

Republic of Iraq
Ministry of Higher Education
and Scientific Research
Al-Nahrain University
College of Science
Department of Physics



Determination of Uranium Concentration in Human Urine for Selected Regions in Iraq Using Laser-Induced Kinetic Phosphorimetry and CR-39 Nuclear Track Detector

A Thesis
Submitted to the College of Science/Al-Nahrain University
in partial fulfillment of
the requirements for the Degree of Master of Science
in
Physics

By
Ahmed F. Saleh Al -Jobouri
(B.Sc. 1996)

Supervised by

Prof. Dr. Mazin M. Elias

Assist. Prof. Dr. Nada F. Tawfiq

Jumada Al-Akhir
April

1433 A.H.
2012 A.D.



جمهورية العراق
وزارة التعليم العالي والبحث العلمي
جامعة النهرين
كلية العلوم
قسم الفيزياء

تحديد تركيز اليورانيوم في الادرار البشري لبعض المناطق المنتخبة في العراق بأستعمال تقنية تحليل الفسفرة المستحثة بالليزر وتقنية كاشف الأثر النووي CR-39

رسالة
مقدمة الى كلية العلوم / جامعة النهرين
وهي جزء من متطلبات نيل درجة ماجستير علوم
في الفيزياء

من قبل
أحمد فرج صالح الجبوري
(بكالوريوس ١٩٩٦)

بإشراف

أ.م.د. ندى فاضل توفيق

أ.د. مازن مانوئيل الياس

١٤٣٣ هـ
٢٠١٢ م

جمادي الآخر
نيسان

Supervisors' Certification

We, certify that this thesis entitled “**Determination of Uranium Concentration in Human Urine for Selected Regions in Iraq Using Laser-Induced Kinetic Phosphorimetry and CR-39 Nuclear Track Detector**” prepared by “**Ahmed F. Saleh Al-Jobouri**” under our supervision at the College of Science/Al-Nahrain University as a partial fulfillment of requirements for the Degree of **Master of Science in Physics**.

Signature:

Name: **Dr. Mazin M. Elias**

Scientific Degree: **Professor**

Address: Institute of Laser for
Postgraduate Studies,
University of Baghdad

Signature:

Name: **Dr. Nada F. Tawfiq**

Scientific Degree: **Assist. Professor**

Address: Dept. of Physics
College of Science
Al-Nahrain University

Date: / /2012

Date: / /2012

In view of the available recommendations, I forward this thesis for debate by the examining committee.

Signature:

Name: **Dr. Salah A. H. Saleh**

Scientific Degree: **Assist. Professor**

Title: Head of the Department of Physics

College of Science/Al-Nahrain University

Date: / /2012

Committee Certification

We, the examining committee certify that we have read the thesis entitled “**Determination of Uranium Concentration in Human Urine for Selected Regions in Iraq Using Laser-Induced Kinetic Phosphorimetry and CR-39 Nuclear Track Detector**” and examined the student “**Ahmed F. Saleh Al-Jobouri**” in its contents and that in our opinion, it is accepted for the Degree of Master of Science in **Physics**.

Signature:

Name: **Dr. Khalid H. Mahdi Al-Ubaidi**

Scientific Degree: **Assist. Professor**

Address: Dept. of Physics, College of Education
/Ibn Al-Haitham, University of Baghdad

Date: / /2012

(Chairman)

Signature:

Name: **Dr. Hana I. Hassan Al-barodee**

Scientific Degree: **Assist. Professor**

Address: Dept. of Physics, College of
Education, University of Mosul

Date: / /2012

(Member)

Signature:

Name: **Dr. Hussain A. Al-jobouri**

Scientific Degree: **Assist. Professor**

Address: Dept. of Physics, College of
Science, Al-Nahrain University

Date: / /2012

(Member)

Signature:

Name: **Dr. Mazin M. Elias**

Scientific Degree: **Professor**

Address: Institute of Laser for Postgraduate
Studies, University of Baghdad

Date: / /2012

(Member & Supervisor)

Signature:

Name: **Dr. Nada F. Tawfiq**

Scientific Degree: **Assist. Professor**

Address: Dept. of Physics, College of
Science, Al-Nahrain University

Date: / /2012

(Member & Supervisor)

I, hereby certify upon the decision of the examining committee

Signature:

Name: **Dr. Khulood Whayeb Abood**

Scientific Degree: **Professor**

Title: Dean of the College of Science

Date: / /2012

*I dedicate this thesis to
the memory of my deceased father,
for his continuous support and encouragement*

Acknowledgements

First, I would like to thank my supervisors Dr. Mazin M. Elias and Dr. Nada F. Tawfiq for giving me the opportunity to complete the work presented here and for their extensive support. Also, I would like to express my gratitude for the great assistance from Ms. Bushra A. Ahmed Director General of Radiation Protection Centre (RPC) in developing this project. Standard preparation and sample measurements would not have been possible without the kind help and assistance from Dr. Scott Miller Director of Research and Development, Chemchek Instruments. Thanks to Dr. Hilal for useful discussions. Further, I am grateful for the excellent service from Radiation Protection Centre employees, for their assistance with the KPA. I am also indebted to all my colleagues for encouragement, help and inspiration. I would also like to thank Ministry of Environment for academic funding for this educational program.

I would also like to express my deep gratitude to State Company for Phosphate, Akashat phosphate mine and Al-Daura refinery authorities for their assessment and tireless efforts.

More importantly, I wish to thank my mother, brothers and sisters, for their knowledge, continuous support, dedication, hard work, confidence and unfaltering love. To them I dedicate this thesis.

Last, but not least, my wife for coming into my life at the right time. Thank you for the incredible amount of patience that you have given me, especially throughout my thesis-writing period. I am deeply grateful to you.

Now let's go sailing!

Ahmed

Abstract

Urine assay is the preferred method for monitoring accidental or chronic internal exposure of uranium in human body. In the present study, two typical methods have been used for determination of uranium in human urine for occupational mining workers and residents of selected regions in Iraq. The main technique is kinetic phosphorescence analysis (KPA). This technique is based on exciting an aqueous solution of uranium using a pulsed dye nitrogen laser source, and measures the emission intensity over time to determine the luminescence decay profile.

Calibration of the system was carried out before analysis utilizing standards of known uranium concentrations to construct the calibration curve between the initial luminescence intensity and uranium concentration. The assay calibration curves are linear and cover the range of uranium concentrations between 0.05 µg/l and 100 µg/l. The limit of quantification in which uranium in urine could be accurately measured above the background was determined to be 0.01 µg/l.

Uranium concentration in urine of all subjects ranged from 0.41 to 5.26 µg/l with an average of 1.315 ± 0.730 µg/l. Higher uranium concentrations were found in the urine of Al-Qaim uranium purification previously workers. The results showed significant correlation with working place and employment duration in Akashat mine and Al-Qaim fertilizer complex. The mean values of different age groups were found to be proportional to age up to 60 years. In addition, the results also show that uranium concentration in urine of Akashat mining area, Tall al-Ragrag and Al-Jesira residents are higher than those living in Al-Qaim. Finally, it has been found that uranium excretion in urine of male is higher than female for each age group.

In order to compare the results all samples were also analysed using the fission track analysis (FTA) with CR-39 solid state nuclear track detector. The results of the comparison demonstrated that the two different techniques were capable of making the measurements, although not with equal degree of bias and uncertainty. It is observed that the kinetic laser phosphorescence technology is more suitable for analysis of uranium in urine samples having high concentration than the fission track technique.

Table of contents

List of symbols and acronyms	vi
Chapter One: Introduction and General Review	1
1.1 Uranium; properties, occurrence and health effects	2
1.1.1 Uranium isotopes.....	2
1.1.2 Uranium natural radioactive series.....	3
1.1.3 Uranium in the environment	3
1.1.4 Uranium exposure pathways and biokinetics	5
1.1.5 Biological half-life of uranium.....	7
1.1.6 Toxicity of uranium	8
1.1.6.1 Chemical toxicity.....	8
1.1.6.2 Radiological toxicity	9
1.1.7 Objective and scope of urine analysis	12
1.2 Uranium analytical techniques	13
1.2.1 Alpha spectrometry	13
1.2.2 Liquid scintillation spectrometry.....	14
1.2.3 Fluorometry.....	14
1.2.4 Laser-induced kinetic phosphorimetry analysis (KPA)	14
1.2.5 Neutron activation analysis.....	15
1.2.6 Fission track analysis (FTA)	15
1.2.7 UV - visible absorption spectrophotometry.....	15
1.2.8 Resonance ionization mass spectrometry (RI-MS)	16
1.2.9 Inductively coupled plasma-mass spectrometry (ICP-MS)	16
1.3 Analytical methods in this study.....	17
1.3.1 Fundamental luminescence theory for kinetic phosphorimetry.....	17
1.3.1.1 Molecular luminescence spectrometry.....	17
1.3.1.2 Emission and excitation energy levels diagrams	18
1.3.1.3 Fluorescence	19
1.3.1.4 Phosphorescence	20
1.3.1.5 Quantum yield	22
1.3.1.6 The use of lasers in photoluminescence spectrometry	23
1.3.1.7 Tunable dye lasers and atomic spectroscopy	24
1.3.1.8 Laser-induced kinetic phosphorimetry analysis (KPA)....	29
1.3.1.9 Calculation of uranium concentration	31
1.3.1.10 Spectroscopic properties of uranyl $[UO_2]^{+2}$	32
1.3.1.11 Lifetime	36
1.3.1.12 Interferences.....	36
1.3.2 Solid state nuclear track detectors SSNTD's	38
1.3.2.1 Track formation mechanism	39
1.3.2.2 Track effecting parameters	39
1.3.2.3 Bulk etch rate velocity (V_B)	39
1.3.2.4 Track etch rate velocity (V_T)	39

1.3.2.5	The chemical etching	40
1.3.2.6	CR-39 track detector	40
1.3.2.7	Fission track analysis	41
1.4	Review of previous studies.....	43
1.4.1	Fission track analysis (FTA)	43
1.4.2	Kinetic phosphorescence analysis (KPA)	44
1.5	The aim of study.....	48
Chapter Two: Materials and Methods	49
2.1	The study regions of interest	49
2.1.1	Akashat phosphate mine (A.M).....	49
2.1.2	Al-Qaim fertilizer complex (Q.F.C)	50
2.1.3	Al-Jesira site (J)	50
2.1.4	Adaya remediation site (A)	51
2.2	Sample collection	54
2.3	Materials and methods for KPA	65
2.3.1	Apparatus	65
2.3.2	Principles and characteristics of the KPA	66
2.3.2.1	Excitation source	66
2.3.2.2	Detection system	66
2.3.2.3	Analytical ranges and detection limit	66
2.3.3	Equipment and glassware	67
2.3.3.1	Muffle furnace	67
2.3.3.2	Analytical balance	67
2.3.3.3	Hot plate	67
2.3.3.4	Fume hood	67
2.3.3.5	Liquid scintillation vials	67
2.3.4	Reagents	68
2.3.5	Uranium standard solutions	68
2.3.6	Linearity of the response to uranium	70
2.3.7	Verification	71
2.3.8	Detection limit (DL) measurement	71
2.3.9	Sample preparation procedure.....	71
2.3.9.1	Principle	71
2.3.9.2	Wet-ashing procedure	72
2.3.10	Sample analysis	72
2.4	Materials and methods for FTA.....	73
2.4.1	Material and apparatuses	73
2.4.1.1	Nuclear track detectors	73
2.4.1.2	Irradiation source	74
2.4.1.3	Etchant solution	74
2.4.1.4	Water bath	75
2.4.1.5	Optical microscope	75
2.4.2	Sample preparation procedure	75

2.4.2.1	Uranium standard solutions	75
2.4.2.2	Irradiation procedure	75
2.4.3	Calibration curve	76
2.4.4	Calculations of uranium concentrations	77
Chapter Three: Results and Discussion	78
3.1	Uranium concentration in urine samples of Akashat mine and Al-Qaim fertilizer complex workers	78
3.2	Uranium concentration in urine samples of Akashat mining region and Al-Qaim residents	89
3.3	Uranium concentration in urine samples of Tall Al-Ragrag and Al-Jesira village residents	92
3.4	Comparison with other countries results	102
3.5	Comparison between KPA and FTA results	104
3.5.1	Outlier data	104
3.5.2	Correlation between KPA and FTA data	105
3.5.3	Uncertainty	106
3.5.4	Detection limit	107
3.5.5	Technical issues	107
3.5.6	Analytical issues	108
3.6	Conclusions	109
3.7	Recommendations and suggestions for future studies	110
References	111

List of symbols and acronyms

Bq	Becquerel
Ci	Curie
C_s	Uranium concentration for standard solution
C_x	Uranium concentration for unknown sample
DL	Detection limit
$E(\lambda)$	Fluorescence line spectrum
E_B	Activation energy of the bulk etch
E_T	Activation energy of the track etch
F_b	Dilution factor (gram sample/ gram dilution)
fs	Femtosecond
I	Intensity
K	Boltzmann constant (1.38×10^{-23} J/K)
k_f	Fluorescence rate constant
k_{isc}	Intersystem crossing rate constant
k_{ic}^S	Internal conversion rate constant
k_p	Phosphorescence rate constant
k_q	rate constant quenching relaxation processes
k_x	Relative rate constants
M	Molarity in mol/l
MDC	Minimum detectable concentration
N	Normality
n	Refractive index
N_A	Avogadro's number (6.023×10^{23} atom/mole)
pH	Acidity of an aqueous solution
ppm	Part per million
RSD	Relative standard deviation
S	Molecules electron spin
S.D _{bg}	Background standard deviation
Sv	Sievert
T	Absolute temperature of the etching solution in K°
U	Uranium
U_0^*	Population of uranyl phosphate
U_c	Uranium concentration
U_t^*	Population of excited uranyl complex
UV	Ultraviolet

V	Volume of drop in milliliter
V	Volume
V_B	Bulk etch rate
V_T	Track etch rate
W	Weight (gram)
W_a	Aliquant weight (gram)
W_{eq}	Equivalent weight (g/mol)
W_t	Atomic weight (g/mol)
η	Etching efficiency
θ_c	Critical angle
λ	Wavelength (nm)
λ_d	Decay constant
ρ	Track density
ρ_s	Induced fission track density for standard solution
ρ_x	Induced fission track density for unknown sample
σ	Fission reaction cross section (4.2×10^{24})
τ_f	Lifetime of fluorescence
τ_p	Lifetime of phosphorescence
φ	Incident angle
$\dot{\Gamma}$	total thermal neutron dose
Φ	Quantum yield
Φ_f^0	Quantum yield for fluorescence
Φ_p^0	Quantum yield for phosphorescence
Φ_{ic}^0	Quantum yield for internal conversion

Chapter One

Introduction and General Review

Environmental radiation originates from a number of naturally occurring and artificial sources. The major sources of natural radioactivity are the nuclides of very long half-lives, which have persisted since the formation of earth and nuclides produced by cosmic rays. Anthropogenic radionuclides can enter into the environment through a variety of different processes. The most relevant sources of artificial radioactivity are nuclear fuel production facilities, spent fuel processing plants and the use of depleted uranium in military armor and munitions, as well as short-lived nuclides from the production of radioisotopes for medical applications. The release of radionuclides from nuclear waste storage areas has also to be considered.

Uranium is a naturally occurring metal, ubiquitous in granites and various other mineral deposits. Its presence in the environment, results from leaching of natural deposits or by manmade sources. The general population is exposed to the naturally occurring background levels of uranium daily through the intake of food, drinking water and air. The health effect of these natural levels on the general population is not fully understood. Much concern has been raised, however, about the accidental and chronic exposure to higher levels of uranium from anthropogenic sources and high uranium dietary intake through contaminated drinking water and food etc. Excessive intake of hazardous uranium materials into body could pose long term health risks from both chemical toxicity and its radioactivity. Such risks to personnel health will depend on the pathway and extent of uranium exposure.

Whatever its route of entry in to the body, uranium is nephrotoxic in both human and animal models. Following absorption, uranium mostly eliminated in the urine. Estimation the potential adverse health effects of uranium is difficult without biological monitoring which is mainly involves in measuring the uranium concentration in the urine.

The objective of this chapter is to develop a simple and rapid description for the uranium radioactive and chemical properties, presence in the environment, biokinetic model and its toxicity. A general description for the uranium determination analytical methods with a brief summary of some previous work will be also presented.

1.1 Uranium; properties, occurrence and health effects

1.1.1 Uranium isotopes

Uranium is a naturally occurring radioactive element. In its pure form, it is a silver-white, lustrous, dense and weakly radioactive metal [1]. Metallic uranium has a high density of 19 g/cm³. It is present in the earth's crust at an average concentration of about 2 ppm (approximately 1 pCi/g) [2].

Naturally occurring uranium (^{nat}U) consists of three isotopes (²³⁴U, ²³⁵U and ²³⁸U), all of which decay by both alpha and gamma emissions [3]. The ²³⁸U isotope is the most abundant by weight (99.28%) with the ²³⁵U and ²³⁴U isotopes constituting about (0.72%) and (0.0054%), respectively. All isotopes of uranium undergo the same chemical reactions in nature and possess almost identical physical characteristics, such as melting point, boiling point and volatility. The radioactive properties (half-life, specific activity, decay mode, etc.) of all uranium isotopes are however different [4]. The total specific activity of natural uranium (i.e. the activity per unit mass of natural uranium metal) is 25.4 Bq/mg [5]. The half-lives, specific activities, relative abundances and average energy per transformation of uranium isotopes ²³⁸U, ²³⁵U and ²³⁴U in natural uranium are given in Table (1.1) .

Uranium occurs in five oxidation states (+2, +3, +4, +5 and +6). Only two oxidation states (+4, +6) are considered stable enough to be of a practical importance [7, 8]. In nature, uranium is primarily (80-90%) present in the hexavalent oxidation state and commonly associated with oxygen as the uranyl ion, [UO₂]⁺² [9].

Table 1.1 Radioactive properties of uranium natural isotopes [6].

Isotope	Half-life (year)	Specific activity (Bq/mg)	Isotopic abundance (%)		Average energy per transformation (MeV/Bq)		
			By mass	By activity	Alpha radiation	Beta radiation	Gamma radiation
^{238}U	4.51×10^9	12.44	99.2746	48.2	4.26	0.010	0.001
^{235}U	7.1×10^8	80	0.7200	2.2	4.47	0.048	0.154
^{234}U	2.47×10^5	230700	0.0054	49.6	4.84	0.001	0.002

1.1.2 Uranium natural radioactive series

Uranium undergoes spontaneously transformation through the decay process to become stable by losing energy and change their atomic number in successive steps and through a serial production of a chain of decay products. Natural uranium consists of two series: The isotope ^{238}U headed the natural $(4n + 2)$ radioactive series (uranium series), and the isotope ^{235}U headed the natural $(4n + 3)$ radioactive series (actinium series). ^{234}U arises from ^{238}U by radioactive decay and these two isotopes are thus linked to each other, but ^{235}U appears to be of independent origin [10].

In nature, uranium isotopes are in radioactive equilibrium with their decay products such as ^{234}Th , ^{231}Th , ^{226}Ra , ^{223}Rn , ^{222}Rn , ^{214}Bi , ^{210}Pb created as a result of radioactive decay [6].

1.1.3 Uranium in the environment

Uranium presents virtually everywhere in the earth's crust in the form of more than 200 minerals [11]. Corresponding concentrations of uranium are also contained in foods of vegetal and animal origin and in groundwater, surface and drinking water. Solubility, mobility and availability of uranium containing compounds in abiotic and biotic systems are very complex and depend, to a high extent; on the respective uranium species present [12].

Uranium presents in the environment as a result of leaching from natural deposits, release in mill tailings, emissions from the nuclear industry, the combustion of coal and other fuels [13, 14]. Additional contamination of arable soils is caused by the use of phosphate fertilizers due to the relatively high uranium levels in phosphate ores (30 - 200 ppm) [15].

In the environment, uranium does not present in metallic form but as uranium compounds. The solubility of uranium compounds are varies greatly. They are dominated by uranium oxides such as UO_2 , which is an anoxic insoluble compound found in minerals, and UO_3 , a moderately soluble compound found in surface waters. The chemical form of the uranium compound determines how easily the compound can move through the environment and its chemical toxicity [5].

International Commission on Radiological Protection (ICRP) summarized the activity concentrations of ^{238}U and ^{235}U of natural origin in some environmental materials as shown in Table (1.2).

Table 1.2 The activity concentrations of ^{238}U and ^{235}U of natural origin in some environmental materials [16].

Material	Activity concentration			
	^{238}U		^{235}U	
	Reference value	Range	Reference value	Range
Soil (Bq/mg)	35×10^{-6}	$(1 - 690) \times 10^{-6}$	—	—
Air ($\mu\text{Bq}/\text{m}^3$)	1	0.02 – 18	0.05	—
Drinking water (Bq/mg)	1×10^{-9}	$9 \times 10^{-11} - 150 \times 10^{-6}$	4×10^{-11}	$0.4 \times 10^{-9} - 0.5 \times 10^{-6}$
Leafy vegetables (Bq/mg)	20×10^{-9}	$6 \times 10^{-9} - 2.2 \times 10^{-6}$	1×10^{-9}	$0.7 \times 10^{-9} - 1.2 \times 10^{-9}$
Root vegetables (Bq/mg)	3×10^{-9}	$0.4 \times 10^{-9} - 2.9 \times 10^{-6}$	0.1×10^{-9}	$5 \times 10^{-11} - 0.6 \times 10^{-9}$
Milk products (Bq/mg)	1×10^{-9}	$0.1 \times 10^{-9} - 17 \times 10^{-9}$	5×10^{-11}	$5 \times 10^{-11} - 0.6 \times 10^{-9}$
Meat products (Bq/mg)	2×10^{-9}	$0.8 \times 10^{-9} - 20 \times 10^{-9}$	5×10^{-11}	$2 \times 10^{-11} - 0.5 \times 10^{-9}$

1.1.4 Uranium exposure pathways and biokinetics

Uranium is incorporated into the human body mainly through the ingestion of food, especially from (vegetables, cereals, and table salt) [17,18], water and the inhalation of air [6].

The daily intake of uranium is estimated to be 1 – 2 μg in food and 1.5 μg in water consumed [19]. On average, the total amount of uranium in the human body is approximately 56 μg (equivalent to 690 μBq ^{238}U) in non-exposed subjects [20]. With 32 μg or 56%, the skeleton accounts for the largest share, followed by muscle tissue 11 μg , fat 9 μg , blood 2 μg and lung, liver and kidney each with less than 1 μg of uranium. The behavior of a substance in the body (intake, uptake, distribution, excretion, retention) is called biokinetics [21].

The systemic availability of uranium after ingestion intake is very low. Depending on the type and bio-solubility of the corresponding uranium compound, only about 0.2 – 2 %, at best 6 % are absorbed from the gastrointestinal tract and thus become systemically available [22-24].

Absorption of inhaled uranium into the systemic circulation depends on the rate at which particles dissolve in the lungs and on their interactions with the ligands present in lung fluid. Generic absorption parameters for fast soluble (Type F), moderately soluble (Type M) and poorly soluble (Type S) compounds have been published by ICRP as shown in Table (1.3).

Table 1.3 Absorption types for uranium compounds [25].

Type	Typical Compounds
F	UF_6 , UO_2F , $\text{UO}_2(\text{NO}_3)_2$
M	UO_3 , UF_4 , UCl_4 , U_3O_8
S	UO_2

- Type F; denotes fast clearance from lung
- Type M; denotes moderate clearance from lung
- Type S; denotes slow clearance from lung

The fate of uranium that enters the blood stream and systemic tissues cannot be observed or easily measured. Therefore, models are used to represent the movement of material around the body. These models can be used to calculate radiation doses to tissues and to predict the retention and excretion of the element [26].

The model used for uranium is that recommended by ICRP in 1995[27] it describes the deposition of material from the blood into various organs or regions, the transfer from region to region, the return of material to blood and the eventual excretion of the material. In keeping with ICRP's move towards physiological realism in its models, this model includes recycling, i.e. the possibility for material to pass from region to region via the blood stream [28].

The principal sites of uranium deposition in the body are kidneys, liver and bones. In addition, some material is deposited in various other tissues generally at lower concentrations than the main sites of deposition; these are usually referred to as 'soft tissues'. Of the amount absorbed into the blood stream, the model assigns 30% to soft tissues (ST) (rapid turnover, ST0), this represents a pool of activity distributed throughout the body which exchanges rapidly with the blood stream. The remaining activity is apportioned as follows, kidneys 12%, liver 2%, bone 15%, red blood cells 1%, soft tissue (intermediate turnover, ST1) 6.7%, soft tissue (slow turnover, ST2) 0.3%, with 63% being promptly excreted in urine via the bladder [26]. Some of the material initially is deposited in these regions can be returned to the blood stream while some is transferred to other regions of tissues.

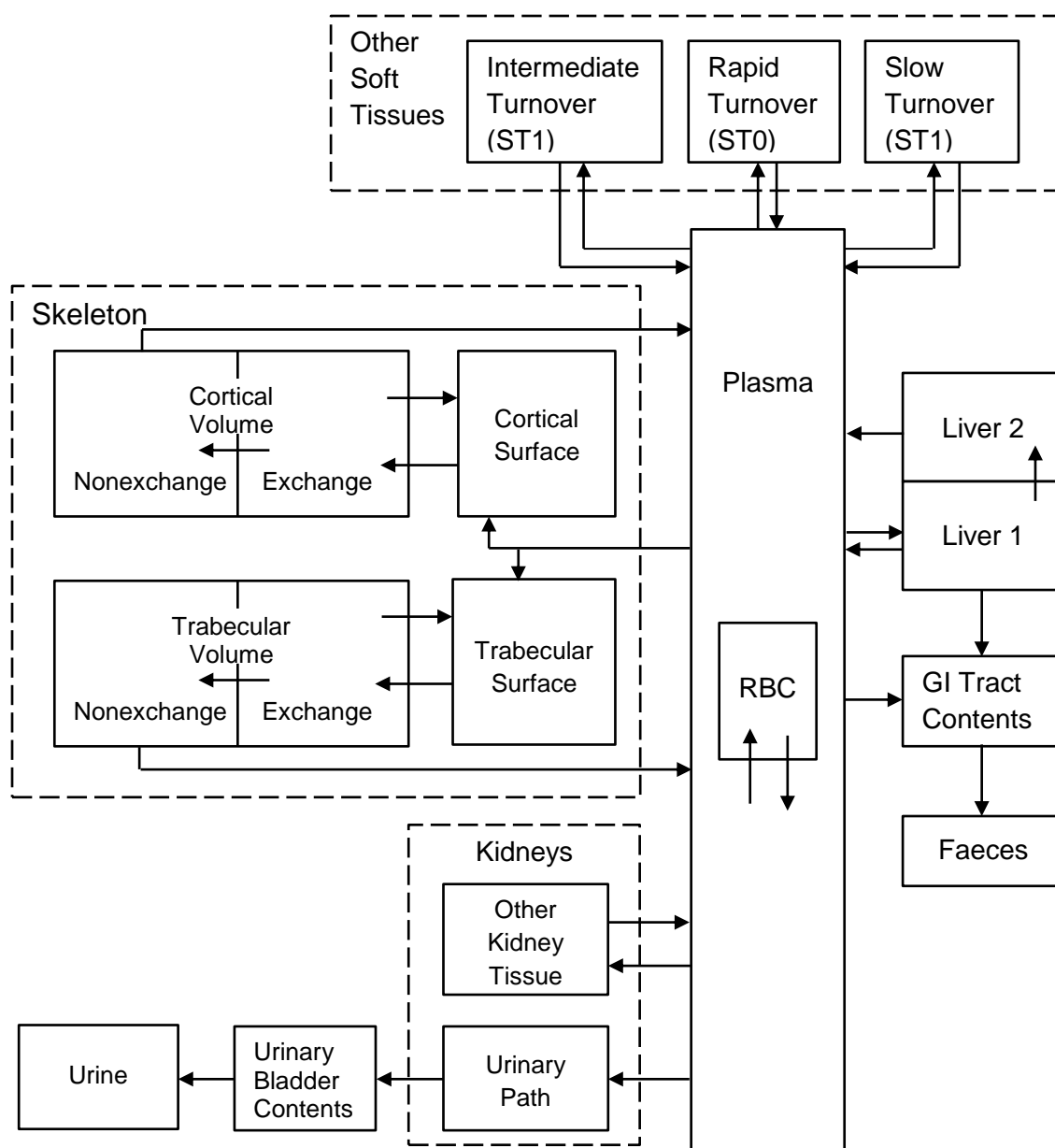


Figure 1.1 The biokinetic model for uranium [27].

1.1.5 Biological half-life of uranium

The biological half-life of uranium in the rat kidney has been estimated to be approximately 15 days. Clearance from the skeleton is considerably slower; half-lives of 300 and 5000 days have been estimated, based on a two-compartment model [22]. Overall half-lives for the clearance of uranium from the rat kidney and skeleton of 5 – 11 and 93 – 165 days, respectively, were determined in another study, based on a 10 – compartment model [29]. The overall elimination half-life of uranium under conditions of normal daily

intake has been estimated to be between 180 and 360 days in humans [30]. For rabbits, uranium half-lives have been estimated to be 14 days in kidney and greater than 200 days in bone. Fourteen percent of absorbed uranium was deposited in bone, and 3% in kidney [31].

1.1.6 Toxicity of uranium

Uranium and its compounds are highly toxic, both from a chemical and radiological standpoint. The maximum permissible total body burden of natural uranium (based on radiotoxicity) is 0.2 μCi (i.e., 7400 Bq) for soluble compounds [7].

1.1.6.1 Chemical toxicity

The chemical toxicity of a heavy elemental compound is related to the interaction of the compound with the biochemical processes of the human body, and identical for all isotopes of the element [26].

Heavy metal compounds may cause a number of cytotoxic effects. For uranium, the most important oxyanions in biological systems are carbonate/bicarbonate compounds, e.g. $[\text{UO}_2(\text{CO}_3)_2]^{2-}$ [32, 33]. While these compounds are stable at a neutral pH value (pH value of blood) and in this form are not very reactive, the highly reactive uranyl ion $[\text{UO}_2]^{+2}$ is released at low pH values (as for example in urine) [21].

The kidney is the most sensitive affected organ for the chemical toxicity of uranium, as other heavy-metal compounds, increased uranium concentrations lead to a reduction of glomerular filtration, of tubular secretion of organic anions and reabsorption of filtered glucose and amino acids in the proximal tubules [34].

There are insufficient data regarding the carcinogenicity of uranium in humans and experimental animals [22]. Uranium has, therefore, been included in Group V (inadequate data for evaluation of carcinogenicity) [35].

For compounds classified in Group V, the maximum acceptable concentration value is derived using a Tolerable Daily Intake (TDI) approach. The World Health Organization (WHO) has established a TDI for uranium of 0.6 µg/kg of body weight per day for humans [36], based on the results of the most extensive subchronic studies, in the most sensitive sex and species, conducted to date in which uranium was administered in drinking water [37].

Typically, an individual may excrete, depending on the dietary intake, between 0.01 and 0.4 µg of uranium in urine each day. Using TDI value of 0.6 µg/kg of body weight per day proposed by WHO for humans and the estimation that 1% of the inhaled or ingested uranium is excreted via urine an uranium concentration value of approximately 0.25 µg/l in urine (obtained by assuming a 60-kg body weight and a daily urine excretion of 1.5 l) is considered to be a reliable safe upper limit for the uranium uptake by humans [38, 39]. However, a concentration of 40 µg of natural uranium in a litre of urine of an individual corresponds to one maximum permissible body burden of natural uranium for that individual [26].

1.1.6.2 Radiological toxicity

Ionizing radiation emitted by different radionuclides differ in their ability to penetrate matter depends on the type of radiation emitted and its energy. The damage caused by ionizing radiation from radionuclide transformations is a result of the energy absorbed by body tissues.

Health effects from external exposure are limited to skin contact. Due to their relatively large size and charge, alpha particles rapidly lose their kinetic energy and have little penetrating power. The penetration range for an alpha particle from ^{238}U is approximately of 28 µm in soft tissue, therefore, provided that redistribution or sorption of uranium into the epidermis does not occur. Alpha particles cannot penetrate to the sensitive lower or basal layers. However, ^{238}U decayed $^{234\text{m}}\text{Pa}$ which emits a 2.29 MeV average energy beta that is capable of irradiating the basal layers of the skin. As a result, uranium principally represents an internal radiation hazard [40].

Internal exposure to ionizing radiation is a function of the route of a given nuclide through the body and its residence time amongst various organs.

Among uranium miners, epidemiological studies provide consistent and convincing evidence of excess lung cancer. The lung cancer risk is associated with alpha particle exposure from ^{222}Rn and its decay products, which arise in uranium mines from the decay of ^{238}U [26].

The period between radiation exposure and an increased risk for cancer is generally quite long [41]. In adults, the median latency period may be about 8 years for leukemia and two- to three-times longer for solid cancers. Generally, the additional cancer risk for low dose exposure is assumed to be proportional to the radiation dose. It is difficult to detect an increased cancer risk due to radiation at doses lower than 100 mSv because the excess risk at low doses is small in comparison to spontaneous rates of cancers of the same type. Therefore, no direct experimental or epidemiological evidence can be obtained [42]. In the absence of any direct evidence, United Nations Scientific Committee on the Effects of Atomic Radiation (UNSCEAR) has estimated that the additional risk of fatal cancer associated with a dose of 1 mSv is about 1 in 20,000 [43].

The dose by inhalation depends on the particle size distribution, and the larger the particle size the lower the dose (particles with aerodynamic diameter of more than 10 μm cannot reach the lungs). In a real case the fraction of radionuclides which is deposited into the lungs is likely below 10% (AMAD 5 μm = 5.8% deposit in the lung; AMAD 1 μm = 11% deposit in the lung) [26].

Internal dose calculations for uranium are based on the use of biokinetic models that describe the passage and kinetics of various given radionuclides throughout the body. The dose coefficient (Sv/Bq) denotes the relationship between the activity intake of a radioactive substance (in Bq)

and the radiation dose caused by this substance. The dose coefficients for committed effective doses of relevant uranium isotopes are listed in Table (1.4).

Table 1.4 Dose coefficients in (Sv/Bq) for uranium isotopes: public and occupational exposure [25, 44]

Intake pathway	Dose coefficient Sv/Bq		
	^{234}U	^{235}U	^{238}U
Inhalation (acute; AMAD = 1 μm) (Public) [25]			
Solubility class F (fast)	5.6×10^{-7}	5.2×10^{-7}	5.0×10^{-7}
Solubility class M (moderate)	3.5×10^{-6}	3.1×10^{-6}	2.9×10^{-6}
Solubility class S (slow)	9.4×10^{-6}	8.5×10^{-6}	8.0×10^{-6}
Inhalation (acute; AMAD = 5 μm) (Occupational) [44]			
Solubility class F (fast)	6.4×10^{-7}	6.0×10^{-7}	5.8×10^{-7}
Solubility class M (moderate)	2.1×10^{-6}	1.8×10^{-6}	1.6×10^{-6}
Solubility class S (slow)	6.8×10^{-6}	6.1×10^{-6}	5.7×10^{-6}
Ingestion (acute; $f_1 = 0.02$) [44]	4.9×10^{-8}	4.7×10^{-8}	4.5×10^{-8}
Direct absorption into blood [44]	2.3×10^{-6}	2.1×10^{-6}	2.0×10^{-6}

- AMAD; Activity median aerodynamic diameter
- f_1 ; Gut transfer factor (i.e. the fraction of an element directly absorbed from the gut to body fluids) through intake by ingestion or inhalation.

1.1.7 Objective and scope of urine analysis

Biochemical analysis of urine can provide information about the condition of the body - both concerning general health, and also specific medical conditions. Approximately 95 % of urine volume is due to water, the remainder consists of solutes, with other remaining constituents. The concentrations of some metals in 10 mg urine ranged as; urea 9.3 – 23.3 mg/l, chloride 1.87– 8.4 mg/l, sodium 1.17 – 4.39 mg/l, potassium 0.75 – 2.61 mg/l, creatinine 0.67 – 2.15 mg/l and other dissolved ions, inorganic and organic compounds. The pH of normal urine is generally in the range 4.6 – 8 [45].

Uranium absorbed into the systemic circulation of the body is mostly excreted through the renal system within a short time. The remainder is stored in different organs as described above and is also excreted through urine within a prolonged half-life [46]. Endogenous fecal excretion of uranium is only of minor importance. Since 98% of inhalation or ingestion uranium passes through the gastrointestinal tract without being absorbed, fecal uranium excretion basically indicates merely the current level of uranium in the food. As this process will be completed within no more than 3 to 4 days, examinations of the feces can prove with reasonable certainty if uranium has recently been incorporated, but fail to detect any incorporation through inhalation.

By assuming that kidneys will efficiently excrete in urine approximately 90% of the uranium solubilized in blood, over a period of approximately three days and uranium excretion in urine is proportional to the uranium level in the body. Thus, urine can be considered as the best body fluid for the detection of uranium, since once in the body any uranium compound soluble, to some extent, will be cleared to the blood and rapidly excreted through the kidneys. The increased urinary uranium excretion can provide a rapid, positive and sensitive quantitative measure of exposure to

ingested, inhaled or embedded uranium, especially in the case of acute exposure.

The background rate of urinary excretion of uranium, occurring from natural sources ranges between 0.05 and 0.5 $\mu\text{g/day}$ [47]. Other studies of unexposed individuals have shown that the excreted uranium concentration in urine averages 12.8 ng/l [48] with daily excretion of 30.9 ± 19.6 ng/day [49].

1.2 Uranium analytical techniques

Uranium analytical techniques are divided into three categories “chemical techniques, nuclear techniques and spectrometric techniques” depending on the detection method. A variety of analytical techniques are available for evaluating uranium in urine and other bioassay samples at levels appropriate for occupational exposure. A few techniques (fluorometry, kinetic phosphorescence analysis, α -spectrometry, neutron irradiation techniques, fission track analysis and inductively-coupled plasma mass spectrometry) have also been demonstrated as capable of determining uranium in these materials at levels comparable to those which occur naturally. Such techniques have also proved of great value in improving our understanding of how uranium behaves in the body. Some of these analytical methods are summarized below; the intent is not to provide an exhaustive list of analytical methods [50]. Rather, the intention is to identify well-established methods that are used as the standard methods of analysis:

1.2.1 Alpha spectrometry

Alpha spectrometry technique based on using solid-state (surface-barrier and passivated ion-implanted) silicon detectors for determine uranium quantitatively in human bioassay. The advantage of α -particle spectrometry is the possibility of isotopic identification.

This technique requires radiochemical separation of the uranium from the biological matrix followed by electrodeposition, evaporation and long counting time ($T = 24$ h). The concentration of uranium in urine or tissue

depends on the detector efficiency, chemical recovery, background, sample size, and counting time. The minimum detectable limit for alpha spectrometry is approximately 0.1 mBq of ^{234}U , ^{235}U or ^{238}U in a 24-hour urine sample. Count times of approximately one week are required to achieve this sensitivity [51].

1.2.2 Liquid scintillation spectrometry

Liquid scintillation spectroscopy is attractive for quantitative determination of α -particle emitters because of its 4π geometry, high counting efficiency (near 100%), and because sample preparation can be relatively straightforward. Liquid scintillation spectroscopy disadvantages are high background (resulting from sensitivity to accompanying β and γ radiation) and sensitivity of scintillator performance to water, acids, or salts which may be introduced along with the analyte [50].

1.2.3 Fluorometry

Fluorometric methods for uranium are commonly variations on classical methods; where in small (usually aqueous) samples are added to solid NaF, or to a NaF/LiF flux, which is then fused by heating. Fusion incorporates the uranium uniformly in the melt and eliminates water, organics, and volatile inorganics. A fluorometer is used to irradiate the cooled sample with UV light in the range from 320 to 370 nm, and fluorescence intensity at 530 to 570 nm is measured at (45° to 90°) to the incident beam. For urine analysis, the minimum detection limit after ion-exchange separation is $0.1 \pm 0.1 \mu\text{g U/l}$ [52].

1.2.4 Laser-induced kinetic phosphorimetry analysis (KPA)

Kinetic phosphorescence analysis is a technique that provides rapid, precise and accurate determination of uranium concentration in aqueous solutions. KPA estimates uranyl ion concentration by observing

phosphorescence intensity with time after pulsed laser excitation. Decay of the resulting $[\text{UO}_2]^{+2}$ excited state follows first-order kinetics.

The initial phosphorescence intensity I_0 is determined from the intercept of the plot of $\ln I_t$ to t , and is related to uranyl ion concentration by calibrations using standard solutions. The KPA limit of detection for U_3O_8 dissolved in nitric acid and complexed with a phosphate solution is about $0.001 \mu\text{g/l}$, with a 4% - 7% CV and (1% - 3% at higher concentrations). Linear response from 0.001 to $5000 \mu\text{g/l}$ is possible if detector saturation is accounted for during early decay times of more concentrated solutions [47].

1.2.5 Neutron activation analysis

In neutron activation analysis, ^{238}U absorbs thermal neutrons in (n- γ) reaction to form ^{239}U , which decays rapidly ($T_{1/2} = 23.5$ min) by β^- decay to ^{239}Np . The ^{239}Np is itself a short-lived isotope ($T_{1/2} = 2.34$ d) which decays by emission of a β^- particle to ^{239}Pu . Photons associated with the decay of either ^{239}U or ^{239}Np can be used to estimate the original amount of ^{238}U present in the sample. The detection limit of the method depends on the thermal neutron fluence rate at which the sample is exposed and the time of exposure [50].

1.2.6 Fission track analysis (FTA)

This technique based on irradiation the sample with thermal neutrons, ^{235}U (n, f) reaction, to produce fission tracks in solid state nuclear track detectors such as polycarbonate films Lexan, mica, or CR-39. These tracks are then developed to a size visible under the microscope, and the amount of ^{235}U present in the sample can be estimated from the track density [50].

1.2.7 UV - visible absorption spectrophotometry

In this technique uranium can be separated directly from urine by anion exchange and then determined spectrophotometrically with arsenazo III (azophenyl arsenic acid). Uranyl ion $[\text{UO}_2]^{+2}$ in the presence of arsenazo III forms a colored complex with high molar absorptivity

1.2.8 Resonance ionization mass spectrometry (RI-MS)

Resonance ionization spectroscopy (RIS) uses tuned laser radiation to selectively raise uranium atoms in the gas phase to one or more intermediate quantum energy states before photoionization and detection. Intermediate excited states can be chosen which are specific for the atom of interest so that isotopic resolution is possible. The charge produced by the free electrons can be measured, or the ions can be analyzed by mass spectrometry. Gaseous neutral atoms are generated from a solid substrate by thermally heating the sample or by bombarding the sample surface with ion beams (sputtering). Pulsed lasers are normally used both to excite and to photoionize the uranium. A detection limit of 1 $\mu\text{g/l}$ using Resonance ionization mass spectrometry is reported [53].

1.2.9 Inductively coupled plasma-mass spectrometry (ICP-MS)

Mass spectrometry provides a sensitive analytical tool which is capable of determining both mass and isotopic composition of an analyte. Exploration of its usefulness in determining uranium in biological materials has increased greatly since the late 1970s. Inductively coupled plasma-mass spectrometry (ICP-MS) uses inductively coupled plasma as an ion source for a mass spectrometer. A sample introduction device introduces samples into the plasma, as either a dry vapor or a fine mist. Options for introducing liquid samples include pneumatic nebulization, electrothermal vaporization, flow injection, and direct injection.

Laser ablation is a common method for introducing solid samples into the plasma. Argon is often used as the carrier gas. Radiofrequency fields at the tip of a quartz torch generate a high-temperature (5000 - 8000 K) plasma at atmospheric pressure in the carrier gas, which desolvates, atomizes, and ionizes the sample; a portion is then drawn into the evacuated mass spectrometer region through a series of small orifices. ICP-MS detection limits are generally competitive with those for methods which depend on natural radioactivity for radionuclides with half-lives exceeding about 10^4 year [53].

1.3 Analytical methods in this study

This work deals with two different analytical methods. The main technique employed within this study is the pulsed-laser kinetic phosphorimetry which form the basis of kinetic phosphorescence analyzer (KPA). The fundamental photoluminescence theory with a general introduction to phosphorescence and the underlying physics will be outlined. Furthermore, this paragraph provides a rapid review for the theoretical principles of tunable dye laser which provide the excitation wavelength for the uranyl ion. A brief theoretical description of kinetic phosphorescence analysis will also be given, together with an overview of uranyl ion spectroscopic properties, including excitation and emission spectral profiles, interferences and phosphorescence lifetime. The second analytical technique for the micro-analysis of uranium concentration in urine samples is based on using solid-state nuclear track detectors (SSNTDs) with fission track registration method. A generic description of this technique and the relevant theory is presented within this paragraph. However, precise experimental details will be described in the next chapter, including the preparation of the samples and their storage and analysis.

1.3.1 Fundamental luminescence theory for kinetic phosphorimetry

1.3.1.1 Molecular luminescence spectrometry

Photoluminescence is the emission of light from any substance and occurs from electronically excited states. Luminescence is formally divided into two categories “*fluorescence and phosphorescence*” depending on the nature of excited state [54].

Fluorescence and phosphorescence are alike in that excitation is brought about by absorption of photons and they are differing in their state multiplicities [55]. The electronic energy transitions responsible for fluorescence have the same multiplicity (i.e. do not involve a change in electron spin). In contrast, a change in electron spin accompanies phosphorescence. Because of highly probable transitions can occur only

when the molecules electron spins (S) are paired $\Delta S = 0$, phosphorescence emissions have relatively long lifetimes [56].

Measurement of intensity of photoluminescence permits the quantitative determination of variety of important inorganic and organic species in trace amounts. Currently the number of fluorometric methods is far greater than the number of applications of phosphorescence procedures.

One of the most attractive features of luminescence methods is their inherent sensitivity. With detection limits that are often one of three orders of magnitude lower than other techniques. In fact for selected species under controlled conditions, single molecular have been detected by fluorescence spectroscopy. The other advantage of photoluminescence methods is their large linear concentration ranges, which are also often significantly greater than other methods. To understand the difference between the two photoluminescence phenomena a review of electron spin and the differences between singlet and triplet excited states are required [55].

1.3.1.2 Emission and excitation energy levels diagram

The processes that occur between the absorption and emission of light are usually illustrated by the Jablonski diagram. This diagram is visualizing in a simple way the possible processes; photon absorption, internal conversion, fluorescence, intersystem crossing, phosphorescence and delayed fluorescence. A typical Jablonski diagram is shown in Fig. 1.2. The singlet ground, first, and second electronic states are depicted by S_0 , S_1 , and S_2 , respectively, while the first triplet electronic state is depicted by T_1 . Vibrational levels are associated with each electronic state. It is important to note that the photon absorption is very fast ($\approx 10^{-15}$ s) with respect to all other procedures [57].

The vertical arrows corresponding to absorption start from the (lowest) vibrational level of the ground electronic state S_0 because majority of molecules occupy this level at room temperature [57].

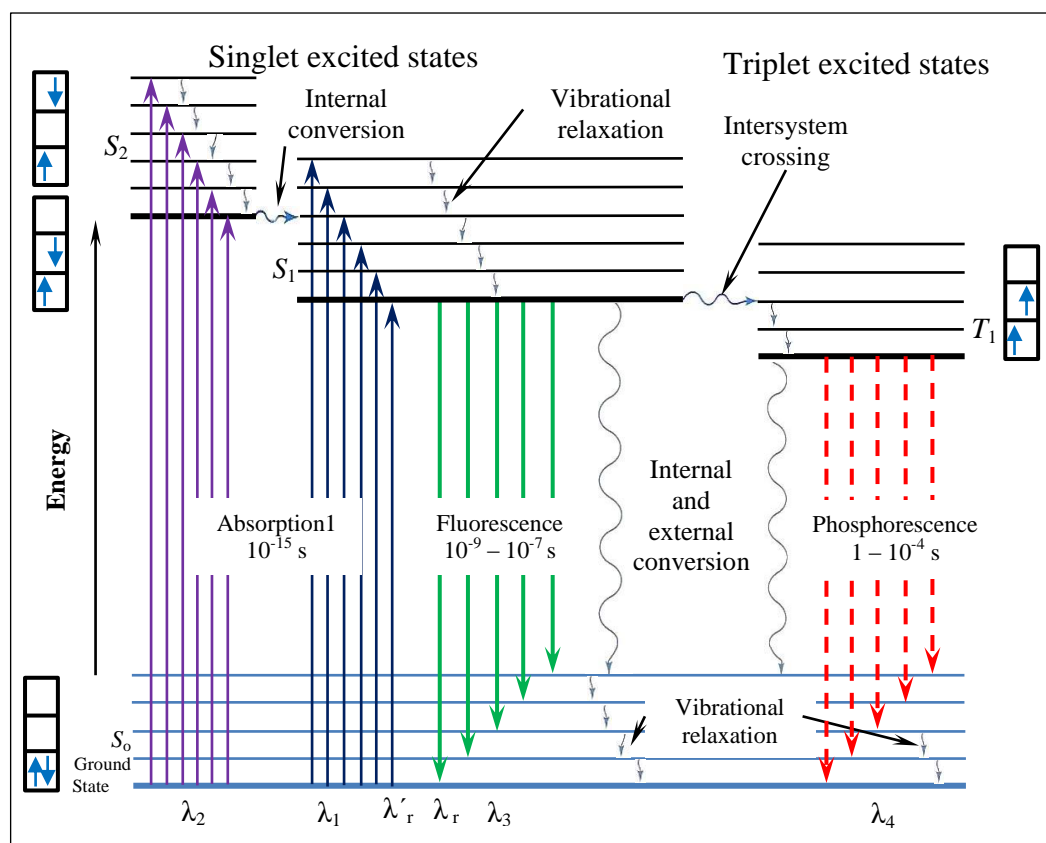


Figure 1.2 Partial energy diagram for photoluminescence system [55].

1.3.1.3 Fluorescence

Emission of photons accompanying the $S_1 \rightarrow S_0$ relaxation is called fluorescence [58]. When photons are absorbed they are elevated to produce excited states. Fig. 1.2 shows the absorption by molecules to produce either the first S_1 , or the second S_2 excited state. Excitation can result in the molecule reaching any of the highest vibration sub-levels associated with each electronic excited state [58]. The energy is absorbed as discrete quanta and this result in a series of distinct absorption bands. However, the above diagram neglects the rotational levels associated with each vibrational level and which normally increase the number of possible absorption bands to such an extent that it becomes impossible to resolve individual transitions. The molecules arrive to the lowest vibrational level of an excited singlet state rapidly by losing their excess of vibrational energy by collision. Almost all molecules occupying any excited singlet state higher than the first undergo

internal conversion and pass from the lowest vibrational level of the upper state to a higher vibrational level of the lower excited state of the same energy. Then the molecules again loss energy until they reach the lowest vibrational level of the first excited state. The molecule can return from this level to any vibrational level of the ground state by a photon emission in the form of fluorescence [59]. Such that fluorescence emission occurs only from the first excited singlet state and therefore its characteristics (except polarization) do not depend on the excitation wavelength [57].

The lifetime of an excited singlet state is approximately 10^{-9} to 10^{-7} s [60] and therefore the decay time of fluorescence is of the same order of magnitude. If fluorescence is unperturbed by competing processes, the lifetime of fluorescence is the intrinsic lifetime of the excited singlet state [61].

The 0-0 transition is usually the same for absorption and fluorescence. However, the fluorescence spectrum is located at longer wavelength (i.e., lower energy) than the absorption spectrum, because of the energy loss in the excited state due to vibrational relaxation. This displacement of the maximum of fluorescence with respect to the maximum of the first absorption band is referred to as *Stocks Shift* [57].

1.3.1.4 Phosphorescence

Although population of triplet states by direct absorption from the ground state is theoretically forbidden, a more efficient process in which a molecule in the lowest vibrational energy level of an excited electronic state can pass into a high vibrational energy level of a lower energy electronic state with a different spin multiplicity. This process is referred to as *intersystem crossing*, and is a spin-dependent internal conversion process. After intersystem crossing to the triplet state, further deactivation can occur either by internal or external conversion or by phosphorescence [57].

Phosphorescence is the radioactive transition between two states of the same molecule which are of different multiplicity. In practice, it is invariably

$T_1 \rightarrow S_0$ [62]. In contrast to fluorescence (singlet to singlet transition), phosphorescence is a spin forbidden process. Nevertheless, it can be observed under specific conditions, due to internal or external spin-orbital coupling which mixes pure singlet and triplet states to produce state with a mixed character in spin multiplicity [63, 64].

As triplet to singlet transitions are generally less probable than singlet-singlet conversion. Transition probability and excited state lifetime are inversely related. Thus, the average lifetime of the triplet excited state with respect to the emission is large and ranges from 10^{-4} to 10 s. or more. Then phosphorescence will have a decay lifetime approximately equal to the lifetime of lowest triplet state [61].

External and internal conversion compete so successfully with phosphorescence that this kind of emission is ordinarily observed at low temperatures and/or in rigid medium where collisional processes are minimized [57].

The phosphorescence occurs at longer wavelengths than fluorescence, as shown in Fig. 1.3, because the energy of the lowest vibrational level of the triplet state T_1 is lower than it's associated with singlet state and the transitions back to the ground state are accompanied with the emission of photons of lower energy than from the singlet state [65].

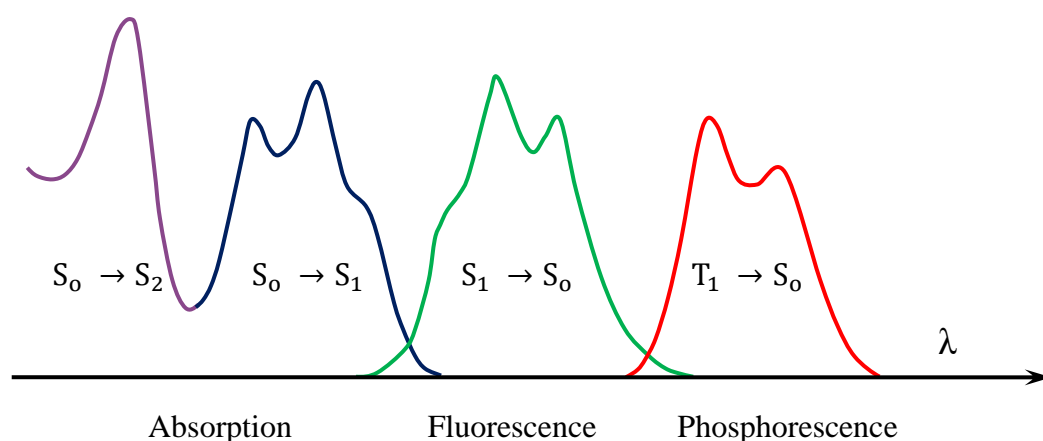


Figure 1.3 Illustration of the relative positions of absorption, fluorescence and phosphorescence spectra [57].

1.3.1.5 Quantum yield

The quantum yield, or quantum efficiency, for fluorescence or phosphorescence is simply the ratio of the number of quanta emitted to the total number of excited quanta absorbed [56] i.e.,

$$\Phi_f = \frac{\text{no. of fluorescence quanta emitted}}{\text{no. of quanta absorbed to a singlet excited state}} \quad (1.1)$$

and:

$$\Phi_p = \frac{\text{no. of phosphorescence quanta emitted}}{\text{no. of quanta absorbed to a singlet excited state}} \quad (1.2)$$

In the absence of external quenching by collisional processes the quantum yields become intrinsic, Φ_f^0 , Φ_p^0 and the following expression is valid:

$$\sum_i \Phi_i^0 = \Phi_f^0 + \Phi_p^0 + \Phi_{ic}^0 = 1 \quad (1.3)$$

where Φ_{ic}^0 is the quantum yield for internal conversion by vibrational deactivation.

The quantum yield (Φ) for a compound is determined by the relative rate constants k_x for various processes by which the lowest excited singlet or triplet states deactivated. These processes are denoted as follows:

k_f : rate constant for radiative deactivation $S_1 \rightarrow S_0$ with emission of fluorescence.

k_{ic}^S : rate constant for internal conversion $S_1 \rightarrow S_0$

k_{isc} : rate constant for intersystem crossing $S_1 \rightarrow T_1$

k_p : rate constant for radiative deactivation $T_1 \rightarrow S_0$ with emission of phosphorescence.

k_{ic}^T : rate constant for internal conversion $T_1 \rightarrow S_0$

Thus quantum yield of fluorescence can be related to several rate constants by the equation [56]:

$$\Phi_f^0 = \frac{k_f}{k_f + k_{ic}^s + k_{isc}} = k_f \tau_f \quad (1.4)$$

where τ_f is the lifetime of fluorescence.

In the case of phosphorescence, if $k_{isc} \gg k_f + k_{ic}^s$, then:

$$\Phi_p^0 = \frac{k_p}{k_p + k_{ic}^T} = k_p \tau_p \quad (1.5)$$

If the above condition does not met, then:

$$\Phi_p^0 = \left(\frac{k_{isc}}{k_f + k_{ic}^s + k_{isc}} \right) \left(\frac{k_p}{k_p + k_{ic}^T} \right) \quad (1.6)$$

In the case of collisional bimolecular quenching (external quenching) the phosphorescence quantum yield is given by [66]:

$$\Phi_p = \left(\frac{k_{isc}}{k_{isc} + k_f + k_{ic}^s + \sum k_{q,f}[Q]} \right) \left(\frac{k_p}{k_p + k_{ic}^T + \sum k_{q,p}[Q]} \right) \quad (1.7)$$

where $\sum k_{q,f}[Q]$ and $\sum k_{q,p}[Q]$ are the sums of all effective (unimolecular) quenching rate constants of fluorescence and phosphorescence, respectively. Collisions effectively shorten the lifetime from that obtained in the absence of collisions.

1.3.1.6 The use of lasers in photoluminescence spectrometry

Since the 1970s, various types of lasers have been used as excitation sources for photoluminescence measurements. Of particular interest are a tunable dye lasers pumped by a pulsed nitrogen laser or Nd:YAG laser. Fixed-wavelength laser are also used, particularly in detectors for chromatography and electrophoresis. Laser sources offer significant advantages in certain instances [67].

1.3.1.7 Tunable dye lasers and atomic spectroscopy

The organic dye laser plays the most prominent role in atomic and molecular spectroscopy.

The narrow spectral bandwidth and great intensity per unit, spectral range of these dye lasers have made it possible to extend the range of spectroscopic methods.

Broad tunability, from the near ultraviolet to the near infrared (i.e. between 300 – 1100 nm), Fig. 1.4, is facilitated by the existence of hundreds of laser dye molecular species. This is adequate for most spectroscopic and other research applications. The tuning range of pulsed narrow bandwidth emission available with a single dye can be up to 50 nm [68]. The intrinsic feature of dye lasers is their inherent ability to yield high-pulse energies and high-average powers in the visible [69]. Single-pulse energies excess of several hundred joules and average powers in excess of 2.5 kW. This unparalleled performance is greatly facilitated by the heat dissipating ability of the gain medium in the liquid phase [70]. The spectral gain profiles of various laser dyes are shown schematically in Fig. 1.5.

On the other hand, highly stabilized single-longitudinal-mode dye lasers can yield frequency drift rates below 1 Hz/s [71]. In the ultrashort-pulse regime dye lasers have demonstrated pulses as short as 19 fs [72] and extra cavity prism-grating compressors have yielded 6-fs pulses [73].

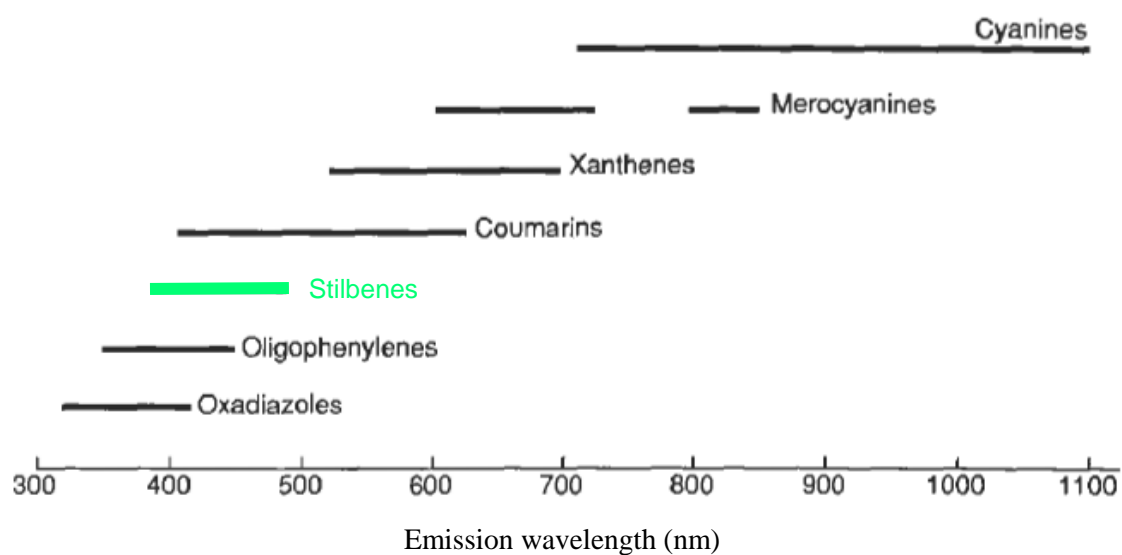


Figure 1.4 Ranges of output wavelengths of KPA Stilbene 420 and various types of organic dyes used in liquid lasers [68].

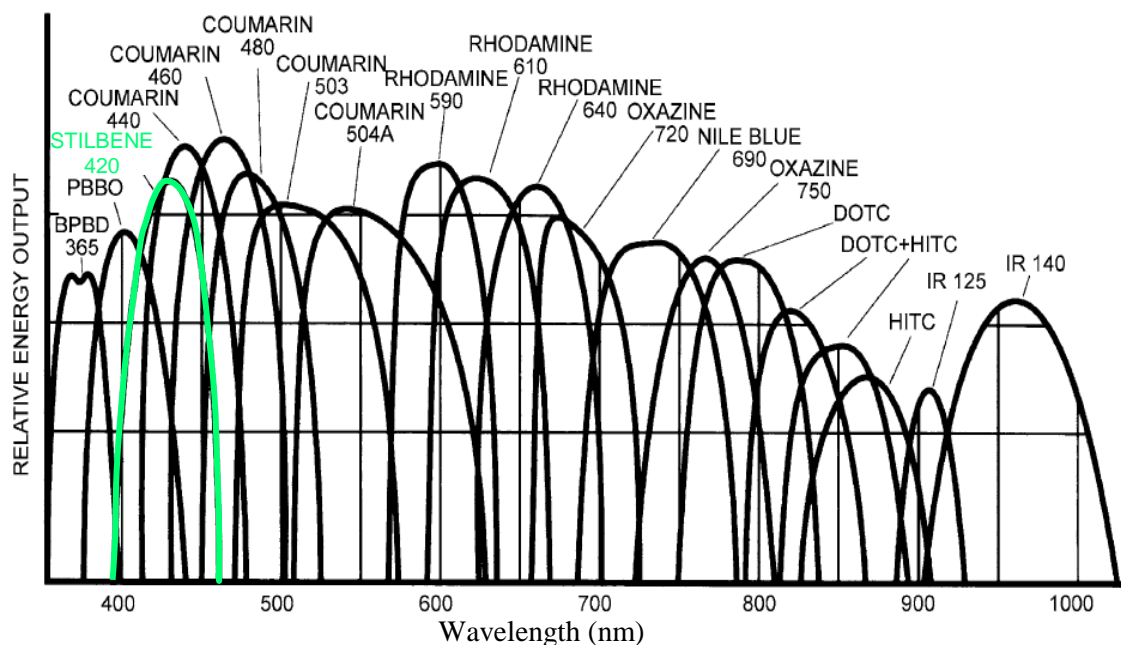


Figure 1.5 Spectral gain profiles of different laser dyes, illustrated by the output power of pulsed lasers [74].

(i) Principles of dye laser operation

Laser dyes are quite large and complex molecules, with atomic weight in the 175 to 1000 amu range which lead to a complex absorption and emission spectra [75].

It is essentially a four levels system where upper and lower energy levels have an extended span, which leads to the broad absorption and tunability corresponding to $S_0 \rightarrow S_n$ electronic transition, [76]. These levels are shown schematically in Fig. 1.6.

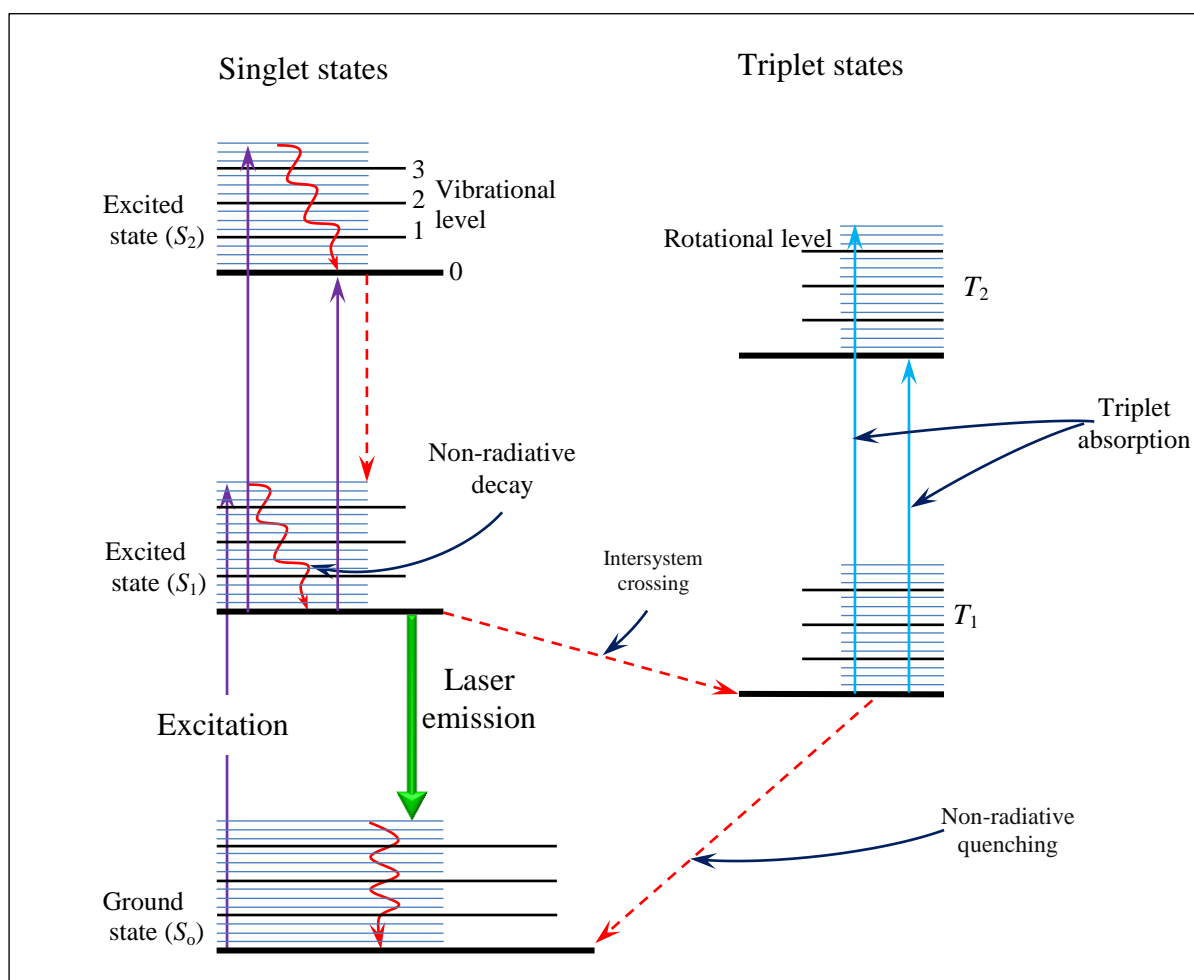


Figure 1.6 Energy-level diagram illustrating excitation and emission transitions of laser dye molecules [76].

These electronic states form the basic structure and transitions between them lead to emission in, or close to, the visible part of the spectrum. The diagram shows that these electronic states have other substates superimposed on them resulting from the vibrational and rotational motion within the molecule. Energy differences caused by rotational motion are small and, when the other line-broadening mechanisms are included, a continuum of states emerges, both for absorption and emission [77]. The diagram shows a continuum of energy levels that enable a laser dye to absorb energy, as well as emit light over a broad range of wavelength, particularly in comparison with other types of laser. The most important of these is that the thermalization time within the vibrational-rotational continuum of a given electronic level band is very fast and the dye therefore can be considered to be homogeneously broadened [76].

Figure 1.6 also shows the processes leading to laser action, with the population of higher vibrational levels of the first S_1 excited electronic singlet states by $S_0 \rightarrow S_1$ or $S_0 \rightarrow S_2$ absorption processes. If excited to S_2 the molecules rapidly decay, in a radiationless transition, to S_1 . After fast radiationless relaxation, the excited dye molecules accumulate in the lowest vibrational level of S_1 , which constitutes the upper level of the laser transition. Laser emission depopulates this level into higher-lying vibrational-rotational levels of the ground electronic state S_0 . Finally, nonradiative processes remove molecules from the lower level of the laser transition. Competing with the radiative depopulation of S_1 are radiationless transitions into the lower triplet state T_1 . This intersystem crossing process populates the lower metastable triplet state and could cause considerable losses if the triplet-triplet absorption bands overlap the lasing band, inhibiting or even halting the lasing process. The triplet losses can be reduced by adding small quantities of appropriate triplet quenchers. These losses are not very important under pulsed excitation with nanosecond pulses because the usual

intersystem crossing rates are not fast enough to build up an appreciable triplet population in the nanosecond time domain [78]. These processes are explained in greater details, with corresponding equations, in [79].

(ii) Molecular nitrogen laser-pumped dye lasers

Radiation emitted by a visible- or near-UV pulse laser is an ideal technique for exciting dye lasers and was used in the first liquid laser demonstration [80, 81]. Many different types of lasers are capable of delivering a very high intensity pulse of radiation, the peak power of which can reach 100 kW or more in a pulse lasting a few nanoseconds. The use of very short pumping pulses avoids the inefficiencies associated with triplet formation. Additionally, this method avoids distortion of the gain medium from acoustic effects.

A particularly reliable and convenient pump source is the pulsed nitrogen laser operating at 337.1 nm. The short wavelength of this laser radiation excites many dyes to high-lying singlet levels, but in all cases the molecules relax very quickly to the bottom edge of the lowest excited singlet level, dissipating the excess energy in the solvent. Since most dyes have a strong absorption band in the ultraviolet region the nitrogen laser provides an almost universal pump source. The short pulse length and high repetition frequency of this laser provide a convenience similar to that of continuous wave operation [82].

A schematic diagram of the nitrogen laser pumped dye laser system is shown in Fig. 1.7. The nitrogen laser consists of a rectangular channel 1 m long through which a rapid discharge is passed from a triggered high-voltage capacitor system [83].

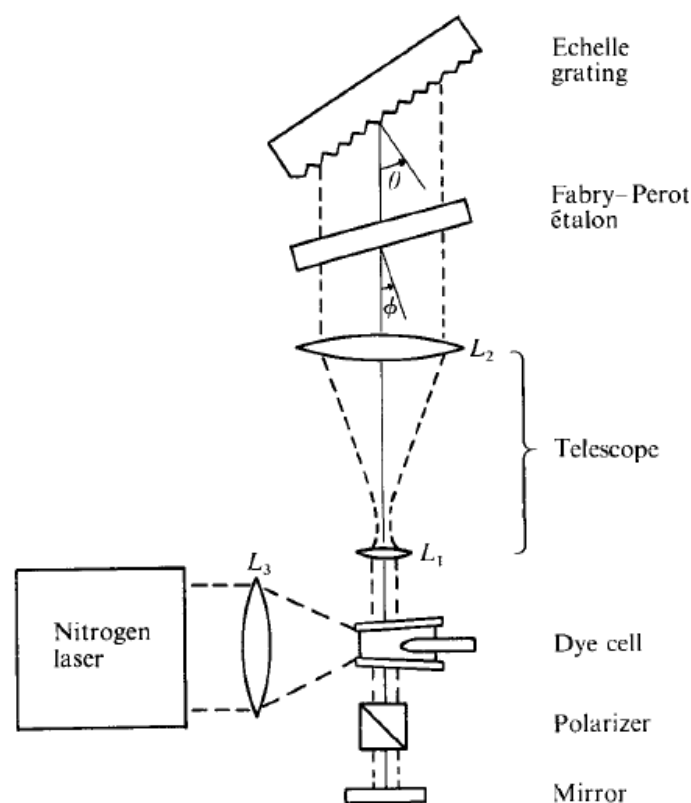


Figure 1.7 Dye laser with narrow bandwidth output pumped by pulsed nitrogen laser [83]

1.3.1.8 Laser-induced kinetic phosphorimetry analysis (KPA)

Phosphorescence provides the basis for many sensitive and selective analytical techniques [84]. Recently, the development of pulsed-source time-resolved phosphorimetry has allowed for the detection of trace amount of metals including uranium, [85] and several lanthanides. This technique significantly simplifies the measurement of phosphorescence [85, 86], by addressing two critical issues with which analysts must be concerned dealing with luminescence measurement in solution; the spectra interference and quenching.

Pulsed-source time-resolved phosphorimetry involve measurement of the luminescence after a specific time delay following excitation.

This reduces the effect of spectral interference when analyzing long-lived luminescence species because the emission is monitored after the short-lived luminescence has decayed to zero [86, 87].

Kinetic phosphorimetry analysis, a pulsed-source time-resolved technique, measure the decay of the phosphorescence signal. This technique assumes that the phosphor decays through a first order process, in which the concentration of the species of interest is related to the rate of change of phosphorescence signal. Figure 1.8 shows the various component of the Kinetic Phosphorimetry Analysis. A nitrogen pumped dye laser, with average power in the (0.1 - 0.5) mW range, provides the wavelength necessary for excitation the sample. The pulse duration is 3ns with repetition rate of 20 pulses/s. The laser beam simultaneously excites the reference and sample cells. These cells are part of two separate and identical detection systems. KPA intensity measurements are taken at fixed time intervals, called time gates, following the pulse [88].

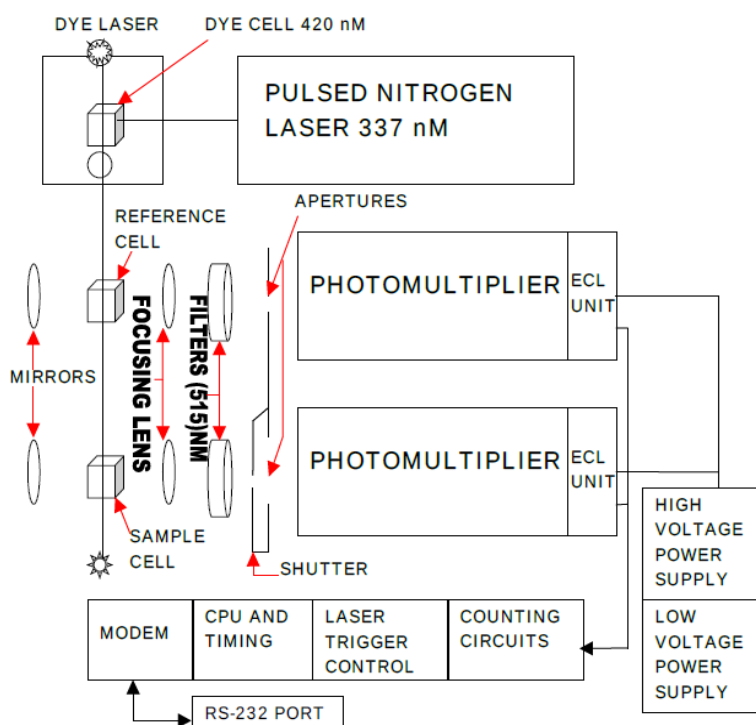


Figure 1.8 Diagram of the Kinetic Phosphorescence Analyzer (Uranium Configuration) [89].

1.3.1.9 Calculation of uranium concentration

Luminescence intensity decreases exponentially with time. If we considered a U_0^* population of uranyl phosphate have reached the excited state. The velocity of decrease in this population with time t is [88, 89]:

$$-\frac{dU_t}{dt} = (k_p + k_q) t \quad (1.8)$$

by integration and linearization Eq. (1.8)

$$\ln U_t^* = \ln U_0^* - (k_p + k_q) t \quad (1.9)$$

Equation 1.9 represents the first order kinetic decay of the excited uranyl complex. U_t^* represents the population of excited uranyl complex at time (t), k_p is the rate constant phosphorescent decay and k_q is the rate constant for all other relaxation processes.

The intensity, I , of the phosphorescence signal is proportional to the concentration of the emitting species, therefore, Eq. 1.9 can be rewritten as:

$$\ln I_t = \ln I_0 - (k_p + k_q) t \quad (1.10)$$

The number of detected photons at any time, t , is proportional to the number of excited uranyl ions. As a result, the least squares fitting of the logarithm of detected intensity versus time-after-pulse yields an intercept proportional to the number of excited uranyl ions. This intercept is independent of nonradiative effects such as quenching. The decay lifetime, τ , is defined as the reciprocal of $k_p + k_q$, which is the time required for the phosphorescent intensity to decrease by the factor $1/e$.

The uranium concentration in the sample U_c is calculated using the following equation [91]:

$$U_c = U_t / (W_a + F_b) \quad (1.11)$$

where U_t is the total uranium, W_a is the aliquant weight in grams and F_b is the dilution factor in 1 gram sample/1 gram dilution.

The percent relative difference (% RD) is calculated by:

$$\% RD = [(U_m - U_r) / U_r] \times 100 \quad (1.12)$$

where U_m , U_r are the measured and reference values, respectively.

1.3.1.10 Spectroscopic properties of uranyl $[\text{UO}_2]^{+2}$

(i) Electronic structure of $[\text{UO}_2]^{+2}$

Minerals of uranium are capable of intrinsic luminescence, which is connected with uranyl ion $[\text{UO}_2]^{+2}$ emissions. Uranyl is formed due to σ and π bonds of $5f$, $6d$ and $7s$ electrons of the uranium atom and $2p$ electrons of two oxygen atoms. Molecular orbitals of uranyl are formed by the interaction of atomic orbitals of uranium and oxygen with the same type of symmetry and close energy levels. Bonding orbitals $1\sigma_u$, $1\sigma_g$, $1\pi_u$, $1\pi_g$ are filled with electrons with antiparallel spin directions. Nonbonding orbitals $1\sigma_g^*$, $1\sigma_u^*$, $1\pi_g^*$, $1\pi_u^*$ and so on are empty and form excitation levels. The ground state of uranyl is $1\Sigma_g^+$, which is a singlet with summary spin 0 and a center of symmetry. The excited state of uranyl is split. It has levels of different symmetry types A_{2g} , E_{2g} , A_{1g} and so on. These levels are split, in their turn, due to electron-phonon interaction forming a system of vibrational sublevels owing to vibration of oxygen atoms in uranyl. Absorption of photon by uranyl results in electron transition from the upper filled orbital $1\pi_g^4$ to one of excited levels of empty orbitals $1\delta_u$ and $1\phi_u$ with vibrational sublevels. Electron transition in the opposite direction results in the emission of photon. Its energy is about $k_0 \approx 2 \times 10^4 \text{ cm}^{-1}$. This is a zero-phonon electron transition [92]. Its peak is accompanied by a series of electron-phonon lines, Figure 1.9. A feature distinguishing the molecular excitation and luminescence spectra of $[\text{UO}_2]^{+2}$ is the fact that they arise from the transitions between electron-vibrational levels [93].

The $[\text{UO}_2]^{+2}$ always exhibits comparably long decay times in the range of 60 – 600 μs [92].

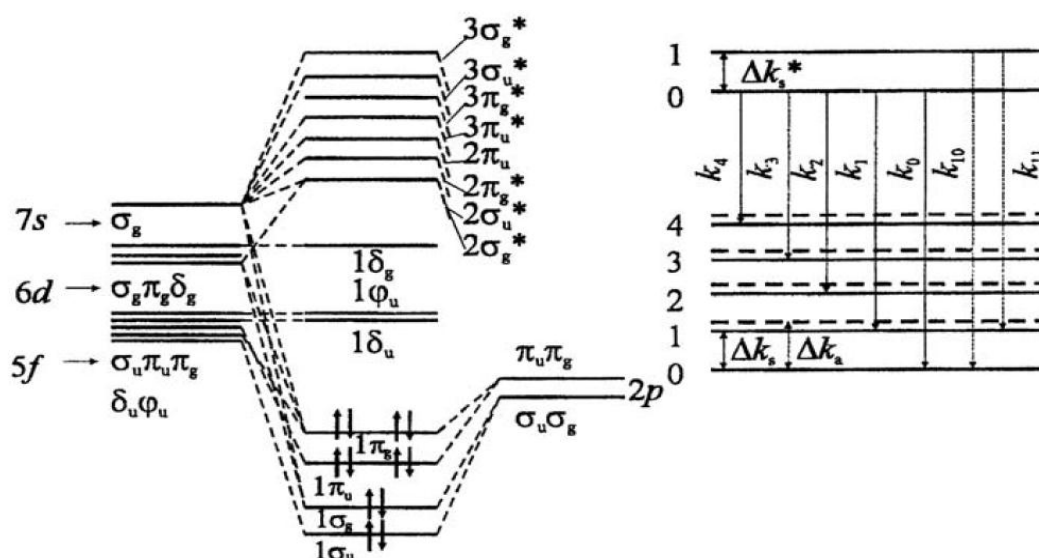


Figure 1.9 Molecular orbitals scheme of UO_2 [93].

(ii) UV-VIS absorption spectrum of uranyl ion

The UV-VIS absorption spectrum of the free uranyl ion is given in Fig. 1.10 in the range 220 nm to 500 nm. The spectrum shows a weak absorption band in the range 480 nm and 330 nm with a characteristic fine structure as well as a nearly continuous spectrum beyond 330 nm without characteristic features. Above 480 nm no further absorption band was observed [94].

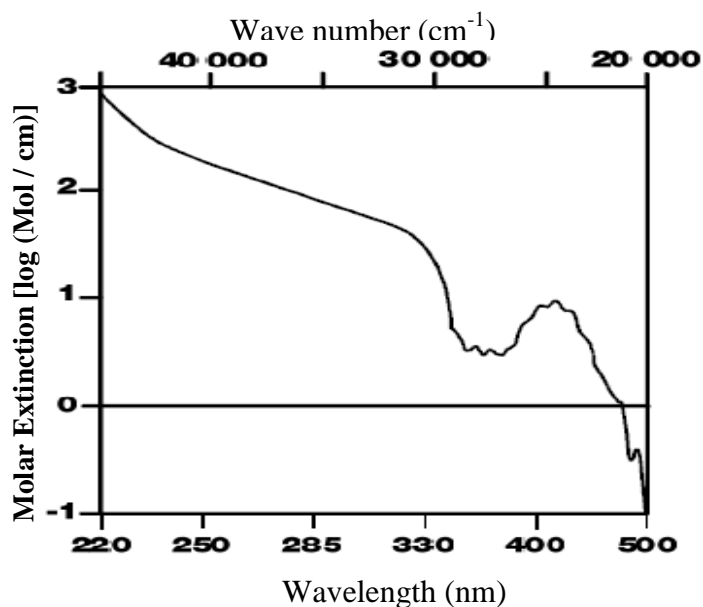


Figure 1.10 UV-VIS spectrum of free uranyl (VI) ions in the range 220 to 500 nm [94]

The characteristic fine structure of the low energy absorption spectrum consists from a nearly regular sequence of bands [95], resulting from coupling of electronic transitions with symmetric stretching vibration of the uranyl (VI) group [96]. This part of the UV-VIS spectrum is shown in Fig. 1.11. The absorption maximum is found at 413.8 nm and a molar extinction coefficient of 9.7 ± 0.2 l/mol.cm.

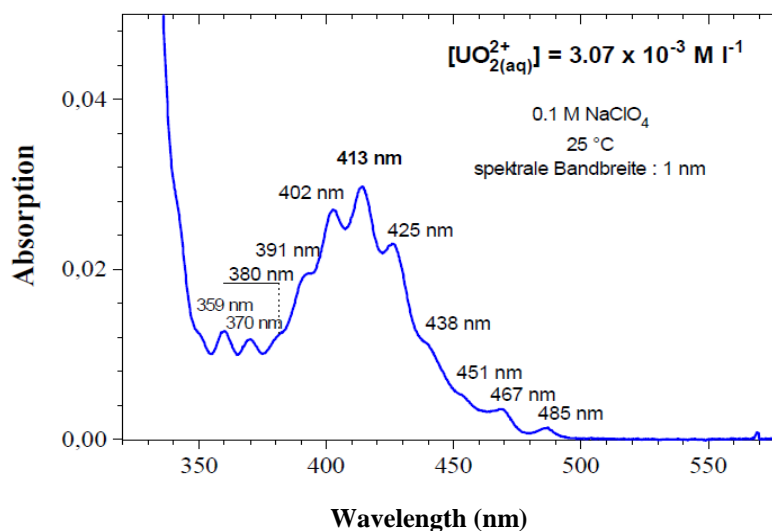


Figure 1.11 UV-VIS spectrum of free uranyl ion in 0.1 N NaClO₄ [95]

(iii) Emission Spectrum

Due to the luminescence emitted by the uranyl (VI) ion by its electronic decay from an electronically excited state, the uranyl ion was considered a ‘model case of inorganic photochemistry’ [94].

The emission spectrum of a 100 µg/l uranyl aqueous solution is given together with its absorption spectrum is shown in Fig. 1.12, with a 2.5 nm band-pass for both spectra. Figure 1.12 (b) shows the characteristic uranyl emission peaks at 494, 515, 540, and 565 nm. The excitation and emission wavelengths for the kinetic phosphorimetric analysis are determined on the basis of these spectrums. The dye selected for the excitation wavelength was stilbene-420, at a concentration of 1.8×10^{-3} M in methanol. At this concentration, the lasing maximum is at about 425 nm. The interference filter used for the photoluminescence detection matches the emission maximum of $[\text{UO}_2]^{+2}$ at 515 nm, with a 10 nm band-pass [90].

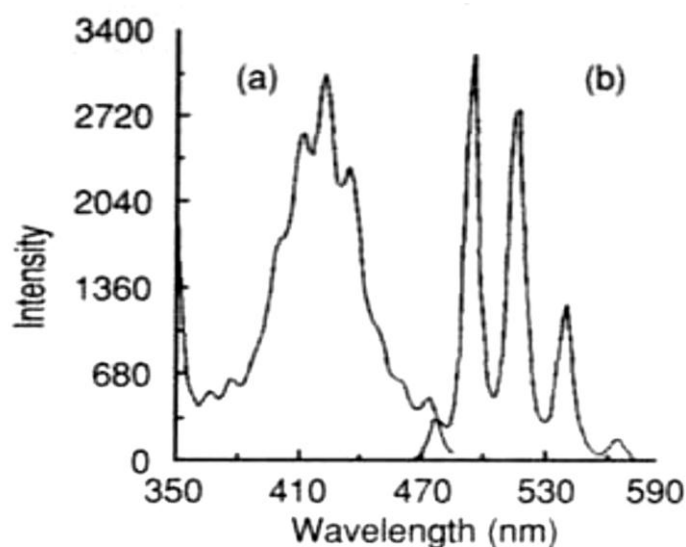


Figure 1.12 (a) Excitation spectrum (b) Emission spectrum of a 100 µg/l uranyl aqueous solution [90]

Under excitation by ultraviolet and visible radiation, many uranium compounds phosphoresce with emission of a characteristic green light [97,98]. The hexavalent uranium present as the uranyl ion $[\text{UO}_2]^{+2}$ is believed to be responsible for the long-lived (10^{-3}) luminescence at room temperature, with uranium in other valences being essentially nonluminescent [99]. In solution, however, the uranyl ion must be protected from quenching in order to observe the long lifetimes [99]. This can be accomplished by complexing $[\text{UO}_2]^{+2}$ with a substance such as phosphoric acid, which yields phosphorescence lifetimes for $[\text{UO}_2]^{+2}$ of a few hundred microseconds [100].

The photoluminescent emission of the uranyl ion has long been used for the determination of trace quantities of uranium [97,99]. The conventional fluorometric method of uranium analysis consists of obtaining a pellet from the uranium sample by fusion with sodium fluoride in a platinum crucible [101, 102]. The chemical separation required before performing the analysis of certain samples, and the strictly regulated conditions for sample preparation make this method marginal for quality analysis. Two major factors limit the precision and accuracy of quantitative photoluminescence measurements of $[\text{UO}_2]^{+2}$ in solutions of real samples. First, the fluorescence from organic components in the samples, with typical lifetimes of 10^{-9} s,

may be superimposed on the long-lived uranyl phosphorescence, thus interfering with the uranium determination [98]. Secondly, species present in the real samples can quench the uranyl luminescence by deactivating the excited state through several possible non-radiative paths [103, 104]. Pulsed-source phosphorimetry has the potential to circumvent these problems, because of the advantages that this technique has over conventional phosphorimetry. First, the greater selectivity between short- and long-lived phosphors possible with time-resolved luminescence techniques can eliminate the problem of interference from fluorescing species present in the aqueous sample. Secondly, the higher signal-to-noise ratio in the pulsed-source time-resolved measurements allows for large dilutions of the original sample to reduce matrix effects (e.g. color, quenching).

1.3.1.11 Lifetime

Lifetimes are temperature dependent, decreasing as temperature increases. For uranium, lifetimes shorter than 100 μs occur when acidity exceeds two molar. Uranium lifetimes in samples are usually shorter than 350 μs . At lower acidities, Uraplex (superior uranium complexant) typically provides lifetimes over 250 μs . Uraplex improves the resistance of uranyl phosphorescence to quenching [88 – 90].

1.3.1.12 Interferences

The development of assays for uranium through kinetic phosphorescence analysis demands the consideration of several interferences issues to maximize the sensitivity and selectivity. These include the following:

(i) Absorption or inner filter effects

Colored solutions may attenuate the excitation beam and/or the emission signal and cause low results. Yellow solutions, e.g., chromate, will absorb the excitation light at 420 nm. The emission at 515 nm is used for

analysis by the KPA and low results will be caused by substances that absorb in the green region [88 – 91].

(ii) Quenching agent

The excited state might interact other species present in the samples to provide competitive nonradiative decay pathways. For uranyl luminescence, reducing agents such as alcohols, halides (except fluoride), biological substances and oxidizable such as silver, iron II, lead, manganese II and thallium are strong quenching agents [88 – 91].

(iii) Fluorescence

Proteinaceous and polyaromatic compounds may fluoresce strongly, depending partly on concentration. Strong fluorescence may excite the KPA optics. The result is phosphorescence which positively interferes, and is easily detected as curved decay and/or unusually long lifetimes [89, 90].

(iv) Turbidity by particles

Particles suspended in the sample cell will strongly reflect and scatter the laser beam, which will cause excitation of the optics and subsequent interfering phosphorescence [89, 90].

(v) Competing reactions

Nonradiative processes compete with uranyl phosphorescence. The uranyl ion must be protected from various intermolecular mechanisms. Complexation fulfills this need, and examples of effective agents are polyphosphates and Uraplex [88, 89].

Typically, the presence of spectral interferences can be determined by examining the decay curve obtained from Eq. 1.10. These potential interferences can overcome using a variety of samples pretreatment processes. The appropriate samples pretreatment process will be discussed in the next chapter.

1.3.2 Solid state nuclear track detectors SSNTD's

Solid state nuclear track detectors are insulating materials have the capabilities for measuring concentration and spatial distribution of isotopes if they emit heavy nuclear particles, either directly or as a result of specific nuclear reactions [105].

The damage of these particles along their path is called track (latent track), may become visible under an ordinary optical microscope after etching with suitable chemicals [106].

The solid state nuclear track detectors are formed in a variety of materials which is fall into two main categories: inorganic solids such as crystals and glasses, and organic solids such as polymers. These types differ in their sensitivity which increases with increasing of incident particle atomic number. Some of commonly used SSNTD's are given in Table 1.5 .

Table 1.5 Commonly used SSNTD's materials [107]

Detector		Atomic composition	General etching conditions	Least ionizing ion seen
Inorganic materials	Quartz	SiO ₂	KOH Soln., 210 °C, 10 min	100 MeV ⁴⁰ Ar
	Muscovite Mica	Kal ₃ Si ₃ O ₁₀ (OH) ₂	48% HF, 23°C, 3 sec - 40 min	2 MeV ²⁰ Ne
	Silica Glass	SiO ₂	48% HF, 23°C, 3 sec	16 MeV ⁴⁰ Ar
	Flint Glass	18SiO ₂ :4PbO:1.5Na ₂ O:K ₂ O	48% HF, 23°C, 3 sec	2-4 MeV ²⁰ Ne
Organic materials	Bisphenol A-polycarbonate (Lexan, Makrofol)	C ₁₆ H ₁₄ O ₃	6 N NaOH, 60°C, 60 min	0.3 MeV ⁴ He
	Cellulose Nitrate (Daicell, LR-115)	C ₆ H ₉ O ₉ N ₂ (CN)	3-6 N NaOH, 50°C, 40 min	0.5 MeV H
	Polyallyl Diglycol Carbonate (CR-39)	C ₁₂ H ₁₈ O ₇ (CR-39)	6 N NaOH, 60°C, 1-6 hrs.	1 MeV H

Nuclear track detection is an excellent tool for making inexpensive *in situ* measurement, the activity and distribution of such alpha emitting radionuclides like radium, radon, and uranium can be determined [108].

1.3.2.1 Track formation mechanism

Operation of the solid state nuclear track detector is based on the fact that a heavy charged particle will cause extensive ionization of the material when it passes through a medium. It produces narrow trails damages at the level of molecular band along their trajectory. Nuclear tracks formed by heavy ions are very small (only about 10 nm in diameter) [109]. As a result of the excitation and ionization of atoms a latent track will formed. There are two different mechanisms exist for the production of damage trails, i.e., formation of latent tracks in solids. In crystals, the latent tracks consists of atomic displacements (ion-explosion spike model) whereas in plastic materials the damage is due to broken molecular chains which produce free radicals [110, 111].

1.3.2.2 Track effecting parameters

The development of a particle track is the resulting effect of two important factors; the track etch rate velocity V_T and the bulk etch rate velocity V_B .

1.3.2.3 Bulk etch rate velocity (V_B)

The bulk etch rate V_B is the rate of chemical etching of the undamaged surface. It is defined as the thickness that is etched out from one of the surfaces of the detector as per time as a result of chemical etching effect [112]. It depends on the construction of the plastic, the constituents of the etching solution, its concentration and temperature [113].

1.3.2.4 Track etch rate velocity (V_T)

The track etch rate V_T is defined as the linear rate at which the detector material is chemically etched out along the particle trajectory, i.e. it measures the amount of the removed layer of the detector along the incident particle trajectory per unit of etching time [110]. The track etching V_T is both a material and particle parameter. It depends on the detector type, the material structural homogeneity and isotropy, etching conditions, and the energy loss

of the incident particle. Experiments prove that V_T increased with increasing the rate of ionization for different organic and inorganic detectors [113, 114].

1.3.2.5 The chemical etching

Ionizing particles passing through polymeric track detectors produce latent track, which are trails of radiation damage. The best means of observing the tracks is by etching the SSNTDs material with a chemical solution, which preferentially attacks the damaged material and enlarges the original track to a size, which is visible in the optical microscope [115].

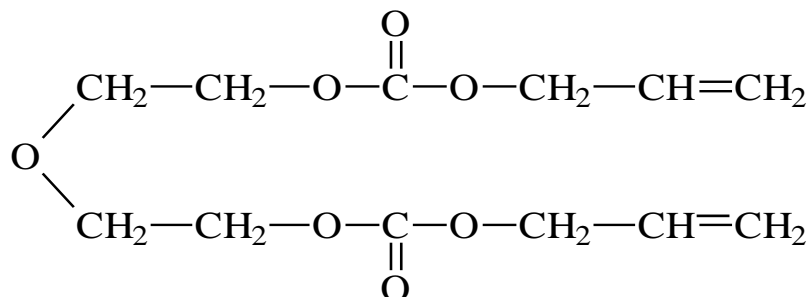
Essentially etching takes place via rapid dissolution of the disordered region of the track core, which exists in a state of higher free energy than the undamaged bulk material [111]. The reagent must be capable of slightly etching the bulk material, while at the same time preferentially attacking the particle damage trails. In fact the radiation damage trails produced by charged particles, consist of disordered structure which in turn are associated with a large free energy. They therefore, represent a region of enhanced chemical activity. These regions get preferentially dissolve and their dimensions are enlarged when they are brought in contact with an etching solution.

The etching conditions are optimized empirically for each detector material [116]. In general, etchants for polymeric detectors are frequently solutions of alkali hydroxides such as NaOH or KOH with 1 – 12 M at 40° – 60° C [117]. For glasses and minerals, crystals such as quartz, mica, and certain pyroxenes are etched in aqueous solutions of acids such as HF with ~ 48% concentration at 20 °C [118].

1.3.2.6 CR-39 track detector

Polyallyl diglycol carbonate (PADC) which is generally referred as CR-39 the most sensitive of the nuclear track recording plastics [119]. The chemical form of CR-39 is $C_{12}H_{18}O_7$. This plastic detector is made by

polymerization of the oxydi-2, 1-ethanediyl, di-2-propenyl ester of carbonic acid. It contains two of monomer ally functional groups [$\text{CH}_2 = \text{CH} - \text{CH}_2 -$] and has the following structure:



It has the unique properties of being inert to light, x-ray, and gamma and beta radiation, but reactive with alpha particles. CR-39 detectors are widely used in different branches of sciences such as nuclear and fission physics, charged-particle radiography, radon dosimetry and radiobiological experiments.

The general characteristics of CR-39 can be summarized as [120]:

1. Amorphous polymer.
2. Optically clear.
3. Environmentally very stable.
4. Having a closed packed and uniform molecular structure.
5. Having non-solvent chemical etchant.
6. Highly cross-linked thermoset.
7. Sensitive to heavy ion damage $Z/\beta > 10$ where β is the ratio of particle velocity to the velocity of light.

1.3.2.7 Fission track analysis

When a neutron enters the nucleus of ^{235}U , the atom splits or fissions into two more or less equally massive smaller atoms 'fission fragments' which move apart at high velocities. When a fission fragment passes through solid

state nuclear track detectors it breaks down the crystal lattice or molecular structure of the material along its path, producing a “fission track” [107].

Since the fraction of ^{235}U in natural materials is a constant, therefore if sample containing uranium is placed in contact with a detector material and irradiated with thermal neutrons in a nuclear reactor and etching the detector surface, the number of fission tracks appearing in the detector material will depend only on the concentration of uranium in the sample material. If a standard of known uranium concentration is irradiated at the same time, the concentration of uranium in the sample material similarly treated can be calculated by simple proportionality [121].

For solid samples analysis, it is usually to place SSNTD's surfaces against them and to irradiate, etch and determine under a microscope the density of tracks (ρ) (i.e. the number of tracks per square centimeter) in the SSNTD's opposite the sample.

$$\frac{[\text{U}] \text{ sample}}{[\text{U}] \text{ standard}} = \frac{\rho \text{ sample}}{\rho \text{ standard}} \quad (1.13)$$

The same technique can be used in the analysis of liquids [122,123], but it is usually more convenient to evaporate the measured drops of a liquid sample on the detector surface, irradiate, etch, and determine the uranium concentration C (in $\mu\text{g/l}$). The following relationship applies [124, 125]:

$$C = (TW_t)/VG\sigma N_A \dot{\Gamma} \eta \quad (1.14)$$

where T is the total number of tracks formed; W_t , the atomic weight of the of uranium isotope ^{238}U ; V , the volume of the drop in milliliters; G , the fraction of the fission events which produce tracks in the detector; σ , the fission reaction cross section (4.2×10^{-24}) cm^2 , N_A the Avogadro's number (6.023×10^{23}); $\dot{\Gamma}$, the total thermal neutron dose in neutrons/ cm^2 ; and η , the etching efficiency factor.

1.4 Review of previous studies

Many studies have been performed to investigate and measure the uranium concentration in urine samples using several techniques. Below we state a summary for some of these studies according to the technique used.

1.4.1 Fission track analysis (FTA)

The trace concentration of uranium in smokers and non-smokers normal human urine was determined by Chakarvarti et al., 1980 [126] using fission track etching technique. Results indicated heterogeneous distribution in both types with levels spread uniform ranging from $(0.9 - 6.5) \times 10^{-3} \mu\text{g/l}$ and in the non-uniform part $(0.14 - 1.0) \times 10^{-3} \mu\text{g/l}$ forming 10 – 52% of the overall contents of the order $(1.2 - 7.1) \times 10^{-3} \mu\text{g/l}$. Igarashi et al., 1985 [127] determined uranium concentrations in several human tissues (lung, liver, kidney, muscle, spleen, heart, cerebrum and bones) from Japanese in Tokyo area using fission track method. This paper showed that the highest average uranium content was in lung $1.70 \mu\text{g/l}$ and then the tissue of each of bone, heart, muscle, kidney, liver, cerebrum and spleen which reached $(0.85, 0.49, 0.43, 0.34, 0.24, 0.15, 0.13 \mu\text{g/l})$ respectively. In 1993, Cheng et al. [128] estimated the uranium contents of beverages and mineral water using fission track analysis technique with polycarbonate detector. The uranium content in beverages was varying from 0.26 ± 0.03 to $1.65 \pm 0.07 \mu\text{g/l}$, the average value was $0.93 \pm 0.05 \mu\text{g/l}$. The mean uranium content in mineral water is $9.20 \pm 0.16 \mu\text{g/l}$, which was approximately 10 times higher than the mean uranium content of beverages. Ciubotariu et al., 1997 [129] studied the uranium bio-distribution in animals contaminated by ingestion using fission track method. Two rats of Wistar-London breed were contaminated at once and after different time intervals, 3 days and 10 days respectively, they were sacrificed. Uranium bio-distribution has been investigated in the vital organs as well as the uranium

retention and elimination. The concentrations of depleted uranium in human blood and tissues for Iraqi subjects were measured by Al-Timimi., in 2000 [130] using fission track method with CR-39 nuclear track detector. The concentrations ranged between 41 – 73 $\mu\text{g/l}$ in the blood and 39 – 46 $\mu\text{g/l}$ in the tissues. In 2003, Singh et al., [131] made a comparison between fission track and laser fluorometry techniques for uranium analysis in water sample. The fission track technique was used for the estimation uranium content. The result showed high values of uranium content in some samples. All samples were reanalyzed using laser fluorometry technique in order to confirm the results. A comparative analysis of the results obtained from these two different techniques observed that the laser fluorometry technique is more suitable for analysis of the water samples having high uranium content than fission track technique. Al-uboode., 2006 [132] determined the variation of alpha emitters concentrations in urine samples of occupational and non-occupational persons in Iraq using PM-355 solid state nuclear track detector (SSNTD). The concentrations of alpha emitters in the urine samples ranged from 0.77 mg/l to 2.87 mg/l. In 2009, Sawant et al. [133] used fission track technique to estimate the trace levels of plutonium in urine samples. Chemically separated plutonium from the samples and a plutonium standard were electrodeposited on planchettes and covered with Lexan solid state nuclear track detector (SSNTD) then irradiated with thermal neutrons. The fission track densities in the Lexan films of the sample and the standard were used to calculate the amount of Pu in the sample.

1.4.2 Kinetic phosphorescence analysis (KPA)

Kinetic phosphorescence analysis (KPA) has been utilized for uranium determination in urine samples. This technique is rapid and accurate with a detection limit of 0.005 $\mu\text{g/l}$ for uranium. However, Moore and Williams, [134] presented a rapid procedure for determining total uranium in urine using a laser-induced kinetic phosphorescence analyzer (KPA). The achieved

detection limit was of 0.006 $\mu\text{g/l}$. For accuracy demonstration six sets of urine samples were prepared, each set consisting of two unspiked samples and four spiked samples. Five laboratories took part in the comparison using methods KPA, alpha spectrometry and fused pellet fluorometry. The results of the KPA method compared to be very well with the results of the other laboratories and with the known added amount. In 1992, Brina and Miller [88] used KPA for assay of uranium in biological, environmental and geological samples. Background urines showed uranium content between 0.015 and 0.045 $\mu\text{g/l}$. The relative standard deviation RSD ranged between 2 – 12 % . Samples from uranium workers had up to 9.38 $\mu\text{g/l}$ of uranium, while RSD values from 2.2 to 8.4% were observed. The larger RSD values obtained in some of the results was likely caused by spattering during the wet-ashing procedure. Urine samples were spiked with known amounts of uranium, to determine the recovery of uranium. The concentration of uranium in the urine samples after these additions varied from 0.056 to 107.96 $\mu\text{g/l}$. The recoveries were generally within the RSD of 100%. A year later, these authors demonstrated the sensitivity of kinetic phosphorescence analysis method for determination of trace levels of uranium and lanthanide elements in a variety of samples of environmental, geological, and biological interest, in the sub-microgram per liter concentration range [90]. Uranium in urine samples of Hanford UO_3 plant workers ranged from 0.015 to 0.03 $\mu\text{g/l}$. In 1997 Hedaya et al., [135] had presented specific, precise and accurate method for the determination of uranium in biological samples utilizing kinetic phosphorescence analysis. The assay calibration curves were linear and covered the range of uranium concentrations between 0.05 $\mu\text{g/l}$ and 1000 $\mu\text{g/l}$. Then the method was used to quantify uranium in different tissue samples obtained over a period of 90 days following a single intraperitoneal uranium dose of 0.1 mg/kg in rats. A year later, Sowder et al., [136] examined the influence of cations, anions and ligands common to natural

water, process and bioassay samples on the quenching of uranyl phosphorescence and the consequences for lower limits of detection and accuracy of measurements of trace uranium concentrations in aqueous solutions using kinetic phosphorimetry method. The potential health risk associated with chronic exposure to depleted uranium was conducted by Pellmar et al., [137] using KPA technique. Sprague Dawley rats were surgically impacted with depleted uranium pellets at three dose levels (low, medium, high). At 1 day and 6, 12, and 18 months after implantation, uranium levels were measured. At all-time points, uranium concentrations in kidney and bone (tibia and skull) were significantly greater than the control group. Significant concentrations of uranium were excreted in the urine throughout the 18 months of the study ($224 \pm 23 \mu\text{g/l}$ urine in low-dose rats and $1010 \pm 87 \mu\text{g/l}$ urine in high-dose rats at 12 months). Many other tissues (muscle, spleen, liver, heart, lung, brain, lymph nodes and testicles) contained significant concentrations of uranium in the implanted animals. From these results, they concluded that kidney and bone were the primary reservoirs for uranium redistributed from intramuscularly embedded fragments. In the same year Miller et al., [138] used kinetic phosphorescence analysis technique for determination of uranium and in urine and serum samples obtained from rats implanted with either depleted uranium or tantalum pellets. In this mutagenicity testing authors studied the relationship between urine uranium levels and mutagenic potential. The data indicated that urine mutagenicity is correlated with increased urine uranium content. Thomas and Gatei, [139] studied the radionuclides concentration ratios in the lichen-caribou-human food chain near uranium mining operations in northern Saskatchewan, Canada. Uranium was determined by either KPA or mass spectroscopy. Uranium was detectable in feces $97 \mu\text{g/l}$, blood $4.8 \mu\text{g/l}$, and liver $2.3 \mu\text{g/l}$. All samples of rumen (stomach) contents and fur and most samples of bone, kidney, and muscle were below detection limits. Uranium in parts per billion

was converted to becquerel per kilogram by multiplying by 0.0252 to account for the activities of ^{235}U , ^{234}U , and ^{238}U in naturally occurring uranium to cancer risk from these doses. Optimal sample preparation conditions for the determination of uranium in biological samples by kinetic phosphorescence analysis presented by Ejnić et al., [140]. The recovery of uranium in urine samples was $99.29 \pm 4.02\%$ between spiked concentrations of 1.98 – 1980 ng 0.198 – 198 $\mu\text{g/l}$ uranium, whereas the recovery in whole blood was $89.99 \pm 7.33\%$ between the same spiked concentrations. The limit of quantification in which uranium in urine and blood could be accurately measured above the background was determined to be 0.05 and 0.6 $\mu\text{g/l}$, respectively. McDiarmid et al., 2000 [141] studied the health effects of depleted uranium on exposed gulf war veterans using kinetic phosphorescence analysis technique for uranium concentration measurements. Finneran et al., 2002 [142] investigated the multiple influences of nitrate on uranium solubility during bioremediation of uranium contaminated subsurface sediments, where dissolved U(VI) in the groundwater was quantified via kinetic phosphorescence analysis. Two years later, McDiarmid et al., [143] studied the health effects of depleted uranium on exposed Gulf War veterans as ten years follow-up using kinetic phosphorescence analysis technique for uranium concentration measurements. Lestaevel et al., [144] studied changes in sleep–wake cycle after chronic exposure to uranium in rats. Uranium content measurement obtained using kinetic phosphorescence analysis. The authors found that after over 90-days exposure period, amounts of uranium increased significantly in the brain (from 75.4 ± 0.6 to 86.1 ± 4.1 ng) and kidneys (from 101.9 ± 4.0 to 579.0 ± 85.5 ng) as compared with control group. Monleau et al., [145] adopted a biokinetic models for rats exposed to repeated inhalation of uranium for the monitoring of nuclear workers implications. Animals were divided into two groups, exposed and clean air group. The first group was

repeatedly exposed by inhalation for one hour to UO_2 with an aerosol concentration of 190 mg/m^3 , (lung intake around $200 \text{ }\mu\text{g}$), twice a week for three weeks (7 inhalations). Uranium content has been determined in daily urine and faeces and lung tissue of sacrificed rats after 1, 3, 6, 15 and 30 days from the end of the repeated exposure using kinetic phosphorescence analysis. Kinetic phosphorescence analysis has been used by Humaid et al., [146] for determination of uranium concentration in ore and reference solid samples after radiochemical separation. The extraction of uranium was carried out with recovery percentage of more than 80%. Urine and water samples spiked by uranium were also investigated for quenching testing. Detection limit as low as $0.004 \text{ }\mu\text{g/l}$ was obtained.

1.5 The aim of study

The main purpose of the present work is to develop a procedure for quantitative determination of uranium concentrations in urine samples using laser-induced kinetic phosphorescence analysis (KPA). Moreover it aims to determine uranium concentrations in urine samples of residents of selected areas in Iraq using KPA. Some important parameters are considered, namely; age, gender, employment duration, and smoking habits. The results were compared with those measured using fission track analysis (FTA) with CR-39 solid state nuclear track detectors (SSNTD's). The evaluation of each technique is extensively investigated.

Chapter Two

Materials and Methods

This chapter describes the use of two methods for determination of uranium concentrations in human urine samples. A brief description for the regions of interest will also be given to explain the reasons of chosen these regions in the present study. The operation principle of apparatus and the materials used are included. Two main sections will be presented in this chapter: the first is the experimental procedure using kinetic phosphorescence analyzer and the second is about the sample preparation, irradiation process and track density measurements using SSNTD's.

2.1 The study regions of interest:

2.1.1 Akashat phosphate mine (A.M)

Phosphate raw materials appear in Iraq in the configurations Cretaceous and Eocene and Paleocene, these geological formations are:

1. Dukma formation (Mastrichtian)
2. Akashat formation (Paleocene)
3. Rutba formation (Eocene)

The most important of these formations is Akashat phosphate layer thickness of up to ten meters in which the proportion of phosphorus pent-oxide P_2O_5 is between 21-22 %.

Akashat mine is located in the western desert at Akashat region sites about 150 km southwest of Al-Qaim, Fig. 2.1. Akashat arises about 600 meters above the sea level, a flat land interspersed with some valleys and hills with no underground water being waged in the region.

2.1.2 Al-Qaim fertilizer complex (Q.F.C)

This complex consists of a set of integrated and interrelated plants, Fig. 2.2B, to produce chemical fertilizers as a final product, these plants are:

1. Ore beneficiation plant (U100)
2. Sulfuric acid plant (U200)
3. Phosphoric acid plant (U300)
4. Fertilizers plants (U400)

Phosphate rock is the most suitable alternative source of uranium. The average uranium concentration in Iraqi phosphate rock is estimated to be about 72 ppm [147]. Several processes have been developed for the recovery of uranium from phosphoric rock. The DEPA/TOPO process, which is based on solvent extraction, using di(2-ethylhexyl) phosphoric acid and trioctyl phosphine oxide as extractants [148].

In this phosphate production site, Unit 340 existed to extract uranium from H_3PO_4 via a DEPA/TOPO solvent extraction process. The final product was yellowcake (refined uranium compounds) which was sent to Al-Jesira site. Unit 340 was destroyed during the 1991 war and never restarted operations.

2.1.3 Al-Jesira site (J)

Al-Jesira site played a pivotal role in the Iraqi former uranium enrichment program. It received yellowcake from Unit 340 plant at Al-Qaim phosphate fertilizer facility. At Al-Jesira site, the yellowcake was further processed to produce uranium dioxide UO_2 and uranium tetrachloride UCl_4 . These uranium compounds were used as feedstock for enrichment processes at other locations in Iraq. This site was bombed during the 1991 war and the UO_2 plant was totally destroyed. Most of the equipments were lost during the looting events in 2003. The majority of materials and contaminated

equipments were moved and buried on a mountain side near the village of Adaya. The aerial photograph of this site is shown in Fig. 2.2D.

The three large concrete waste ponds still exist. In the present time, some of the administration structures have been occupied by local residents. Five of the occupied structures were being used as residences. The remaining five occupied buildings were being used to store household materials and to house livestock and fowl.

2.1.4 Adaya remediation site (A)

Adaya site is a very large burial ground on a gradually sloping mountain side. This site is located at 50 km to the west of Mosul city. After the 1991 war, destroyed equipment, concrete rubble and miscellaneous solid wastes were trucked to this burial site near the village of Adaya (about 4 km north) and Tall Al-Ragrag (about 3 km west), and about 35 km west of Al-Jesira. The materials were dumped into excavations in the soil and subsequently covered. Most of the equipment and rubble contained uranium compounds as yellowcake, ammonium diuranate ADU $(\text{NH}_4)_2\text{U}_2\text{O}_7$, UO_3 and UO_2 .

The site was likely chosen because it has deep soil deposited as alluvium from the upper slopes of the mountain ridge. The terrain is gently rolling hills separated by deeply carved ravines resulting from water runoff resulting from periodic rains. The trenches converge upon a main drainage channel that flows westward toward the nearby village of Tall Al-Ragrag. The aerial photograph, Fig. 2.2C, show that water occasionally pools adjacent to the road near the village

As result, people living near; Akashat phosphate mining area, Al-Jesira site, Adaya site, and the workers in Al-Qaim fertilizer complex and Akashat phosphate mine may be exposed to high concentrations of uranium.



Figure 2.1 Aerial photograph of Iraq. The study regions of interest are labeled.

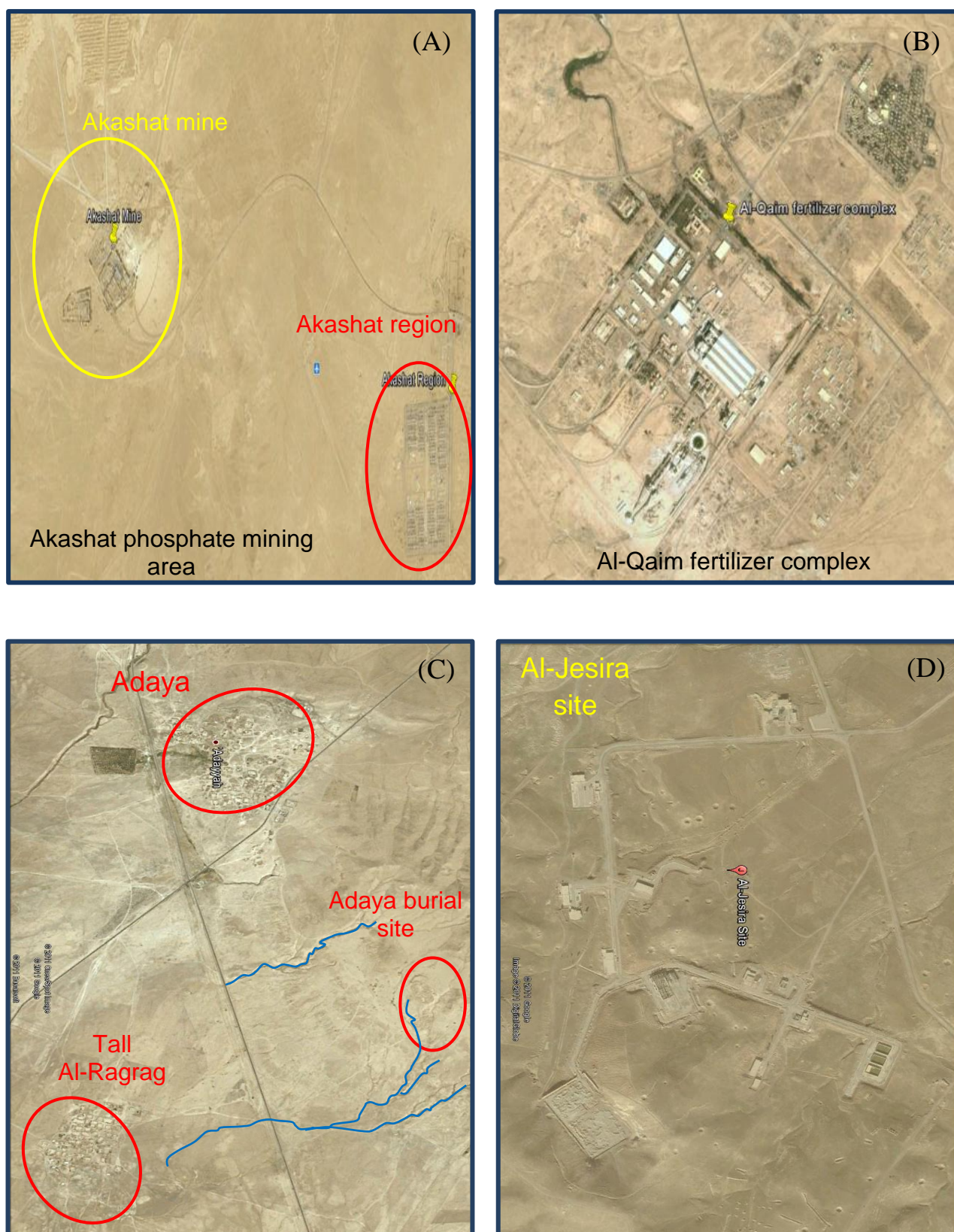


Figure 2.2 Aerial photographs for the study regions of interest, (A) Akashat phosphate mining area, (B) Al-Qaim fertilizer complex, (C) Adaya remediation site, (D) Al-Jesira site.

2.2 Sample collection

A total of 194 urine samples were collected from healthy individual volunteers under normal living habits. Volunteers were from the workers of Akashat phosphate mine, Al-Qaim fertilizer complex, residents of Akashat region, Tall Al-Ragrag village, Al-Jesira village and workers at Al-Qaim hospital.

The subjects were asked to collect urine in extra clean polyethylene containers, then acidified with 0.5 ml HNO₃ (70%). Participants were given instructions on how to collect the samples without contamination (e.g. by using only the clean containers provided). Samples were stored in cool boxes initially, then transported to the research laboratories of Radiation Protection Centre (RPC) and stored in refrigerator at 4 °C until analysis.

Each adult participant were asked to sign informed consent form and record their food and drink consumed and other habits like smoking, before testing. For participants less than 18 years old, the child's assent and the parent's signed consent were obtained. The participant's ages were between 2 and 65 years old, and the average age was 34 years old. These samples were classified according to area of study, gender, age and the employment duration in the following tables.

Table 2.1 Urine samples characteristics of Akashat phosphate mine (A.M) workers

Sample code	Age (Years)	Gender	Work duration (years)	Smoking habit
AM 1	53	Male	24	P
AM 2	41	Male	17	S
AM 3	60	Male	35	N
AM 4	42	Male	18	N
AM 5	40	Male	5	P
AM 6	38	Male	14	S
AM 7	48	Male	14	S
AM 8	54	Male	20	P
AM 9	45	Male	7	S
AM 10	53	Male	17	S
AM 11	55	Male	21	S
AM 12	45	Male	18	P
AM 13	37	Male	15	P
AM 14	45	Male	18	N
AM 15	47	Male	11	P
AM 16	58	Male	15	N
AM 17	50	Male	12	S
AM 18	39	Male	11	N
AM 19	41	Male	11	S
AM 20	42	Male	18	N
AM 21	42	Male	22	N
AM 23	46	Male	20	S
AM 24	43	Male	5	N
AM 25	34	Male	7	N
AM 26	47	Male	19	N

N: Non smoker

P: Past smoker

S: Smoker

Table 2.2 Urine samples characteristics of Al-Qaim fertilizer complex, Beneficiation plant (Unit 100) workers

Sample code	Age (Years)	Gender	Work duration (years)	Smoking habit
U 100	41	Male	18	N
U 101	50	Male	15	N
U 102	48	Male	18	N
U 103	52	Male	8	P
U 104	45	Male	20	N
U 105	46	Male	20	N
U 106	45	Male	19	N
U 107	53	Male	21	P
U 110	42	Male	17	N
U 111	42	Male	16	N
U 112	44	Male	19	N
U 113	52	Male	23	S
U 114	42	Male	20	N
U 115	45	Male	25	N

Table 2.3 Urine samples characteristics of Al-Qaim fertilizer complex, Sulfuric acid plant (Unit 200) workers

Sample code	Age (Years)	Gender	Work duration (years)	Smoking habit
U 200	52	Male	15	N
U 201	43	Male	11	S
U 202	48	Male	6	S
U 206	34	Male	8	N
U 208	35	Male	12	N
U 210	52	Male	15	N
U 211	34	Male	8	N
U 212	31	Male	8	S
U 213	44	Male	21	S
U 214	42	Male	12	N
U 215	57	Male	29	N
U 216	45	Male	13	S
U 217	56	Male	12	S

Table 2.4 Urine samples characteristics of Al-Qaim fertilizer complex, Phosphoric acid plant (Unit 300) workers

Sample code	Age (Years)	Gender	Work duration (years)	Smoking habit
U 300	38	Male	16	N
U 301	41	Male	11	N
U 302	43	Male	20	N
U 303	30	Male	8	N
U 304	57	Male	29	N
U 305	30	Male	4	P
U 306	56	Male	27	P
U 307	40	Male	14	N
U 308	40	Male	10	S

Table 2.5 Urine samples characteristics of Al-Qaim fertilizer complex, Fertilizers plants (Unit 400) and laboratories workers (L)

Sample code	Age (Years)	Gender	Work duration (years)	Smoking habit
U 400	43	Male	18	N
U 401	41	Male	10	S
U 402	43	Male	10	P
U 403	45	Male	17	P
U 404	39	Male	10	N
U 405	45	Male	22	N
U 406	40	Male	8	N
U 407	40	Male	11	N
U 408	46	Male	18	P
L 1	38	Male	12	N
L 2	41	Male	16	N
L 3	39	Male	10	N

Table 2.6 Urine samples characteristics of Akashat phosphate region residents (APR)

Sample code	Age (Years)	Gender	Smoking habit
APR 1	40	Male	N
APR 2	18	Male	N
APR 3	20	Male	N
APR 4	20	Male	N
APR 5	18	Male	N
APR 6	13	Female	N
APR 7	15	Female	N
APR 8	14	Female	N
APR 9	13	Female	N
APR 10	11	Male	N
APR 11	12	Male	N
APR 12	6	Female	N
APR 13	14	Male	N

Table 2.7 Urine samples characteristics of Al-Qaim hospital workers (H)

Sample code	Age (Years)	Gender	Smoking habit
H 1	20	Male	N
H 2	33	Male	N
H 3	20	Male	N
H 4	20	Male	S
H 5	23	Male	S
H 6	22	Male	S

Table 2.8 Urine samples characteristics of Tall Al-Ragrag residents (A)

Sample code	Age (Years)	Gender	Smoking habit
A 001	25	Male	N
A 002	25	Female	N
A 003	30	Female	N
A 004	35	Female	N
A 005	62	Male	P
A 006	50	Female	P
A 007	50	Female	N
A 008	55	Female	N
A 009	40	Female	P
A 010	14	Female	N
A 011	11	Female	N
A 012	40	Female	N
A 013	2	Male	N
A 014	32	Female	N
A 015	51	Female	N
A 016	5	Male	N
A 017	7	Male	N
A 018	6	Male	N
A 019	3	Male	N
A 020	55	Female	P
A 021	13	Male	N
A 022	5	Male	N
A 023	30	Male	N
A 024	40	Male	S
A 025	23	Female	N
A 026	37	Male	N
A 027	48	Male	N
A 028	39	Male	N
A 029	8	Male	N
A 030	29	Male	N
A 031	33	Female	N
A 032	35	Female	N
A 033	40	Female	N
A 034	60	Male	N
A 035	22	Male	N
A 036	28	Male	P
A 037	41	Female	N
A 038	50	Female	P
A 039	40	Female	N

Continuous table 2.8

Sample code	Age (Years)	Gender	Smoking habit
A 040	9	Female	N
A 041	30	Female	N
A 042	60	Female	N
A 043	55	Female	N
A 044	65	Female	N
A 045	50	Female	N
A 046	37	Female	N
A 047	45	Female	N
A 048	18	Female	N
A 049	32	Female	N
A 050	28	Female	N
A 051	30	Female	N
A 052	3.5	Male	N
A 053	3	Male	N
A 054	6	Male	N
A 055	12	Female	N
A 056	9	Female	N
A 057	34	Male	N
A 058	8	Female	N
A 059	7	Female	N
A 060	25	Female	N
A 061	4	Male	N
A 062	23	Female	N
A 063	15	Female	N
A 064	23	Male	P
A 065	16	Male	N
A 066	28	Male	N
A 067	21	Male	N
A 068	22	Male	N
A 069	60	Male	P
A 070	3	Male	N
A 071	19	Male	N
A 072	5	Female	N
A 073	7	Male	N
A 074	35	Female	N
A 075	39	Male	N
A 076	60	Male	N
A 077	36	Male	N

Table 2.9 Urine samples characteristics of Al-Jesira residents (J)

Sample code	Age (Years)	Gender	Smoking habit
J 078	40	Male	N
J 079	40	Male	N
J 080	9	Male	N
J 081	50	Male	N
J 082	9	Male	N
J 083	14	Male	N
J 084	45	Male	N
J 085	12	Male	N
J 086	21	Male	N
J 087	18	Male	N
J 088	12	Male	N
J 089	9	Male	N
J 090	19	Male	N
J 091	42	Female	N
J 092	33	Female	N
J 093	35	Female	N
J 094	20	Female	N
J 095	45	Female	N
J 096	19	Male	N
J 097	53	Male	P
J 098	58	Male	P
J 099	10	Male	N
J 100	60	Female	N
J 101	16	Male	N
J 102	50	Female	N

Table 2.10 Demographic characteristics of the occupational and non-occupational from Akashat phosphate mine and Al-Qaim fertilizer complex

Classification			(number of subjects) n	Percentage %
Place of work				
Beneficiation plant (Unit 100)			14	15
Sulphuric acid plant (Unit 200)			13	14
Phosphoric acid plant (Unit 300)			9	10
Fertilizers plants (Unit 400)			9	10
Laboratories			3	3
Akashat mine			25	27
Akashat residents			13	14
Al-Qaim residents			6	7
Total			92	100 %
Smoking				
Non smokers			58	63
Past smokers			13	14
Smokers			21	23
Total			92	100 %
Employment duration				
	Q.F.C	A.M		
Less than 5 years	1		1	1
From 5 to 10 years	12	4	16	22
From 11 to 15 years	12	8	20	27
From 16 to 20 years	15	9	24	33
From 21 to 25 years	5	3	8	11
Over 25 years	3	1	4	6
Total	48	25	73	100 %
Age (years)				
From 5 to 10			1	1
From 11 to 20			14	15
From 21 to 30			4	4
From 31 to 40			19	21
From 41 to 50			39	43
From 51 to 60			15	16
Total			92	100 %

Q.F.C: Al-Qaim fertilizer complex

A.M: Akashat mine

Table 2.11 Demographic characteristics of the non-occupational from Tall Al-Ragrag and Al-Jesira residents

Classification	(number of subjects)			Percentage %
	n			
Gender	Adaya	Al-Jesira	Total	
Males	36	18	54	53
Females	41	7	48	47
Total	77	25	102	100
Age (years)	Male	Female	Total	
Under 5 years old	6	---	6	6
From 5 to 10	11	5	16	16
From 11 to 20	10	6	16	16
From 21 to 30	10	8	18	17
From 31 to 40	8	13	21	20
From 41 to 50	3	9	12	12
From 51 to 60	5	6	11	11
Over 60	1	1	2	2
Total	54	48	102	100
Smoking	Adaya	Al-Jesira	Total	
Non smokers	68	23	91	89
Past smokers	8	2	10	10
Smokers	1	--	1	1
Total	77	25	102	100

Table 2.12 General demographic characteristics all occupational and non-occupational

Classification	(number of subjects) n	Percentage %
Working or living place		
Beneficiation plant (Unit 100)	14	7
Sulphuric acid plant (Unit 200)	13	7
Phosphoric acid plant (Unit 300)	9	5
Fertilizers plants (Unit 400)	9	5
Laboratories	3	1
Akashat mine	25	13
Akashat residents	13	7
Al-Qaim residents	6	3
Tall Al-Ragrag residents	77	39
Al-Jesira residents	25	13
Total	194	100 %
Gender		
Males	146	75
Females	48	25
Total	194	100 %
Smoking		
Non smokers	149	77
Past smokers	23	12
Smokers	22	11
Total	194	100 %
Age (years)		
Under 5 years old	6	3
From 5 to 10	17	9
From 11 to 20	30	16
From 21 to 30	22	11
From 31 to 40	40	21
From 41 to 50	51	26
From 51 to 60	26	13
Over 60	2	1
Total	194	100 %

2.3 Materials and methods for KPA

2.3.1 Apparatus

The kinetic phosphorescence analyzer model KPA-11 manufactured by Chemchek Instruments (Richland, USA) was utilized for uranium analysis. This instrument is equipped with a pulsed nitrogen/dye laser to supply monochromatic ultraviolet light to excite uranium atoms in the sample solution. The KPA-11 is a fully integrated computerized system for data collection and analysis. Chemchek's KPA Win software controls the KPA-11 along with storing and interpreting the analytical data returned from the KPA.

KPA is equipped with a Gilson 223 sample changer (XYZ robot that can automate sample handling procedures) and 402 syringe pump (auto-sampler dilutor) for mixes 1 ml of standard or sample solution to 1.5 ml of Uraplex and injects 1.9 ml of mixed solution into the KPA's flow cell. Figure 2.3 shows the various component of KPA.

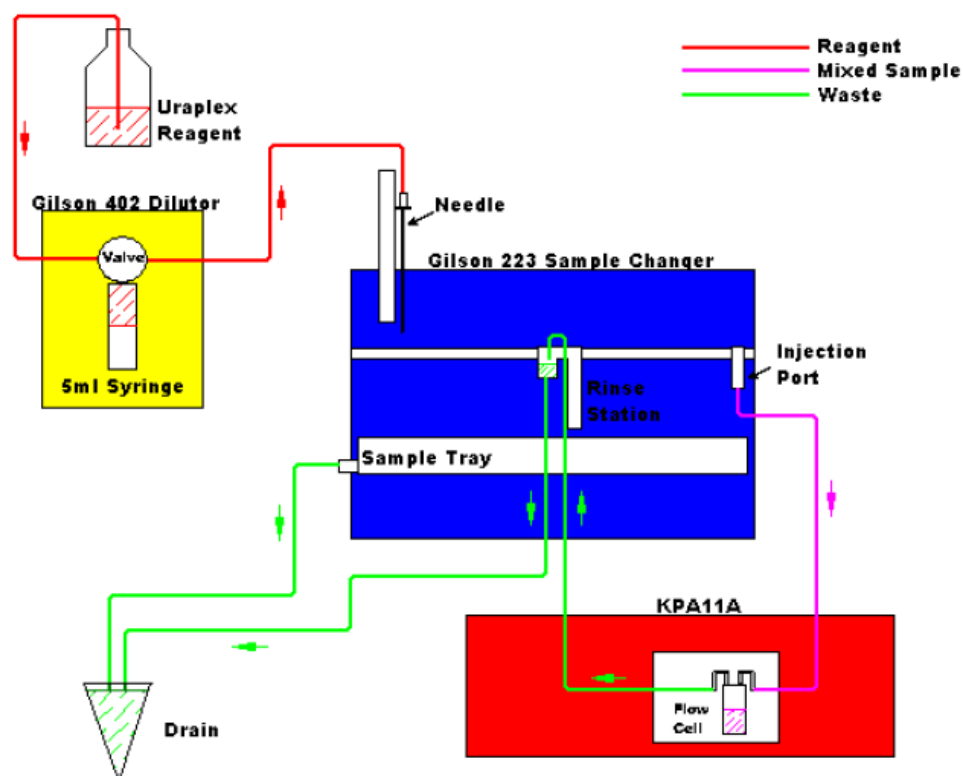


Figure 2.3 Tubing diagram of the Kinetic Phosphorescence Analyzer [89]

2.3.2 Principles and characteristics of the KPA

2.3.2.1 Excitation source

KPA utilizes a pulsed nitrogen laser operating at 337 nm coupled with a Stilbene 420 dye. This provides an excitation wavelength of 420 nm which is close to the uranyl ion absorption maximum of 415 nm [89].

2.3.2.2 Detection system

The light intensity is measured with a photomultiplier tube operated in the photon counting mode to improve signal to noise ratios S/N. The emitted light passes through 515 nm interference filters having a 10 nm band-pass to filter the emission signal and to pass the 515 nm uranium peak [89, 90].

The pulse of light which excites the uranyl complex occurs at time zero, and ensuing luminescence intensity measurements are taken at fixed time intervals after excitation. Each laser pulse triggers a multichannel scaler (MCS) photon-counting sweep of 1.65 ms duration. During this sweep, the signal from the detector is fed into a counting circuit, which is read and reset by the microprocessor. Each successive reading of the counter occurs after a constant interval of time and forms a time gate. A dwell time of 13 μ s per time gate is used, which corresponds to 128 time gates per MCS sweep. The luminescence intensities recorded at each time gate are summed over the number of laser pulses used in the measurement [88].

2.3.2.3 Analytical ranges and detection limit

Kinetic phosphorimetry technique provides for the direct detection of uranium ranged from 1ng/l to 5 mg/l.

The linear response range of electronics and photomultiplier tubes limits the range of concentration that can be determined with optical instruments. In KPA the range has been substantially extended by using apertures to limit signal light. The result is two ranges:

- Low concentration range around 10-15 μ g/l with 1.5875 cm aperture.
- High concentration range with 0.508 cm aperture

This extends the analytical range of the instrument, allowing analysis of concentrated samples that would cause saturation of the detector in the low range [89].

2.3.3 Equipment and glassware

2.3.3.1 Muffle furnace

A muffle furnace of the type “Paragon” was used for sample dry-ashing. It is supplied with “Sentry 2.0” digital temperature controller and four thermocouples, which can operated over range of 25 °C to 1200 °C. However, in sample preparation, the dry-ashing temperature applied in the furnace proves to be one of the major contributing parameters affecting the chemical yield. The optimum conditions are found to be drying at 450 °C for 60 minutes.

2.3.3.2 Analytical balance

A sensitive analytical balance with readability of 0.0001g and maximum weight of 200 g manufactured by Kern & Sohn, DKD calibration laboratory, Germany was used for weight standards.

2.3.3.3 Hot plate

The wet-ashing was carried out using hot plates at 60 °C.

2.3.3.4 Fume hood

Standard and sample preparation was carried inside a fume hood to reduce the exposure to hazardous or noxious fumes.

2.3.3.5 Liquid scintillation vials

Standard 20 ml glass liquid scintillation vials with poly seal liner screw caps were used to contain the samples during processing. Since naturally occurring uranium can leach from glass, all new glassware was soaked in 4 M nitric acid at sub-boiling temperature for 48 h to remove any leachable uranium. The glassware was then rinsed with deionized water and air dried. Plasticware was boiled in deionized water for 48 h and then rinsed and dried to remove potential interference from leachable plasticizers.

In addition, acid dispenser, micropipettes (1000 µl and 100 µl) with disposable plastic tips were used to transfer the reagents and uranium standard solutions to avoid cross-contamination.

2.3.4 Reagents

Because the detection limit of this technique is very low, great care have been taken to avoid uranium contamination from all sources. Reagent grade chemicals contain varying amounts of uranium; a reagent blank was run on the concentrated nitric acid to analyze for the level of uranium. All reagents used were American Chemical Society (ACS) analytical reagent grade unless otherwise specified. Uranium octoxide U_3O_8 was obtained from department of chemistry at College of Sciences and supplied by Johnson Matthey and company limited; UK. Nitric acid HNO_3 and hydrogen peroxide H_2O_2 were obtained from J.T. Baker (Phillipsburg, NJ). Double distilled deionized water used for reagent preparation, glassware cleaning and rinsing and obtained from Al-Dora refinery. The water was analyzed with KPA to ensure that uranium is not present. Uraplex, which was used as complexing agent to enhance the phosphorescence of the uranyl ion in solution, thereby reducing interference and the quenching was also supplied by Chemchek Instruments.

2.3.5 Uranium standard solutions

Uranium standard solutions were prepared using uranium octoxide U_3O_8 . Firstly a stock standard solution of 1000 mg/l (1000 ppm) was prepared by dissolving 117.9 mg of U_3O_8 in 100 ml of 0.82 M nitric acid HNO_3 in volumetric flask. To construct the calibration curve for kinetic phosphorescence analysis two different series of calibration standard were prepared to cover a wide range of uranium concentrations. Uranium concentrations in the first series of standards were (0.05, 0.1, 0.5, 1, 5 and 10 $\mu\text{g/l}$), while that of the second series were (20, 100, 200, 500 and 1000 $\mu\text{g/l}$) and 250 $\mu\text{g/l}$ for reference. These two sets of standards were used to construct the calibration curves for the low and high ranges of uranium concentrations. The two standard series were prepared by further diluting the stock solution in 0.82 M nitric acid HNO_3 to the desired concentration of uranium utilizing the dilution formula:

$$1^{\text{st}} \text{ volume} \times 1^{\text{st}} \text{ concentration} = 2^{\text{nd}} \text{ volume} \times 2^{\text{nd}} \text{ concentration} \quad (2.1)$$

Table 2.13 represents the procedure of preparing uranium standard solutions for the desired concentrations. Uranium standard solutions were stored in glass containers which have been soaked in worm 4 M HNO₃ for 48 h then rinsed with ultrapure deionized water.

Table 2.13 Procedure of preparing uranium standard solutions

Standard concentration	Procedure
High range concentrations	
1000 µg/l (1000 ppb)	0.1 ml of 1000 mg/l diluting with 0.82 M HNO ₃ to 100 ml
500 µg/l (500 ppb)	50 ml of 1000 µg/l diluting with 0.82 M HNO ₃ to 100 ml
200 µg/l (200 ppb)	20 ml of 1000 µg/l diluting with 0.82 M HNO ₃ to 100 ml
100 µg/l (100 ppb)	10 ml of 1000 µg/l diluting with 0.82 M HNO ₃ to 100 ml
50 µg/l (50 ppb)	5 ml of 1000 µg/l diluting with 0.82 M HNO ₃ to 100 ml
20 µg/l (20ppb)	2 ml of 1000 µg/l diluting with 0.82 M HNO ₃ to 100 ml
Reference	
250 µg/l (250ppb)	25 ml of 1000 µg/l diluting with 0.82 M HNO ₃ to 100 ml
Low range concentrations	
10 µg/l (10 ppb)	10 ml of 100 µg/l diluting with 0.82 M HNO ₃ to 100 ml
5 µg/l (5 ppb)	5 ml of 100 µg/l diluting with 0.82 M HNO ₃ to 100 ml
1 µg/l (1 ppb)	1 ml of 100 µg/l diluting with 0.82 M HNO ₃ to 100 ml
0.5 µg/l (0.5 ppb)	0.5 ml of 100 µg/l diluting with 0.82 M HNO ₃ to 100 ml
0.1 µg/l (0.1 ppb)	0.1 ml of 100 µg/l diluting with 0.82 M HNO ₃ to 100 ml
0.05 µg/l (0.05 ppb)	0.5 ml of 10 µg/l diluting with 0.82 M HNO ₃ to 100 ml

2.3.6 Linearity of the response to uranium

A daily background measurement and calibration were performed using four calibration standard solutions for each analytical range, ranging in concentration from the detection limit up to 1000 $\mu\text{g/l}$. A blank sample of 0.82 M HNO_3 was used to determine the background and reagent uranium concentration. The blank's phosphorescence intensity was subtracted from all KPA measurements. The values of the intercept of the $\ln I$ versus time t plots using Eq. (1.10) for every concentration were then plotted as a function of the uranium concentration. A linear fit with zero intercept was used for the regression to fit the analytical response. The results show that the response to uranium is linear with correlation coefficient of 0.999, with eight points. The low range calibration curve is displayed in the Fig. 2.4. Background, calibration and all sample measurements were performed using a reference solution of the same concentration as used with this original calibration.

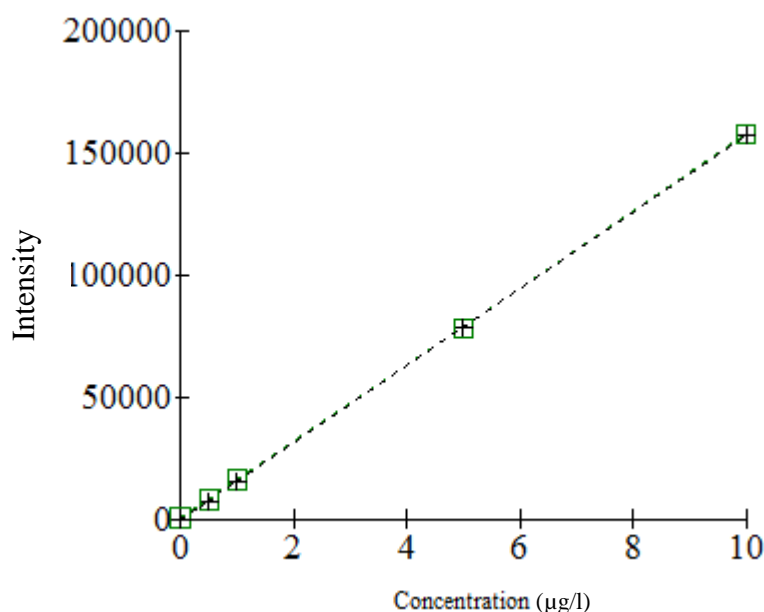


Figure 2.4 Low range calibration curve

2.3.7 Verification

KPA calibration was verified using traceable standard solutions obtained from different stock solution immediately following the calibration. The measurement results produced an average of $0.992 \pm 0.010 \mu\text{g/l}$ for $1\mu\text{g/l}$ standard solution. A complete recalibration of the system was performed for every sample set measurements.

2.3.8 Detection limit (DL) measurement

The KPA detection limit (DL) is an estimate of the minimum sample concentration that can be detected with a 99% confidence. The detection limit for uranium by KPA was determined by analyzing the same standard solution of $0.05 \mu\text{g/l}$ for ten different times. The standard deviation ($S.D_{bg}$) of the background measurements was then determined in terms of concentration, the calculation of the detection limit at the 99% confidence level using the formula of $(DL=2.8 \times S.D_{bg})$ [91]. The obtained value of standard deviation was $0.0035 \mu\text{g/l}$ with detection limit of $0.01 \mu\text{g/l}$.

2.3.9 Sample preparation procedure

2.3.9.1 Principle

Raw urine cannot be analyzed without pretreatment except at levels well above $20 \mu\text{g/l}$. If the concentration of uranium in the samples is high enough, they can be diluted one hundredfold with 1 M HNO_3 to reduce the matrix effects. The reasons for this are due to the presence of chloride and organic constituents which may fluoresce, complex uranium, or quench uranyl phosphorescence. Chemical separations are only required for very low levels of uranium with a substantially complex matrix.

2.3.9.2 Wet-ashing procedure

For low detection limits, wet-ashing process was performed to destroy proteinaceous compounds. In wet-ashing procedure for urine, 2 ml of concentrated nitric acid and 0.5 ml of 30% hydrogen peroxide were added to a 5 ml aliquot of the sample in 20 ml glass liquid scintillation vial which previously soaked as described in 2.3.3.5. Samples with solids were homogenized, for the uranium concentrates in solids. The vial containing the mixture solution was then placed on a hot plate at moderated temperature for six to eight hours and slowly boiled to dryness. The oxidant was replenished one to two times until white solid residue is obtained. After wet-ashing, the vial was placed in muffle furnace at 450 °C for 1 h. After cooling, the residue was dissolved in 1 ml of 4M nitric acid with warming and then diluted to the desired volume with deionized water and swirled to mix. The final volume was determined by weight. Although the sample preparation procedure takes a few days because of the repeated wet-ashing and dry-ashing steps, large numbers of samples can be analyzed simultaneously. This is because only small urine samples were needed for the analysis due to the high sensitivity of the KPA technique. Typically 16 samples were analyzed during each analysis run.

2.3.10 Sample analysis

Aliquot sample solutions were analyzed by combining 1 ml of the sample with 1.5 ml of complexing reagent (Uraplex) and determination of the phosphorescence decay profile.

The sample resulting phosphorescence intensities were measured at timed intervals (every 13 μ s) after the laser pulse termination. The accumulated data were plotted as the logarithm of the intensities versus the interval times, Fig. 2.5, which produces an intercept proportional to the number of excited uranyl ion. The intercept was then compared to

the standard calibration curve to determine the concentration of uranium. One thousand laser pulses were used for each measurement. Deionized water blank was analyzed for each batch of 16 samples.

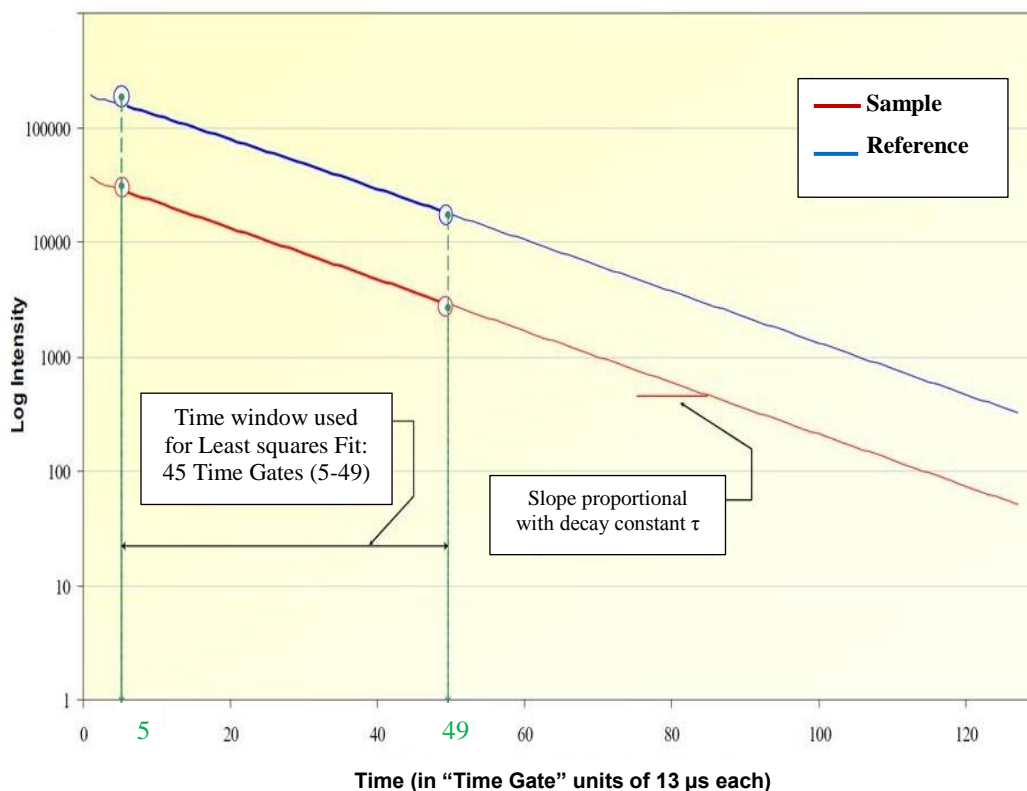


Figure 2.5 Relationship between log intensities and interval times

2.4 Materials and methods for FTA

The apparatus and experimental details for determination of uranium concentration in urine samples using fission track analysis are summarized below;

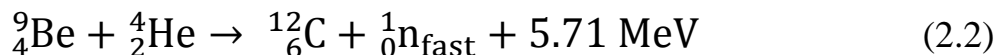
2.4.1 Material and apparatuses

2.4.1.1 Nuclear track detectors

CR-39 nuclear track detector sheets of 500 μm thick obtained from (Pershore Moulding LTD Company, UK) were used to record fission tracks. These sheets were cut into small pieces each of (1×1) cm² area. The detector sheets were stored at normal laboratory conditions.

2.4.1.2 Irradiation source

For irradiation samples, an Am-Be neutron source with neutron flux of $10^5 \text{ n.cm}^{-2}.\text{s}^{-1}$ was used. It emits fast neutrons by (α , n) reaction:



The irradiation system consists of a rod of (Am-Be) source surrounded by a paraffin wax. The paraffin wax was used to moderating the fast neutrons to thermal neutrons ${}^1_0\text{n}_{\text{thermal}}$ energies.

2.4.1.3 Etchant solution

Sodium hydroxide (NaOH) solution with 6.25 N has been used for the etching process. The etchant solution was prepared using volumetric flask and applying the following equation [149]:

$$W = W_{\text{eq}} \times N \times V \quad (2.3)$$

where:

W: weight of NaOH needed to prepare the given normality

W_{eq} : equivalent weight of NaOH

N: normality and equals to 6.25

V: volume of distilled water (250 ml)

$$W_{\text{eq}} = \sum_{t=0}^3 W_n \quad (2.4)$$

where W_n is the atomic weight of sodium, oxygen and hydrogen

$$W_{\text{eq}} = 22.98977 + 15.9994 + 1.00794 = 39.99711 \text{ g/mol}$$

So that:

$$W = 40 \text{ g/mol} \times 6.25 \text{ N} \times 250 \text{ ml} = 62.5 \text{ gm}$$

The etchant compartment has a volume of about 250 ml of NaOH solution with 6.25 N. This apparatus is a closed assembly, except for small vent at the top of the condenser tube, which prevents any change of etchant normality (concentration) during the experiment due to evaporation. The etching was performed at 60°C while the etching time was 5 hours.

2.4.1.4 Water bath

Water bath (type Labsco, Germany) was used to regulate the etchant solution temperature. It included a thermostat operating over a range of 20 °C to 110 °C and temperature regulation accuracy better than ± 0.1 °C. The chemical etching was carried out at 60 °C. Distilled water was used as the bath liquid.

2.4.1.5 Optical Microscope

The counting of chemically etched tracks was carried out using optical microscope (type Motic, Malaysia). It is capable of giving magnifications of 400x and eyepiece 10x to measure the number of tracks.

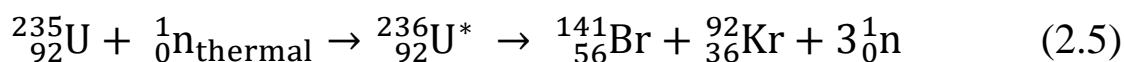
2.4.2 Sample preparation procedure

2.4.2.1 Uranium standard solutions

Uranium standard samples were prepared in a similar procedure to that mentioned before. Four standard uranium samples of concentration (0.5, 1, 3 and 5 $\mu\text{g/l}$) were prepared by dilution of 1000 $\mu\text{g/l}$ stock solution with double distilled deionized water.

2.4.2.2 Irradiation procedure

Uranium concentration in urine samples has been determined using the fission track registration technique. In this technique two drops of urine of known volume 100 μl were dried on a square CR-39 piece in a dust free atmosphere at normally room temperature as shown in Fig. 2.6. A non-volatile constituent of the sample was left over the detector in the form of a thin film. It was then covered with another piece of detector to make it a pair. All such pairs were then irradiated with thermal neutrons from (Am-Be) neutron source with 5 cm paraffin wax for seven days. The total thermal neutron fluence was $3.024 \times 10^9 \text{ n.cm}^{-2}$. The induced fission fragments were obtained according to the (n,f) reactions, one of them:



Uranium standard samples were prepared in the same procedure. A blank CR-39 detector was also irradiated along with the sample pair in order to calculate the background.

After irradiation the base detectors were etched in 6.25 N NaOH at 60 °C for five hours. The etched detectors were then rinsed in distilled water. The whole area of the droplet was manually scanned using the optical microscope at a magnification of (400x).

The fission track density (ρ) was calculated according to the following equation [150]:

$$\text{Track density } (\rho) = \frac{\text{average of total pits (tracks)}}{\text{area of field view}} \quad (2.6)$$

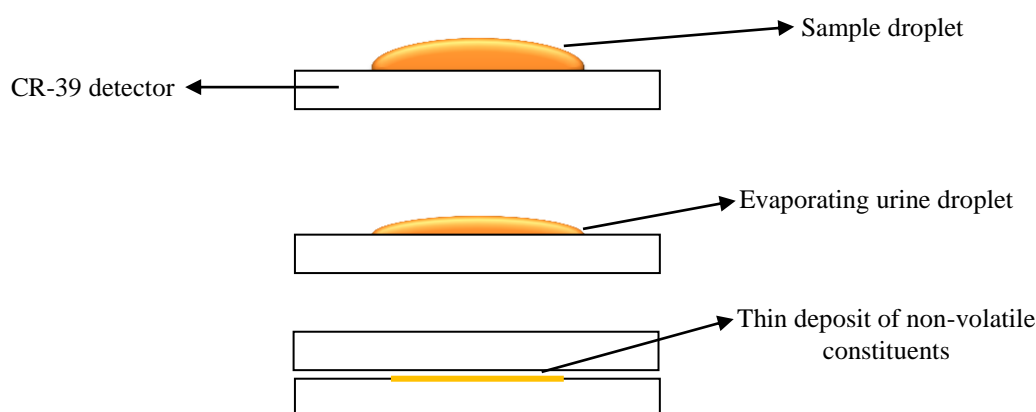


Figure 2.6 Evaporation of the sample droplet and the formation of a thin deposit [149]

2.4.3 Calibration curve

The accumulated data of the registered induced tracks density for standard solutions was plotted as a function of the uranium concentration. The blank's tracks density was subtracted from all measurements.

Figure 2.7 represents the calibrations curve for uranium standard samples and track density.

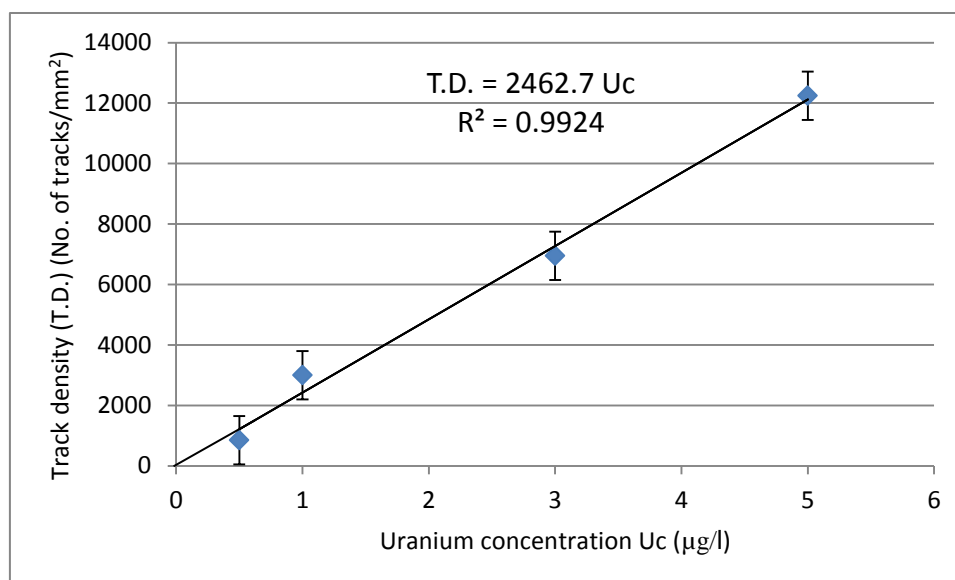


Figure 2.7 The relation between track density and uranium concentration in ($\mu\text{g/l}$) for standard samples

2.4.4 Calculations of uranium concentrations

Uranium concentration in urine samples was measured by comparison between track densities registered on the detector of urine samples and that of the standard solutions by Eq. (1.13) so that:

$$C_x = \rho_x \cdot (C_s / \rho_s) \quad (2.7)$$

where ρ_x and ρ_s are the induced fission track density for unknown sample and standard solution (in tracks/mm²), C_x and C_s denote the uranium concentration for unknown sample and standard solution (in $\mu\text{g/l}$). The slope of the linear relation between track density and uranium concentration for standard samples, Fig. 2.7, is equal to the reciprocal of the second term on the right-hand side of Eq. (2.7), then:

$$C_x = \rho_x / \text{slope} \quad (2.8)$$

Chapter Three

Results and Discussion

In this study, 194 samples of urine were collected from the workers of Akashat phosphate mine, Al-Qaim fertilizer complex, residents of Al-Qaim, Akashat region, Tall Al-Ragrag village and Al-Jesira village. The characteristics of these participants are shown in Table (2.12). They were classified into ten groups according to the area of study.

The measurements of uranium concentration in urine sample were obtained using kinetic phosphorescence analysis (KPA) and fission track analysis (FTA) with CR-39 solid state nuclear track detectors.

In this chapter, the results those include the uranium concentration in each sample are presented and classified according to some important parameters, namely; age, gender, employment duration and smoking habits. Comparison between KPA and FTA analysis is included. Moreover discussions, conclusions extracted from the present results and suggestions for future works are presented.

3.1 Uranium concentration in urine samples of Akashat mine and Al-Qaim fertilizer complex workers

The results of the uranium concentration in urine samples collected from the worker at Akashat phosphate mine and Al-Qaim fertilizer plants; beneficiation plant (U100), sulfuric acid plant (U200), phosphoric acid plant (U300) and fertilizers plants (U400) using KPA and FTA techniques are given in Tables (3.1), (3.2), (3.3), (3.4) and (3.5), respectively. Uranium excretion in the urine of these participants varied from $0.487 \pm 0.009 \mu\text{g/l}$ to $5.260 \pm 0.062 \mu\text{g/l}$ with a total average value of $1.468 \pm 0.002 \mu\text{g/l}$. Higher uranium concentrations were observed in the urine of U 215, U 304 and U 200 fertilizer occupational workers who had previously working in Al-Qaim uranium purification unit, with values of (5.260 ± 0.062 , 4.261 ± 0.072 and $4.104 \pm 0.055 \mu\text{g/l}$) respectively. Therefore, the uranium

detected in these samples was likely due to uranium that was being slowly released from bone and other tissue storage sites in the body.

The average, maximum and minimum uranium concentration values for each plant are presented in Table (3.6). From this Table it can be seen that the concentration of uranium in urine samples of sulfuric acid plant workers ranges from 1.048 ± 0.012 to 5.260 ± 0.062 $\mu\text{g/l}$ with an average value of 2.648 ± 0.008 $\mu\text{g/l}$ and uranium concentration in urine samples collected from phosphoric acid plant workers ranges from 1.043 ± 0.013 to 4.261 ± 0.072 $\mu\text{g/l}$ with an average of 1.744 ± 0.005 $\mu\text{g/l}$. While uranium concentration in urine samples of fertilizers plants workers ranges from 0.723 ± 0.010 to 2.105 ± 0.025 $\mu\text{g/l}$ with an average of 1.451 ± 0.006 $\mu\text{g/l}$ and uranium concentration in urine samples collected from beneficiation plant workers ranges from 0.620 ± 0.008 to 2.049 ± 0.030 $\mu\text{g/l}$ with an average value of 1.163 ± 0.003 $\mu\text{g/l}$. Similarly, uranium concentration in urine samples selected for analysis from Akashat mine workers ranges from 0.487 ± 0.009 to 2.222 ± 0.034 $\mu\text{g/l}$ with an average of 1.299 ± 0.003 $\mu\text{g/l}$. Finally for Al-Qaim laboratories workers the uranium concentration in urine ranges from 0.591 ± 0.008 to 0.806 ± 0.012 $\mu\text{g/l}$ with an average value of 0.722 ± 0.005 $\mu\text{g/l}$.

Figure 3.1 illustrates these average values as a function of work place, which shows that the higher uranium concentrations were for sulfuric acid plant (U200) workers because most of them were working in the past in uranium purification unit or their present work is nearby this site. The average uranium concentration in urine of sulfuric acid plant (U200) workers is a factor of 3.7 higher than that for laboratories workers and about twofold higher than that for beneficiation plant (U100) workers and Akashat phosphate mine workers. Similarly the average uranium concentration in urine of phosphoric acid plant (U300) workers is a factor of 2.4 higher than for laboratories workers. These results also shows that uranium concentrations in urine of beneficiation plant (U100) workers were closer to the measured values of Akashat phosphate mine workers and higher than the values for laboratories workers but lower than those values of fertilizers plants (U400) workers. This present that the phosphoric acid plant workers were exposed to uranium levels higher than those work in other plants.

The results of these study groups are about a factor of 1.5 to 5 higher than ICRP reference man value of 0.5 $\mu\text{g/l}$ [47].

In general, the uranium concentration found in urine of this study group may result from the dusty climate condition in the phosphate mine and fertilizer factory, a slightly higher uptake and thereafter excretion of uranium in urine might occur through inhalation of additionally suspended dust in the air.

Table 3.1 Uranium concentration in urine samples of Akashat phosphate mine workers

Sample code	Age (years)	work duration (years)	Smoking	Uranium concentration in ($\mu\text{g/l}$) \pm S.D	
				FTA	KPA
AM 1	53	24	P	2.057 \pm 0.273	1.302 \pm 0.020
AM 2	41	17	S	1.877 \pm 0.235	1.713 \pm 0.022
AM 3	60	35	N	1.930 \pm 0.286	2.065 \pm 0.030
AM 4	42	18	N	1.231 \pm 0.226	0.973 \pm 0.017
AM 5	40	5	P	1.689 \pm 0.177	1.158 \pm 0.018
AM 6	38	14	S	1.314 \pm 0.264	0.976 \pm 0.016
AM 7	48	14	S	1.915 \pm 0.195	2.222 \pm 0.034
AM 8	54	20	P	1.877 \pm 0.215	2.150 \pm 0.033
AM 9	45	7	S	1.629 \pm 0.152	1.600 \pm 0.024
AM 10	53	17	S	2.155 \pm 0.186	1.845 \pm 0.030
AM 11	55	21	S	1.374 \pm 0.278	1.342 \pm 0.021
AM 12	45	18	P	2.110 \pm 0.210	1.861 \pm 0.023
AM 13	37	15	P	1.389 \pm 0.246	1.433 \pm 0.022
AM 14	45	18	N	1.359 \pm 0.287	1.033 \pm 0.017
AM 15	47	11	P	1.780 \pm 0.290	1.239 \pm 0.027
AM 16	58	15	N	1.877 \pm 0.187	2.015 \pm 0.029
AM 17	50	12	S	1.299 \pm 0.266	0.994 \pm 0.021
AM 18	39	11	N	1.051 \pm 0.233	0.762 \pm 0.011
AM 19	41	11	S	1.584 \pm 0.225	0.976 \pm 0.017
AM 20	42	18	N	1.397 \pm 0.285	0.768 \pm 0.010
AM 21	42	22	N	1.194 \pm 0.146	0.882 \pm 0.013
AM 23	46	20	S	1.539 \pm 0.255	0.856 \pm 0.011
AM 24	43	5	N	1.089 \pm 0.217	0.487 \pm 0.009
AM 25	34	7	N	1.307 \pm 0.261	0.881 \pm 0.013
AM 26	47	19	N	1.156 \pm 0.213	0.955 \pm 0.014
Average				1.567 \pm 0.044	1.300 \pm 0.003

Table 3.2 Uranium concentration in urine samples of Al-Qaim fertilizer complex, Beneficiation plant (Unit 100) workers

Sample code	Age (years)	work duration (years)	Smoking	Uranium concentration in ($\mu\text{g/l}$) \pm S.D	
				FTA	KPA
U 100	41	18	N	1.434 \pm 0.283	1.047 \pm 0.020
U 101	50	15	N	1.051 \pm 0.242	0.620 \pm 0.008
U 102	48	18	N	1.757 \pm 0.252	1.662 \pm 0.020
U 103	52	8	P	1.847 \pm 0.243	1.429 \pm 0.026
U 104	45	20	N	1.246 \pm 0.233	0.837 \pm 0.012
U 105	46	20	N	1.614 \pm 0.206	1.346 \pm 0.019
U 106	45	19	N	1.382 \pm 0.194	0.851 \pm 0.013
U 107	53	21	P	1.397 \pm 0.218	1.212 \pm 0.011
U 110	42	17	N	1.442 \pm 0.209	1.022 \pm 0.008
U 111	42	16	N	1.239 \pm 0.217	1.063 \pm 0.008
U 112	44	19	N	1.096 \pm 0.233	1.129 \pm 0.009
U 113	52	23	S	2.065 \pm 0.170	2.049 \pm 0.030
U 114	42	20	N	1.367 \pm 0.246	0.784 \pm 0.012
U 115	45	25	N	1.697 \pm 0.218	1.226 \pm 0.010
Average				1.474 \pm 0.059	1.163 \pm 0.003

Table 3.3 Uranium concentration in urine samples of Al-Qaim fertilizer complex, Sulfuric acid plant (Unit 200) workers

Sample code	Age (years)	work duration (years)	Smoking	Uranium concentration in ($\mu\text{g/l}$) \pm S.D	
				FTA	KPA
U 200	52	15	N	2.823 \pm 0.254	4.104 \pm 0.055
U 201	43	11	S	1.817 \pm 0.251	1.686 \pm 0.046
U 202	48	6	S	2.590 \pm 0.217	2.884 \pm 0.058
U 206	34	8	N	1.967 \pm 0.195	2.217 \pm 0.049
U 208	35	12	N	1.870 \pm 0.210	1.146 \pm 0.015
U 210	52	15	N	1.892 \pm 0.209	1.681 \pm 0.045
U 211	34	8	N	1.517 \pm 0.242	1.048 \pm 0.012
U 212	31	8	S	3.041 \pm 0.251	2.991 \pm 0.049
U 213	44	21	S	3.289 \pm 0.355	3.934 \pm 0.047
U 214	42	12	N	2.358 \pm 0.178	2.315 \pm 0.052
U 215	57	29	N	2.170 \pm 0.283	5.260 \pm 0.062
U 216	45	13	S	2.253 \pm 0.171	2.877 \pm 0.046
U 217	56	12	S	1.960 \pm 0.279	2.277 \pm 0.054
Average				2.273 \pm 0.063	2.648 \pm 0.008

Table 3.4 Uranium concentration in urine samples of Al-Qaim fertilizer complex, Phosphoric acid plant (Unit 300) workers

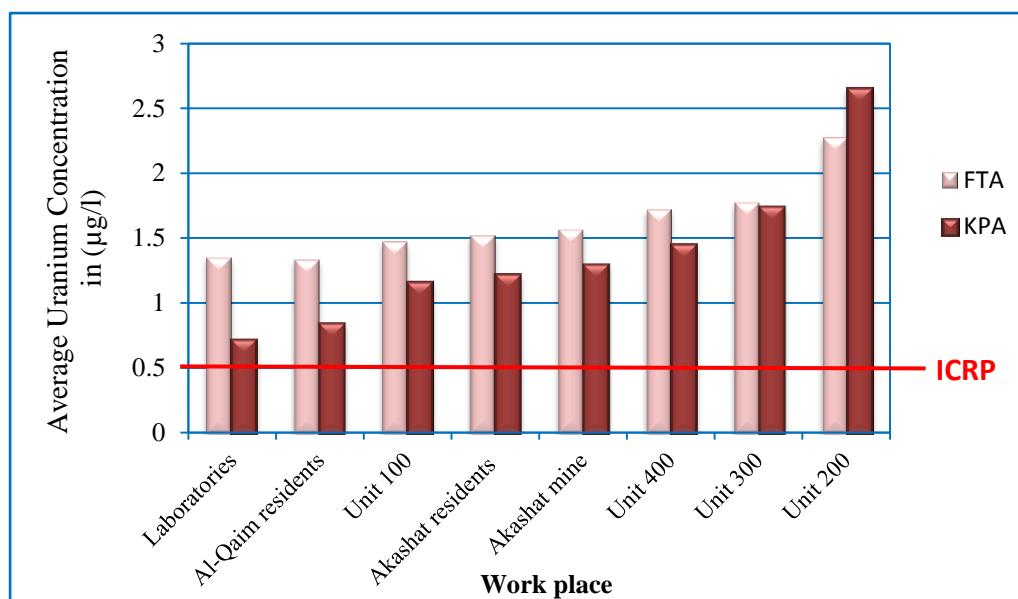
Sample code	Age (years)	work duration (years)	Smoking	Uranium concentration in ($\mu\text{g/l}$) \pm S.D	
				FTA	KPA
U 300	38	16	N	1.952 ± 0.264	1.863 ± 0.044
U 301	41	11	N	1.682 ± 0.210	1.254 ± 0.017
U 302	43	20	N	1.554 ± 0.192	1.043 ± 0.013
U 303	30	8	N	1.224 ± 0.214	1.092 ± 0.013
U 304	57	29	N	2.718 ± 0.255	4.261 ± 0.072
U 305	30	4	P	1.659 ± 0.266	0.925 ± 0.011
U 306	56	27	P	1.659 ± 0.174	1.966 ± 0.011
U 307	40	14	N	1.682 ± 0.258	1.645 ± 0.041
U 308	40	10	S	1.840 ± 0.206	1.649 ± 0.019
Average				1.775 ± 0.073	1.744 ± 0.005

Table 3.5 Uranium concentration in urine samples of Al-Qaim fertilizer complex, Fertilizers plants (Unit 400) and laboratories workers

Sample code	Age (years)	work duration (years)	Smoking	Uranium concentration in ($\mu\text{g/l}$) \pm S.D	
				FTA	KPA
U 400	43	18	N	1.802 ± 0.190	1.444 ± 0.019
U 401	41	10	S	1.915 ± 0.260	1.691 ± 0.020
U 402	43	10	P	1.802 ± 0.202	1.671 ± 0.021
U 403	45	17	P	1.547 ± 0.223	1.427 ± 0.018
U 404	39	10	N	1.772 ± 0.199	1.454 ± 0.023
U 405	45	22	N	1.562 ± 0.230	1.200 ± 0.035
U 406	40	8	N	1.104 ± 0.203	0.723 ± 0.010
U 407	40	11	N	1.937 ± 0.246	1.344 ± 0.020
U 408	46	18	P	2.050 ± 0.209	2.105 ± 0.025
Average				1.721 ± 0.072	1.451 ± 0.006
L 1	38	12	N	1.224 ± 0.197	0.591 ± 0.008
L 2	41	16	N	1.584 ± 0.244	0.770 ± 0.010
L 3	39	10	N	1.246 ± 0.223	0.806 ± 0.012
Average				1.352 ± 0.126	0.722 ± 0.005

Table 3.6 Average, maximum and minimum uranium concentration in urine samples of Al-Qaim fertilizer complex and Akashat phosphate mine workers

Work place	No. of Subject	Average uranium concentration in ($\mu\text{g/l}$) \pm S.D		Maximum uranium concentration in ($\mu\text{g/l}$) \pm S.D		Minimum uranium concentration in ($\mu\text{g/l}$) \pm S.D	
		FTA	KPA	FTA	KPA	FTA	KPA
Akashat mine	25	1.567 ± 0.044	1.299 ± 0.003	2.155 ± 0.186	2.222 ± 0.034	1.051 ± 0.233	0.487 ± 0.009
Beneficiation plant (Unit 100)	14	1.474 ± 0.059	1.163 ± 0.003	2.065 ± 0.170	2.049 ± 0.030	1.051 ± 0.242	0.620 ± 0.008
Sulphuric acid plant (Unit 200)	13	2.273 ± 0.063	2.648 ± 0.008	3.289 ± 0.355	5.260 ± 0.062	1.517 ± 0.242	1.048 ± 0.012
Phosphoric acid plant (Unit 300)	9	1.775 ± 0.073	1.744 ± 0.005	2.718 ± 0.255	4.261 ± 0.072	1.224 ± 0.214	1.043 ± 0.013
Fertilizers plants (Unit 400)	9	1.721 ± 0.072	1.451 ± 0.006	2.050 ± 0.209	2.105 ± 0.025	1.104 ± 0.203	0.723 ± 0.010
Laboratories	3	1.352 ± 0.126	0.722 ± 0.005	1.584 ± 0.244	0.806 ± 0.012	1.224 ± 0.197	0.591 ± 0.008



ICRP: Reference man value

Figure 3.1 The relation between average uranium concentration in ($\mu\text{g/l}$) and work place

To explain these results, workers were divided into groups according to the employment duration: (A) 1 – 5 years, (B) 6 – 10 years, (C) 11 – 15 years, (D) 16 – 20 years, (E) 21 – 25 years and (G) more than 25 years.

In order to analyze these results, the range, mean, dispersion and standard deviation were calculated for each group. The results of average uranium concentration for each group are presented in Table (3.7) and plotted graphically in Figs. 3.2 and 3.3 for Al-Qaim fertilizer complex workers and Akashat miners, respectively.

Figs 3.2 and 3.3 show that the uranium concentration in the urine of Al-Qaim workers and Akashat phosphate miners increase with the increasing of the number of working years. The average concentration of uranium for group G occupational worker at Al-Qaim fertilizer was $3.829 \pm 0.010 \mu\text{g/l}$ and a factor of 2 higher than for group E. It also is a factor of 2.2 higher than for group D and about fourfold higher than that for group A. Similar results were observed for Akashat phosphate miners.

The recorded average uranium concentration values for each plant workers at Al-Qaim fertilizer complex as a function of employment duration are presented in Table (3.8) and plotted graphically in Figs. 3.4, 3.5, 3.6 and 3.7 for beneficiation plant (U100), sulfuric acid plant (U200), phosphoric acid plant (U300) and fertilizers plants (U400), respectively.

For individual cases it can be seen from Table (3.1) that UM 2 and UM 19 are in the same age (41 years old) and they are smokers but they have different work duration at Akashat mine 17 and 11 years, respectively. Nevertheless, the uranium concentration in urine of UM 2 is $1.713 \pm 0.022 \mu\text{g/l}$ and a factor of 1.7 higher than for UM 19. Similarly from Table (3.2), U 115, U 104 and U 106 are in the same age (45 years old), nonsmokers but have different work duration at Al-Qaim fertilizer complex 25, 20 and 19 years respectively and the uranium concentration in urine of U 115 is a factor of 1.4 higher than for U 104 and U 106. And U 113 and U 103 they are in the same age (52 years old), smokers but they have different work duration at Al-Qaim fertilizer complex 23 and 8 years respectively and the uranium concentration in urine of U 113 is a factor of 1.5 higher than for U 103.

Table 3.7 Average uranium concentration in urine samples of Al-Qaim fertilizer complex and Akashat mine workers according to the number of working years

Work place	No. of working years	Average uranium concentration in ($\mu\text{g/l}$) \pm S.D	
		FTA	KPA
Al-Qaim fertilizer complex (Q.F.C)	Group A (1 – 5)	1.659 ± 0.266	0.925 ± 0.011
	Group B (6 – 10)	1.822 ± 0.062	1.638 ± 0.005
	Group C (11 – 15)	1.879 ± 0.063	1.795 ± 0.005
	Group D (16 – 20)	1.848 ± 0.060	1.893 ± 0.004
	Group E (21 – 25)	2.002 ± 0.098	1.924 ± 0.007
	Group G (More than 25)	2.183 ± 0.128	3.829 ± 0.010
Akashat phosphate mine (A.M)	Group A (1 – 5)	1.389 ± 0.137	0.823 ± 0.008
	Group B (6 – 10)	1.468 ± 0.131	1.241 ± 0.011
	Group C (11 – 15)	1.526 ± 0.082	1.327 ± 0.007
	Group D (16 – 20)	1.634 ± 0.076	1.350 ± 0.005
	Group E (21 – 25)	1.716 ± 0.195	1.322 ± 0.010
	Group G (More than 25)	1.930 ± 0.286	2.065 ± 0.030

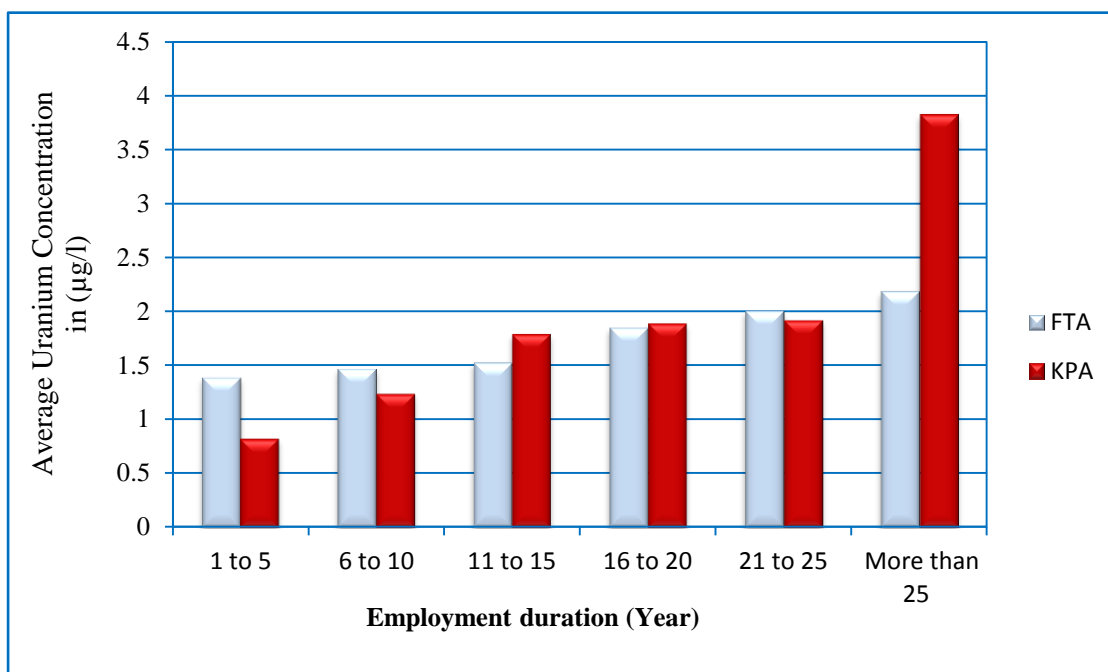


Figure 3.2 The relation between average uranium concentration in ($\mu\text{g/l}$) and employment duration (years) for Al-Qaim complex workers

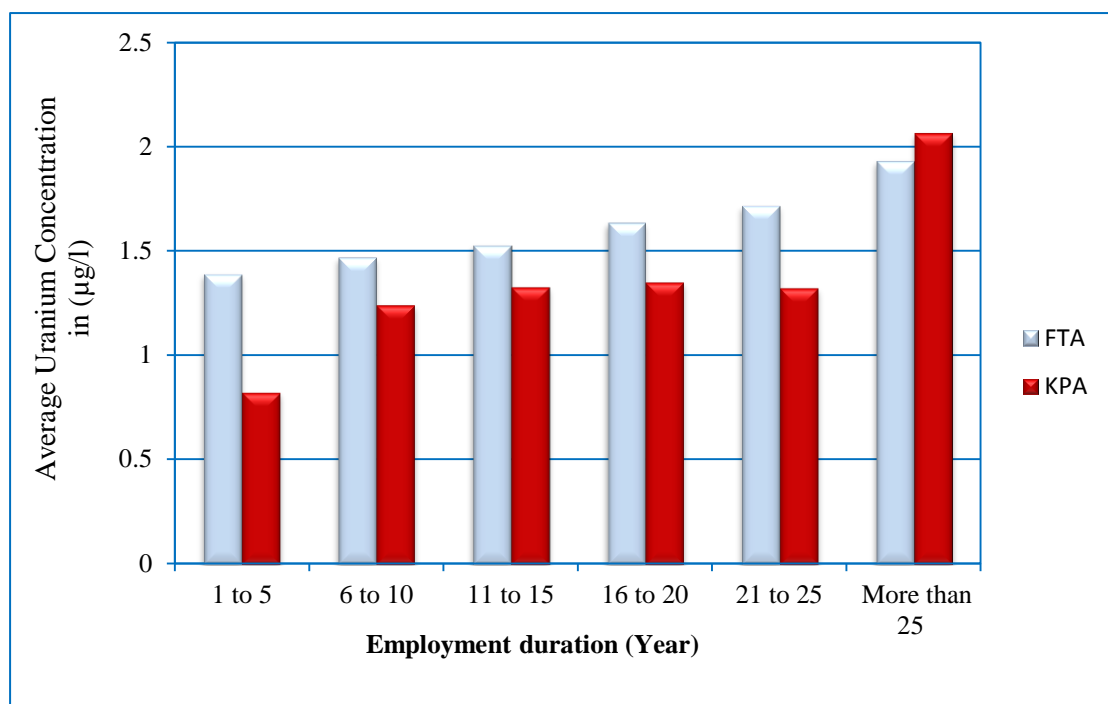


Figure 3.3 The relation between average uranium concentration in ($\mu\text{g/l}$) and employment duration (years) for Akashat mine workers

Table 3.8 Average uranium concentration in urine samples for each plant workers at Al-Qaim fertilizer complex as a function of employment duration

Employment duration groups (years)	Average uranium concentration in ($\mu\text{g/l}$) \pm S.D	
	FTA	KPA
Beneficiation plant (Unit 100)		
11 – 15	1.051 \pm 0.242	0.620 \pm 0.008
16 – 20	1.404 \pm 0.086	1.158 \pm 0.004
Over 25	1.719 \pm 0.114	1.495 \pm 0.007
Sulphuric acid plant (Unit 200)		
5 – 10	2.279 \pm 0.111	2.285 \pm 0.011
11 – 15	2.139 \pm 0.080	2.298 \pm 0.012
16 – 20	2.253 \pm 0.171	2.877 \pm 0.046
21 – 25	3.289 \pm 0.355	3.934 \pm 0.047
Over 25	2.170 \pm 0.283	5.260 \pm 0.062
Phosphoric acid plant (Unit 300)		
5 – 10	1.574 \pm 0.129	1.222 \pm 0.008
11 – 15	1.682 \pm 0.163	1.450 \pm 0.016
16 – 20	1.753 \pm 0.155	1.453 \pm 0.012
Over 25	2.189 \pm 0.144	3.113 \pm 0.011
Fertilizers plants (Unit 400)		
5 – 10	1.568 \pm 0.096	1.269 \pm 0.007
11 – 15	1.937 \pm 0.246	1.344 \pm 0.020
16 – 20	1.800 \pm 0.118	1.659 \pm 0.012

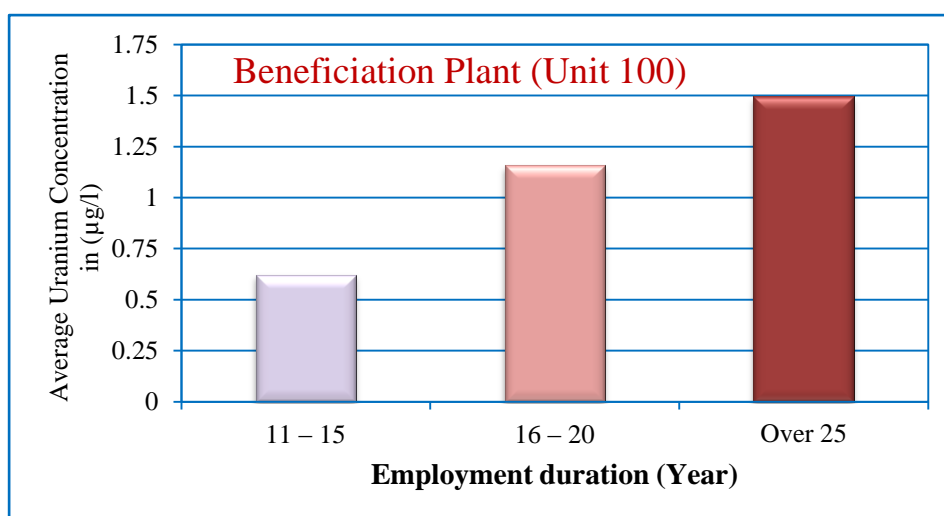


Figure 3.4 The relation between average uranium concentration in ($\mu\text{g/l}$) and employment duration (years) for beneficiation plant workers using KPA technique

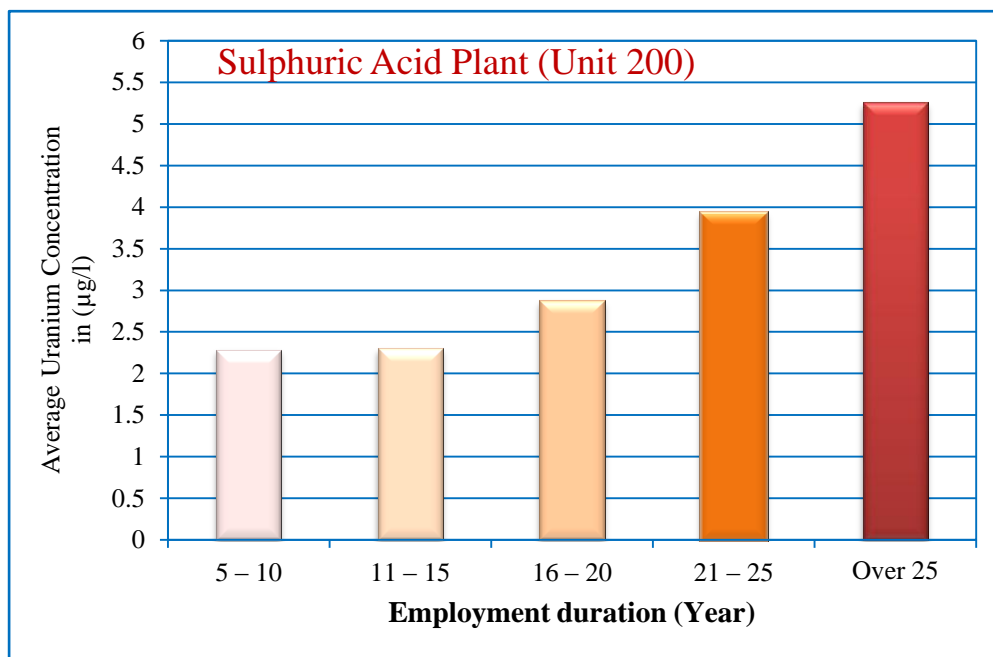


Figure 3.5 The relation between average uranium concentration in ($\mu\text{g/l}$) and employment duration (years) for Sulphuric acid plant workers using KPA technique

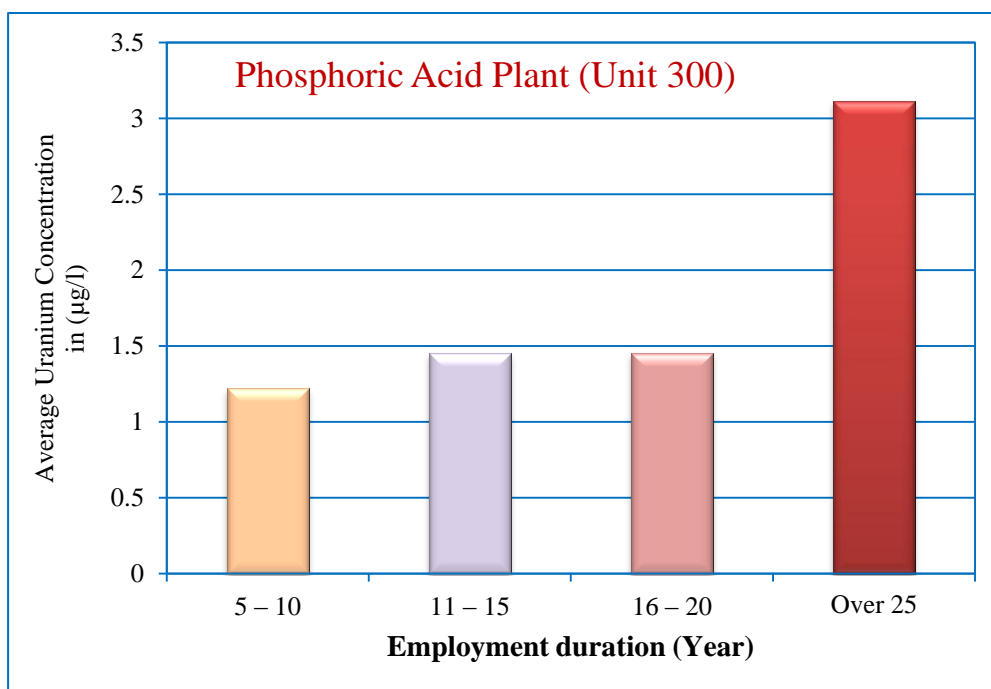


Figure 3.6 The relation between average uranium concentration in ($\mu\text{g/l}$) and employment duration (years) for phosphoric acid plant workers using KPA technique

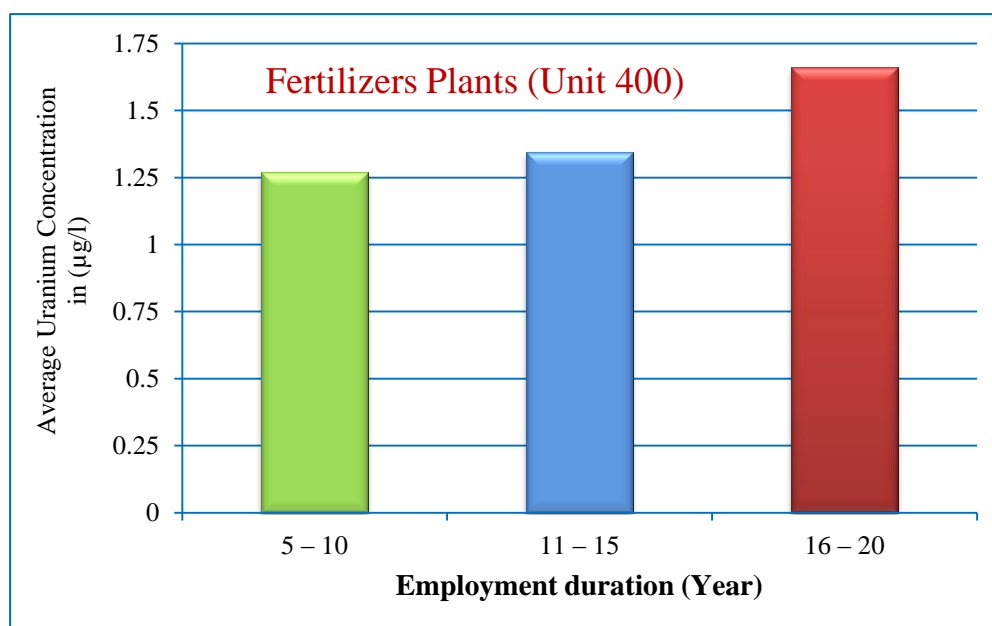


Figure 3.7 The relation between average uranium concentration in ($\mu\text{g/l}$) and employment duration (years) for fertilizers plants workers using KPA technique

3.2 Uranium concentration in urine samples of Akashat mining region and Al-Qaim residents

Tables (3.9) and (3.10) show the uranium concentration in urine samples collected from non-occupational persons living in Akashat mining region and from control population living in Al-Qaim city. Uranium excretion in the urine of Akashat residents varied from 0.621 ± 0.010 to 2.012 ± 0.031 $\mu\text{g/l}$ with an average value of 1.222 ± 0.004 $\mu\text{g/l}$ and uranium concentration in urine samples collected from residents in Al-Qaim city ranges from 0.733 ± 0.015 to 1.025 ± 0.014 $\mu\text{g/l}$ with an average of 0.846 ± 0.005 $\mu\text{g/l}$. These results show that the uranium concentration in urine of Akashat mining region residents were closer to the recorded values for Akashat mine workers, Table (3.5), and higher than the values for the control group in Al-Qaim. This indicates that all people (occupational and non-occupational) living in the phosphate mining areas exposed to uranium levels higher than those living outside that region.

The uranium concentration found in urine of the Akashat mining region study group may be resulted from the variable uranium intake through food and beverages. However, Akashat and the mining regions (in the middle of the western desert) are considered to be in a dry area where dusty climate is likely to occur at most times of the year, even in the rainy season in Iraq. Therefore, air particulates are also considered to be a health hazard; dust carrying phosphate ore particulates containing naturally occurring radioactive materials NORM being also a radiation health hazard.

Table 3.9 Uranium concentration in urine samples of Akashat residents

Sample code	Gender	Age (years)	Smoking	Uranium concentration in ($\mu\text{g/l}$) \pm S.D	
				FTA	KPA
APR 1	Male	40	N	1.254 ± 0.224	0.862 ± 0.011
APR 2	Male	18	N	1.562 ± 0.192	1.148 ± 0.016
APR 3	Male	20	N	1.149 ± 0.186	0.806 ± 0.011
APR 4	Male	20	N	1.141 ± 0.153	0.820 ± 0.011
APR 5	Male	18	N	1.479 ± 0.229	0.904 ± 0.012
APR 6	Female	13	N	1.765 ± 0.227	1.527 ± 0.022
APR 7	Female	15	N	1.224 ± 0.219	0.830 ± 0.011
APR 8	Female	14	N	1.081 ± 0.236	0.621 ± 0.010
APR 9	Female	13	N	1.457 ± 0.178	1.227 ± 0.019
APR 10	Male	11	N	1.494 ± 0.181	1.204 ± 0.019
APR 11	Male	12	N	1.937 ± 0.242	1.946 ± 0.029
APR 12	Female	6	N	2.283 ± 0.188	1.981 ± 0.031
APR 13	Male	14	N	1.952 ± 0.202	2.012 ± 0.031
Average				1.521 ± 0.055	1.222 ± 0.004

Table 3.10 Uranium concentration in urine samples of Al-Qaim residents

Sample code	Gender	Age (years)	Smoking	Uranium concentration in ($\mu\text{g/l}$) \pm S.D	
				FTA	KPA
H 1	Male	20	N	1.322 ± 0.181	0.733 ± 0.015
H 2	Male	33	N	1.562 ± 0.174	1.025 ± 0.014
H 3	Male	20	N	1.389 ± 0.232	0.837 ± 0.012
H 4	Male	20	N	1.224 ± 0.197	0.830 ± 0.011
H 5	Male	23	N	1.322 ± 0.175	0.910 ± 0.011
H 6	Male	22	N	1.194 ± 0.235	0.741 ± 0.010
Average				1.335 ± 0.079	0.846 ± 0.005

Table (3.11) and Fig. 3.8 show the uranium concentration in urine of Akashat mining region and Al-Qaim complex workers as a function of age group. The average values were found to be proportional to the age group except for ages between 21 and 30 years, where a drop in concentration is observed. The average concentration of uranium in the age between 51 and 60 years was $(2.275 \pm 0.006) \mu\text{g/l}$ and a factor of 1.6 higher than for age 41 – 50 years. It also is a factor of 1.8 higher than for 31 – 40 years and about twofold higher than that for the age between 11 and 20 years. From these results a significant increase of uranium concentration with age was observed.

Tale 4.11 Uranium concentration in urine samples of Akashat mining residents and Al-Qaim fertilizer complex as a function of age

Age group (years)	No. of Subject	Average uranium concentration in ($\mu\text{g/l}$) \pm S.D	
		FTA	KPA
11 – 20	14	1.476 ± 0.059	1.186 ± 0.004
21 – 30	4	1.442 ± 0.166	1.009 ± 0.008
31 – 40	19	1.620 ± 0.053	1.308 ± 0.003
41 – 50	39	1.848 ± 0.035	1.417 ± 0.002
51 – 60	15	1.977 ± 0.058	2.275 ± 0.006

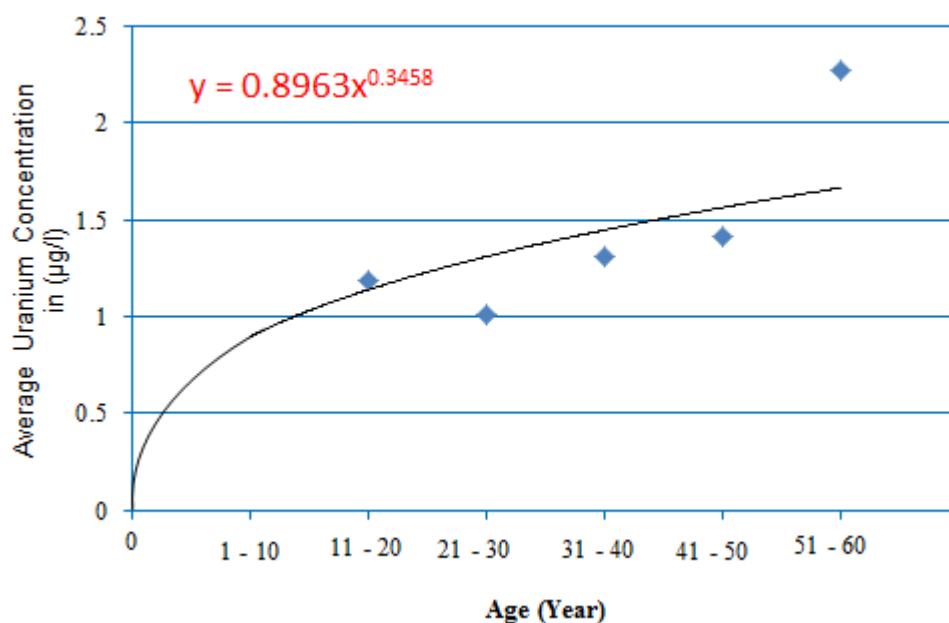


Figure 3.8 KPA results of uranium concentration in urine samples of Akashat mining residents and Al-Qaim fertilizer complex as a function of age

3.3 Uranium concentration in urine samples of Tall Al-Ragrag and Al-Jesira village residents

Uranium concentrations in urine samples collected from Tall Al-Ragrag and Al-Jesira villagers are given in Tables (3.12) and (3.13), respectively. Table (3.12) shows that the uranium concentration in urine of Tall Al-Ragrag residents are in the range of 0.410 ± 0.008 to 3.011 ± 0.072 $\mu\text{g/l}$ with mean value of 1.125 ± 0.001 $\mu\text{g/l}$. Table (3.13) shows that the uranium concentration in urine of Al-Jesira residents are in the range of 0.552 ± 0.009 to 2.925 ± 0.053 $\mu\text{g/l}$ with mean value of 1.338 ± 0.003 $\mu\text{g/l}$. The analysis results for Tall Al-Ragrag and Al-Jesira villagers were separated into gender and summarized in Table (3.14) and plotted graphically in Fig. 3.9. Uranium concentration in the urine of Al-Jesira residents are higher than the values of Tall Al-Ragrag as they living in/or closer to the structures of the former nuclear facility.

Table 3.12 Uranium concentration in urine samples of Tall Al-Ragrag residents (A)

Sample code	Gender	Age (Years)	Uranium concentration in ($\mu\text{g/l}$) \pm S.D	
			FTA	KPA
A 001	Male	25	1.254 \pm 0.239	1.177 \pm 0.017
A 002	Female	25	0.999 \pm 0.224	0.570 \pm 0.008
A 003	Female	30	1.727 \pm 0.230	1.614 \pm 0.024
A 004	Female	35	1.494 \pm 0.275	1.073 \pm 0.014
A 005	Male	62	2.208 \pm 0.293	2.591 \pm 0.055
A 006	Female	50	1.915 \pm 0.212	2.324 \pm 0.040
A 007	Female	50	1.044 \pm 0.210	0.720 \pm 0.011
A 008	Female	55	1.246 \pm 0.228	0.961 \pm 0.018
A 009	Female	40	1.216 \pm 0.222	0.950 \pm 0.012
A 010	Female	14	1.081 \pm 0.205	0.772 \pm 0.014
A 011	Female	11	0.803 \pm 0.192	0.763 \pm 0.011
A 012	Female	40	0.984 \pm 0.168	0.779 \pm 0.012
A 013	Male	2	1.021 \pm 0.181	0.967 \pm 0.040
A 014	Female	32	1.141 \pm 0.235	0.941 \pm 0.020
A 015	Female	51	1.547 \pm 0.228	1.505 \pm 0.019
A 016	Male	5	1.171 \pm 0.199	0.981 \pm 0.016
A 017	Male	7	1.201 \pm 0.207	0.891 \pm 0.018
A 018	Male	6	1.231 \pm 0.254	1.209 \pm 0.015
A 019	Male	3	1.156 \pm 0.196	1.154 \pm 0.021
A 020	Female	55	1.982 \pm 0.210	1.739 \pm 0.023
A 021	Male	13	1.134 \pm 0.220	0.844 \pm 0.011
A 022	Male	5	1.081 \pm 0.205	0.675 \pm 0.017
A 023	Male	30	1.629 \pm 0.192	1.704 \pm 0.020
A 024	Male	40	2.418 \pm 0.329	2.598 \pm 0.070
A 025	Female	23	1.036 \pm 0.206	0.923 \pm 0.011

Continuous table 3.12

Sample code	Gender	Age (Years)	Uranium concentration in ($\mu\text{g/l}$) \pm S.D	
			FTA	KPA
A 026	Male	37	1.772 \pm 0.210	1.530 \pm 0.019
A 027	Male	48	1.457 \pm 0.218	1.319 \pm 0.016
A 028	Male	39	1.344 \pm 0.266	1.159 \pm 0.015
A 029	Male	8	1.119 \pm 0.253	1.075 \pm 0.020
A 030	Male	29	1.412 \pm 0.215	1.268 \pm 0.036
A 031	Female	33	1.569 \pm 0.220	1.585 \pm 0.024
A 032	Female	35	1.397 \pm 0.247	1.313 \pm 0.050
A 033	Female	40	1.344 \pm 0.168	1.487 \pm 0.067
A 034	Male	60	1.930 \pm 0.224	1.913 \pm 0.043
A 035	Male	22	1.036 \pm 0.212	0.542 \pm 0.009
A 036	Male	28	1.780 \pm 0.278	1.732 \pm 0.029
A 037	Female	41	1.772 \pm 0.226	1.905 \pm 0.030
A 038	Female	50	1.382 \pm 0.216	1.680 \pm 0.027
A 039	Female	40	1.359 \pm 0.210	1.518 \pm 0.028
A 040	Female	9	0.781 \pm 0.147	0.758 \pm 0.011
A 041	Female	30	0.781 \pm 0.175	0.971 \pm 0.014
A 042	Female	60	1.757 \pm 0.289	1.942 \pm 0.031
A 043	Female	55	1.502 \pm 0.260	1.770 \pm 0.029
A 044	Female	65	0.916 \pm 0.206	0.715 \pm 0.012
A 045	Female	50	1.201 \pm 0.202	0.683 \pm 0.019
A 046	Female	37	1.472 \pm 0.188	1.119 \pm 0.042
A 047	Female	45	1.074 \pm 0.219	0.853 \pm 0.023
A 048	Female	18	0.976 \pm 0.210	0.646 \pm 0.017
A 049	Female	32	1.299 \pm 0.243	0.923 \pm 0.029
A 050	Female	28	0.991 \pm 0.198	0.853 \pm 0.021
A 051	Female	30	1.494 \pm 0.230	1.251 \pm 0.031

Continuous table 3.12

Sample code	Gender	Continuous table 3.12	Continuous table 3.12	
			FTA	KPA
A 052	Male	3.5	1.517 ± 0.255	1.101 ± 0.029
A 053	Male	3	1.269 ± 0.235	0.739 ± 0.021
A 054	Male	6	1.254 ± 0.219	0.946 ± 0.029
A 055	Female	12	1.164 ± 0.189	0.990 ± 0.051
A 056	Female	9	1.081 ± 0.226	0.801 ± 0.020
A 057	Male	34	1.254 ± 0.179	1.010 ± 0.041
A 058	Female	8	1.186 ± 0.206	0.730 ± 0.010
A 059	Female	7	1.066 ± 0.212	0.824 ± 0.012
A 060	Female	25	1.036 ± 0.227	0.748 ± 0.019
A 061	Male	4	1.081 ± 0.194	0.719 ± 0.009
A 062	Female	23	1.006 ± 0.196	0.644 ± 0.006
A 063	Female	15	0.976 ± 0.204	0.759 ± 0.015
A 064	Male	23	1.119 ± 0.235	0.637 ± 0.010
A 065	Male	16	0.946 ± 0.191	0.717 ± 0.005
A 066	Male	28	0.901 ± 0.237	0.760 ± 0.008
A 067	Male	21	1.134 ± 0.262	0.722 ± 0.010
A 068	Male	22	1.382 ± 0.199	1.422 ± 0.018
A 069	Male	60	2.335 ± 0.253	3.011 ± 0.072
A 070	Male	3	1.171 ± 0.155	0.561 ± 0.003
A 071	Male	19	1.036 ± 0.217	0.622 ± 0.011
A 072	Female	5	0.931 ± 0.194	0.863 ± 0.008
A 073	Male	7	1.096 ± 0.165	0.821 ± 0.010
A 074	Female	35	1.074 ± 0.214	0.817 ± 0.012
A 075	Male	39	1.111 ± 0.204	0.458 ± 0.011
A 076	Male	60	1.111 ± 0.198	0.410 ± 0.008
A 077	Male	36	1.629 ± 0.214	1.874 ± 0.033
Average			1.293 ± 0.024	1.125 ± 0.001

Table 3.13 Uranium concentration in urine samples of Al-Jesira residents (J)

Sample code	Gender	Age (Years)	Uranium concentration in ($\mu\text{g/l}$) \pm S.D	
			FTA	KPA
J 078	Male	40	1.442 \pm 0.225	1.102 \pm 0.020
J 079	Male	40	1.472 \pm 0.181	1.501 \pm 0.027
J 080	Male	9	1.307 \pm 0.208	0.899 \pm 0.023
J 081	Male	50	1.614 \pm 0.206	1.933 \pm 0.035
J 082	Male	9	1.036 \pm 0.195	0.732 \pm 0.016
J 083	Male	14	1.179 \pm 0.239	0.784 \pm 0.015
J 084	Male	45	2.193 \pm 0.316	2.831 \pm 0.050
J 085	Male	12	1.239 \pm 0.217	1.171 \pm 0.021
J 086	Male	21	1.674 \pm 0.261	1.994 \pm 0.036
J 087	Male	18	1.644 \pm 0.210	1.441 \pm 0.021
J 088	Male	12	1.194 \pm 0.220	1.082 \pm 0.023
J 089	Male	9	1.119 \pm 0.210	0.552 \pm 0.009
J 090	Male	19	1.239 \pm 0.189	0.832 \pm 0.020
J 091	Female	42	1.239 \pm 0.251	0.914 \pm 0.013
J 092	Female	33	0.811 \pm 0.160	0.630 \pm 0.009
J 093	Female	35	1.719 \pm 0.220	1.466 \pm 0.019
J 094	Female	20	1.171 \pm 0.199	1.047 \pm 0.013
J 095	Female	45	2.132 \pm 0.254	2.567 \pm 0.057
J 096	Male	19	1.021 \pm 0.221	0.564 \pm 0.025
J 097	Male	53	2.268 \pm 0.206	2.591 \pm 0.055
J 098	Male	58	2.508 \pm 0.362	2.925 \pm 0.053
J 099	Male	10	1.179 \pm 0.219	0.658 \pm 0.013
J 100	Female	60	1.997 \pm 0.315	1.850 \pm 0.059
J 101	Male	16	0.999 \pm 0.224	0.593 \pm 0.018
J 102	Female	50	1.111 \pm 0.266	0.791 \pm 0.011
Average			1.460 \pm 0.044	1.338 \pm 0.003

Table 3.14 Average uranium concentration in urine samples of Tall Al-Ragrag (A) and Al-Jesira (J) residents as a function of gender

Residential region	No. of subject	Average uranium concentration in ($\mu\text{g/l}$) \pm S.D	
		FTA	KPA
Tall Al-Ragrag	77	1.293 ± 0.024	1.125 ± 0.001
Male	36	1.353 ± 0.036	1.163 ± 0.002
Female	41	1.239 ± 0.033	1.092 ± 0.002
Al-Jesira	25	1.460 ± 0.044	1.338 ± 0.003
Male	18	1.495 ± 0.053	1.344 ± 0.005
Female	7	1.454 ± 0.084	1.324 ± 0.005

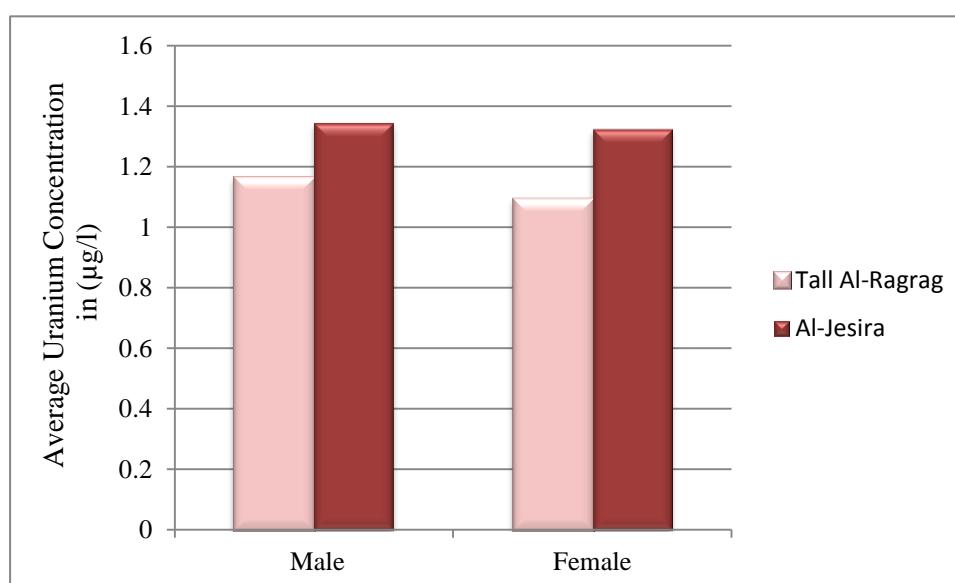


Figure 3.9 Average uranium concentration in urine samples of Tall Al-Ragrag (A) and Al-Jesira (J) residents as a function of gender using KPA technique

To find an age-dependency, Tall Al-Ragrag and Al-Jesira residents were further subdivided into seven age groups: 1 – 10 y, 11 – 20 y, 21 – 30 y, 31 – 40 y, 41 – 50 y, 51 – 60 y, and up to 60 y. Table (3.15), illustrates the results. The average values were found to be proportional to the age group. Figure 3.10 shows that the uranium concentration in the urine of Tall Al-Ragrag increased with age except for ages between 11 and 20 years, where a drop in concentration is observed. The average concentration of uranium in the age between 51 and 60 years was $1.840 \pm 0.037 \mu\text{g/l}$

and a factor of 1.4 higher than for age 41 – 50 years. It also is a factor of 1.5 higher than for 31 – 40 years and about twofold higher than that for the age between 1 and 10 years.

As shown in Fig. 3.11, for Al-Jesira volunteers, a significant increase of uranium concentration with age was observed. The excretion of uranium values in the age between 51 and 60 years was $2.455 \pm 0.032 \mu\text{g/l}$ and it is also about twofold higher than that for the age between 11 and 20 years and about threefold higher than that for the age between 1 and 10 years.

In earlier studies a dependency of the daily uranium excretion with age was postulated [130, 151]. The results of their smaller studies indicated that uranium excretion rates increased with age. Such an increase is also predicted by the ICRP uranium model [25, 27] under conditions of continuous level of intake. Moreover, such an increase with age is expected for several reasons ; for example dietary intake, especially during childhood, is correlated with age. Also under conditions of continuous intake uranium body burden (skeletal burden) will increase as a function of exposure period and the amount of uranium excreted because of bone turnover will increase in line with body burden.

Figure 3.12 illustrates the uranium concentration as a function of gender and age group. The uranium concentrations in urine of both male and female subjects less than 20 years were comparable. By contrast, the data of the adult age groups showed a wider distribution and differed between male and female. The lowest median value of $0.795 \pm 0.005 \mu\text{g/l}$ was determined for the female subjects between 1 – 10 years. In total , the uranium concentration of all adult male age groups is a factor of 1.4 higher than the uranium concentrations of the adult female groups.

The gender-specific difference may be resulted from the lower daily urine volumes of the female subjects. Possibly, the males ingested a little more uranium through food and beverages as they had a better opportunity to drinking water in sufficient amounts during work. The fact that the adult male showed a higher urine volume than female could also result from a larger daily intake of fluid.

A comprehensive study on uranium concentration in blood of occupational radiation field workers and residents of some Iraqi governorates revealed that uranium concentrations in blood samples of female are higher than those of male subjects [152]. Therefore, the lowest uranium excretion results of adult female were likely due to the uranium slowly release from bone and other tissue storage sites in the body.

Table 3.15 Uranium concentration in urine samples of Tall Al-Ragrag (A) and Al-Jesira residents (J) as a function of age

Area of study	Age group (years)	No. of subject			Average uranium concentration in ($\mu\text{g/l}$) \pm S.D	
		Male	Female	Total	FTA	KPA
Tall Al-Ragrag (A)	1 – 10	13	5	18	1.134 ± 0.046	0.879 ± 0.002
	11 – 20	3	5	8	1.017 ± 0.081	0.808 ± 0.004
	21 – 30	9	8	17	1.245 ± 0.055	1.095 ± 0.004
	31 – 40	6	11	17	1.405 ± 0.051	1.243 ± 0.004
	41 – 50	1	6	7	1.406 ± 0.081	1.355 ± 0.007
	51 – 60	3	5	8	1.653 ± 0.082	1.656 ± 0.006
	Up to 60	1	1	2	1.562 ± 0.168	1.658 ± 0.011
Al-Jesira (J)	1 – 10	4	0	4	1.308 ± 0.112	0.710 ± 0.006
	11 – 20	7	1	8	1.262 ± 0.075	1.056 ± 0.006
	31 – 40	2	2	4	1.361 ± 0.095	1.175 ± 0.007
	41 – 50	2	3	5	1.658 ± 0.113	1.807 ± 0.008
	51 – 60	2	1	3	2.258 ± 0.156	2.455 ± 0.032

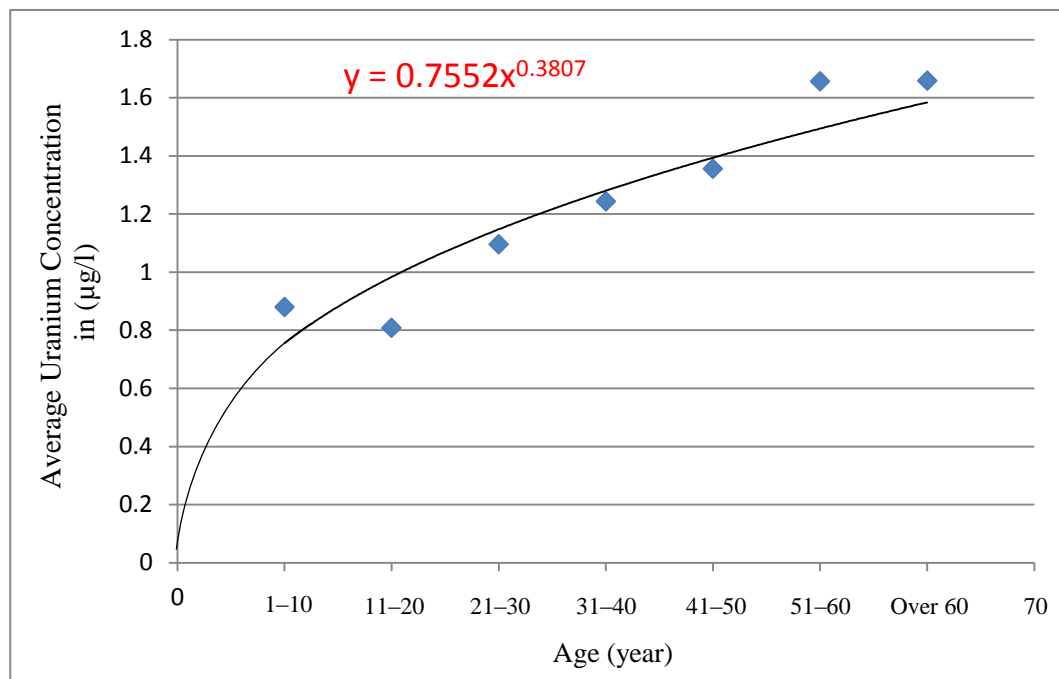


Figure 3.10 Uranium concentration in urine samples of Tall Al-Ragrag residents (A) as a function of age

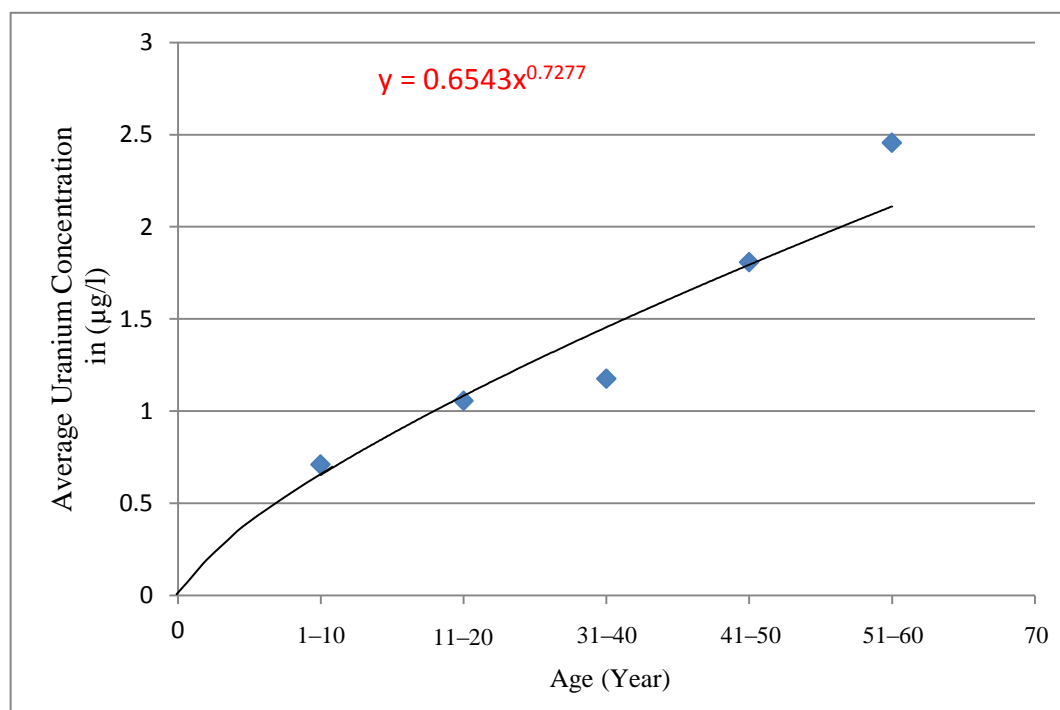


Figure 3.11 Uranium concentration in urine samples of Al-Jesira residents (J) as a function of age

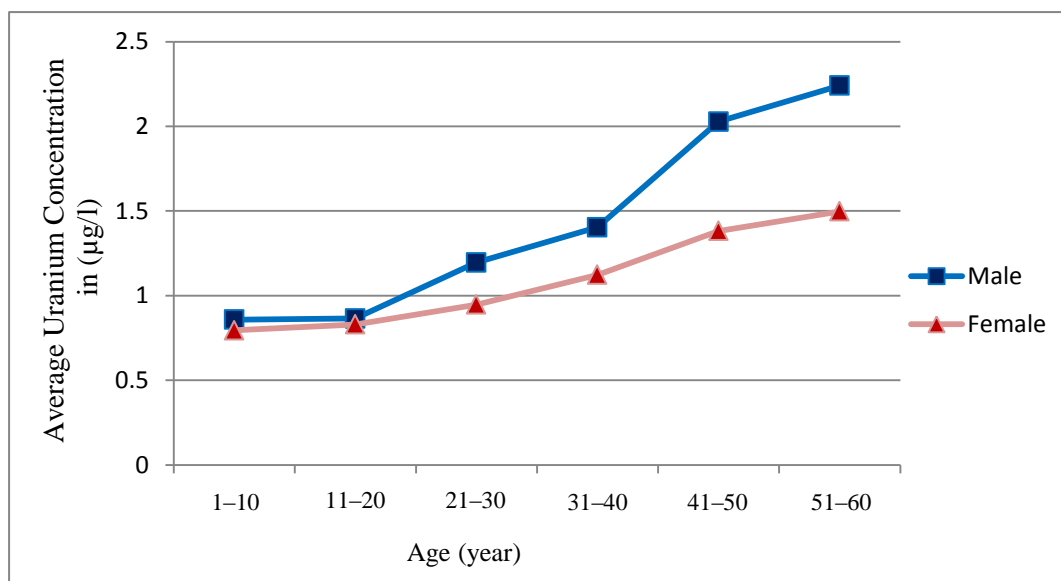


Figure 3.12 Uranium concentration in urine samples of Tall Al-Ragrag and Al-Jesira residents as a function of gender and age group

Figure 3.13 illustrates the uranium concentration as a function of smoking habit. From this figure we notice that the uranium concentration in urine of smokers is 2.025 ± 0.004 µg/l and a factor of 1.3 higher than for those of past-smokers. It also is a factor of 1.7 higher than for non-smokers. This suggested that smoker peoples are exposed to uranium levels greater than those non-smoker peoples. The same results obtained by using fission track method.

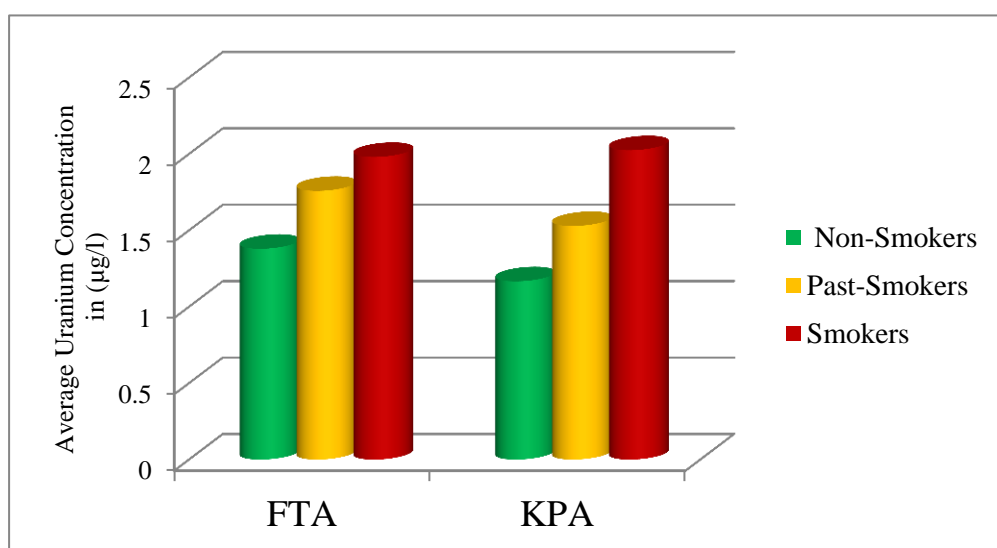


Figure 3.13 Uranium concentration in urine as a function of smoking habit

3.4 Comparison with other countries results

The elimination of uranium from the body is complex and involves multiple compartments and transfer rates. In experimental studies from the 1950s, the biokinetics of uranium were studied in humans after intravenous injections of uranium [23]. About two-thirds of the injected uranium dose was excreted over the first 24 h, and about 75 percent was excreted within 5 days. Of the remainder, most was slowly excreted over a period of several months, but a small portion was retained and excreted over a period of years.

In the present investigation study, uranium excretion in the urine of the all participants varied from 0.41 ± 0.008 to 5.26 ± 0.062 $\mu\text{g/l}$ with total average of 1.315 ± 0.001 $\mu\text{g/l}$. The obtained median value is about threefold higher than the ICRP reference man value of 0.5 $\mu\text{g/l}$. In other countries the levels of uranium excretion are different. Table (3.16) briefly summarizes recent studies from the last 20 years. This table shows that the highest recorded uranium excretion values were observed in unexposed resident subjects in Jordan [153] and in Southern Finland, where exceptionally high concentrations of uranium have been determined in private drilled wells in the granite areas of Southern Finland [154]. However, similar high mean excretion values of uranium were presented with occupational and non-occupational Syrian phosphate workers [155]. For most other countries the values reported are in the range of few tens of ng/l. The figures of the present study are higher than those of non-exposed subjects from Germany and USA, but lower than the values measured in Jordan or Southern Finland. Moreover, the results of uranium concentrations in urine of Akashat mining area and Al-Qaim fertilizer workers are almost matched the reported data of occupational and non-occupational Syrian phosphate workers obtained by Othman in 1993 [155].

In general, the uranium concentration found in urine of the Tall Al-Ragrag and Al-Jesira study group may result from the variable uranium intake through food and beverages or may be due to the use of well water for drinking in these areas which is might be rich in natural uranium.

Table 3.16 Urinary uranium excretion in unexposed subjects for different countries

Country	No. of subjects	Urinary uranium excretion values $\mu\text{g/l}$	Ranges $\mu\text{g/l}$	Reference
India	27	0.017 ± 0.014 (M \pm SD)	--	Dang et al. (1992) [48]
Syria	200	--	1.140–7.060	Othman (1993) [155]
USA	6	0.031 ± 0.020 (M \pm SD)	--	Medley et al. (1994) [49]
Germany	37	0.023 ± 0.018 (M \pm SD)	--	Schramel et al. (1997) [151]
USA	500	0.007 (GM), 0.035 (95th)	0.006 – 4.080	Ting et al. (1999) [156]
Jordan	60	0.320 (mean)	0.018 – 3.425	Al-Jundi et al. (2004) [153]
Kuwait	70	0.041 (mean)	0.058 – 0.390	Mohagheghi et al. (2005) [157]
Southern Finland	205	0.064 (median), 2.647 (95th)	1 – 8.450	Karpas et al. (2005) [154]
Selected regions in Iraq	194	1.315 (mean)	0.410 – 5.260	Present work

(M \pm SD) arithmetic mean \pm standard deviation

(GM) geometric mean

(95th) 95th percentile

Nevertheless, the overall mean of 33.4 mBq and the f_1 value of 0.02 would result in a yearly intake of 609.6 Bq. Applying the ingestion dose coefficient of 4.5×10^{-8} Sv/Bq [27, 44] the resulting effective internal dose would be only 27.4 $\mu\text{Sv/y}$. Even for the highest uranium excretion obtained in this study would be increased only by a factor of 4. The annual radiation effective dose for the members of the public according to the ICRP recommendation is 1 mSv [41]. These data show that even a significant increase of uranium intake as found in selected area in Iraq will not lead to substantial changes of internal radiation exposure.

The US Nuclear Regulatory Commission (NRC) has recommended that corrective actions must be taken when urine uranium concentrations in uranium mill workers exceed 15 $\mu\text{g/l}$ [158]. None of the participants' urine uranium concentrations exceeded this concentration. However, the participants' urine uranium concentrations were probably higher in the past.

Furthermore, standards for occupational exposures are derived for healthy adult workers and may not be protective of more sensitive members of the general population. In particular, people with preexisting renal disease, or taking potentially nephrotoxic medications (such as aminoglycoside antibiotics), may be more susceptible to the nephrotoxic effects of uranium.

3.5 Comparison between KPA and FTA results

One of the objectives of this study is to evaluate the kinetic phosphorescence analysis (KPA) and fission track analysis (FTA) techniques for their ability to measure microgram quantities of uranium in urine. The resulting data were evaluated to determine the outlier data, data correlation, uncertainty, detection limit and limitation of analysis due to analytical and technical issues. Table (3.17) summarizes the main comparison parameters of the two methods.

Table 3.17 Comparison of the main parameters of KPA and FTA methods

Item	KPA	FTA
Sample volume (ml)	5	0.1
Sample digestion	Needed	Not needed
Sample preparation time (days)	3	3
Irradiation (days)	Not needed	7
Reagent needed	Large volumes	Very limited
Analysis time (min)	5	360 with the etching time
Counting time (min)	1	5
Minimum detection limit ($\mu\text{g/l}$)	0.01	0.01 – 0.1 [111]
Uncertainty	2%	10 – 18%
Analysed isotopes	Total uranium	Total uranium, ^{235}U , ^{238}U

3.5.1 Outlier data:

Tables (3.1 – 3.6) and (3.9 – 3.13) represents comparative results of the uranium concentration obtained by kinetic phosphorescence analysis (KPA) and fission track analysis (FTA) techniques. No significant differences

or tendency of the results are seen. Except for high concentrations, the differences become more significant.

Out of the 194 samples analysed, 58% of samples showed less uranium concentration when determined by kinetic phosphorescence analysis as compared to the fission track technique, while 28% gave comparable values and the rest 14% gave higher values. As most of the samples showed less uranium content by kinetic phosphorescence analysis than from track etch technique, the reason may be attributed to the background tracks existence in the later.

The ratio of uranium concentration determined by kinetic phosphorescence analysis to that of the fission track technique varied from a minimum of 0.37 to maximum of 2.42, with a mean value of 0.85. Only 3 % samples showed a ratio < 0.5 and only 2 % showed a ratio ≥ 1.2 . A ratio ≥ 1.5 has been found in samples having very high uranium concentration (e.g., U 215 and U 304).

The high ratio (about 1.5) may also be attributed to the suspended uranium particulate matter recorded by KPA technique as it involves the analysis of a considerable volume of urine (about 5 ml), but probably missed in the track etch technique as it involves the analysis of a small amount of urine (about 0.1 ml).

3.5.2 Correlation between KPA and FTA data

Figure 3.14 illustrates the correlation between the uranium concentrations data obtained by KPA and those by FTA. The red solid line represents the condition at which KPA data coincide that of FTA. The figure is subdivided into three regions; the first region for the concentration below 1.5 $\mu\text{g/l}$, as poor correlation between the two methods is observed. The figure also shows a good linear correlation in the region between 1.5 and 3 $\mu\text{g/l}$ with correlation coefficient of 0.92, which shows good agreement between the two techniques in this region. For higher uranium concentration the linear correlation coefficient between the two measurements was 0.70 and the FTA results are lower than KPA results by a factor of 1.4.

In general, the FTA results are somewhat higher than that of KPA at the low concentrations and lower at higher concentrations. As mentioned

before, poor FTA performance is related to track density, sample inhomogeneity, background radiation from cosmic ray and other environmental storing conditions. The residues left by evaporating urine droplets may be redistributed with sufficient homogeneity for fission track determination of their uranium content by placing drops of diluted collodion on the residue.

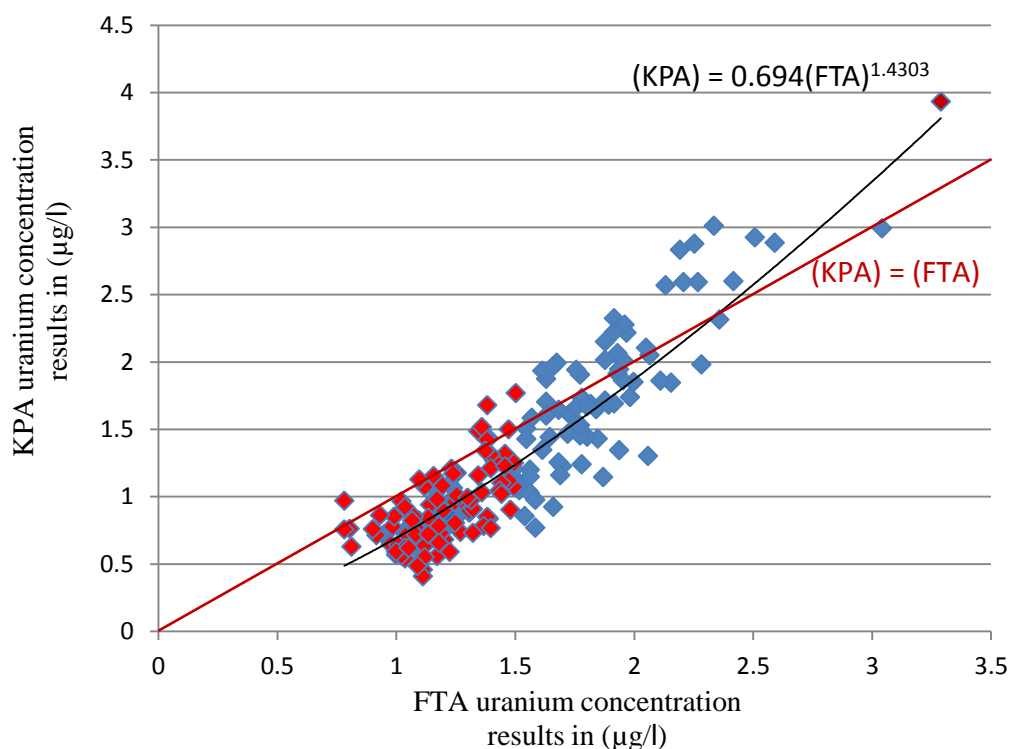


Figure 3.14 Correlation between uranium concentrations determined by KPA and uranium concentrations by FTA for all investigated urine samples, red labels for poor correlation regions and blue labels for good correlation region.

3.5.3 Uncertainty

KPA gave the best uncertainty among all of the measurements of uranium concentration in urine. It is likely that the analytical blank control by KPA played a key role in their well-controlled performance for measurement uncertainty. FTA had wider uncertainty (by a factor of about tenfold larger than for KPA) because of the inherent uncertainty limitations for FTA due to counting problems. For few tracks the resolution is good with poor uncertainty and for high track density the resolution is poor due to the track overlapping and the presence of clusters, so uncertainty and bias are adversely affected.

3.5.4 Detection limit

The detection limit (DL) is an estimate of the minimum sample concentration that can be detected with a 99% confidence. The obtained value of detection limit for uranium by KPA was 0.01 $\mu\text{g/l}$. In Brina and Miller study [88] KPA detection limit of 0.005 $\mu\text{g/l}$ in urine samples was achieved.

FTA method gives a detection limit of 0.1 $\mu\text{g/l}$ in water samples. The detection sensitivity of 0.01 $\mu\text{g/l}$ for uranium determination in natural water was achieved [111]. The use of different irradiation times and neutron fluxes may control this limit.

3.5.5 Technical issues

KPA technique is fast and the phosphorescence lifetime determination capabilities of the KPA offer additional selectivity. The accuracy of the method was $\pm 2\%$ RD, with a precision of ± 2 to $\pm 6\%$ RSD for the range of 0.05 to 100 $\mu\text{g/l}$ of solution. Statistical analysis showed that by level (high or low), no significant analyst-to-analyst or day-to-day variations were found.

It should be recognized that the diluted standards may not be stable for long periods of time due to uranium adsorption onto glass container walls. For example, a 100 $\mu\text{g/l}$ standard solution has been successfully stored in extra clean previously soaked glass container for 6 months, but standard solutions of 0.5 and 1 $\mu\text{g/l}$ had to be prepared on a weekly basis.

The stability of response and the sensitivity of SSNTD's are depended on environmental conditions. Large variations in the efficiency for alpha-particle detection were observed in some detectors exposed to solar light. Exposure to oxygen distorts the surface quality of un-doped CR-39, and creates poor transparency, thus resulting in decreased accuracy of measurement when using transmitted illumination. Ultraviolet exposure can also dramatically change the properties of polymeric track detectors.

3.5.6 Analytical issues

Sample preparation procedure in terms of duration, complexity, the counting time and interferences are also parameters should be considered in the choice of the analytical method. Recent KPA devices give the possibility to prepare up to 20 samples together. There is no need of big sample volumes and the method is less time consuming; the analysis of 20 samples takes about an hour. The FTA method is quick and there is no need for special sample preparation. The track counting and analysis takes only few minutes and the usual sample volume is 0.1 ml but the sample irradiation takes 7 days. The advantages of FTA are also that the method does not produce waste, no interference and the amount of reagent needed is very limited.

A disadvantage of KPA arises from the colour quenching and the organic materials content of the sample. Another disadvantage is that only total uranium content can be estimated. With the kinetic phosphorescence analysis method, it is not possible to analyze coloured samples. Several rare earth elements like calcium, magnesium, manganese, iron, etc. are quenching agents. Furthermore, higher uranium concentrations of different samples need higher dilution. If the uranium concentration is high, the sample is diluted prior the analysis. The lifetime should be between 200 and 300 μ s. If the lifetime is out of this range there may be a quenching problem and the sample may need to be diluted.

In Moore and Williams's study [134], the effect of potential interferences on KPA analysis was determined for K, Na, Mg, Ca and transition metals Cr, Mn, Fe, Co, Ni and Cu. These elements are commonly found in milk and urine. They reported that the concentrations of possible interfering elements in normal, routine urine samples are too low to affect the results of the total uranium in urine analysis using this KPA method.

3.6 Conclusions

This study highlights the importance of having individual or at minimum local reference baseline values for uranium concentration in urine of potentially exposed subjects. This reference is essential in order to accurately determine the severity of accidental incorporations which are potentially chemically and radiologically toxic. The result of the present study leads to the following conclusions:

1. The data presented in this study revealed current KPA and FTA capabilities for uranium determinations in urine. It is apparent that kinetic phosphorescence analyzer is currently capable of successfully competing with FTA's sensitivity, and at considerably higher uncertainty down to the 0.01 $\mu\text{g}/\text{sample}$ level. In addition, KPA has the potential to provide more accurate and precise measurements than FTA. Furthermore, it is feasible that KPA can provide higher sensitivity measurements of uranium for routine occupational radiobioassay programs and emergency assessment evaluations than alpha spectrometry.
2. KPA results indicated the tremendous ability to accurately and precisely measure microgram quantities of uranium in urine. FTA can also measure microgram quantities of uranium in urine, but with considerably larger uncertainty than kinetic phosphorescence analyzer.
3. Uranium concentration in urine from a normal human population exposed only to natural sources in the environment is higher when measured by the older fission track techniques than by more sensitive modern kinetic phosphorescence analysis technique.
4. The uranium concentration in the urine of phosphate mine and fertilizer workers increased with the increasing of employment duration.
5. The uranium level in the urine of the phosphate mine residents is higher than the control value from people living in Al-Qaim.
6. The persistence of high excretion rates of uranium in urine of former uranium purification workers, more than 20 years since active exposure, indicates that the body burden of uranium must still be significant, whether retained in lungs, lymphatic system, kidneys or bone.

7. The uranium levels in the urine of Tall Al-Ragrag and Al-Jesira sites are higher than the value of control group and closer to the phosphate workers value.
8. The results show that even with a chronic exposure to uranium in phosphate mine and fertilizer sites, the uranium concentration in urine is far below the concentration of 40 μg of natural uranium in a litre of urine of an individual that corresponds to the maximum permissible body burden [26].
9. The uranium mean values of different age groups were found to be proportional to age up to 60 years and uranium concentration in urine of male is higher than female for each age group
10. In addition the results presented here support previous studies which suggested that the uranium concentration in normal population is appearing to have a certain dependence on the smoking habits of the individuals.

3.7 Recommendations and suggestions for future studies

In addition to the present study and according to our results and conclusions, many ideas for the suggestions concerning the accomplishments and development of these measurements in future can be considered here:

1. Establishment of biological monitoring program to estimate the radiation internal doses for Iraqi population and the radiation workers occupationally exposed to uranium and other radioactive elements high concentrations.
2. Studying uranium transfer in the food chain from soil to plants, animals and man.
3. Using the pulsed laser induced kinetic phosphorimetry technique for uranium routine analysis of environmental, geological and biological samples.
4. Comparison of direct and chemical recovery corrected kinetic phosphorescence analysis for determination of uranium in urine and other biological samples.

References:

- [1] Greenwood N.N. and Earnshaw A., "Chemistry of the Elements", Pergamon Press, Oxford, (1984).
- [2] Favre-Réguillon A., Lebuzy G., Murat D., Foos J., Mansour C. and Drayed M., *Selective removal of dissolved uranium in drinking water by nanofiltration*, Water Res. **42**, 1160-1166, (2008).
- [3] Budavari S., "The Merck Index: An Encyclopedia of Chemicals, Drugs, and Biologicals", 14th edition. Merck & Co., New Jersey, (2008).
- [4] European Food Safety Authority (EFSA), *Uranium in foodstuffs, in particular mineral water; scientific opinion of the panel on contaminants in the food chain*, EFSA J. **1018**, 1-59, (2009).
- [5] International Atomic Energy Agency (IAEA), "Management of Reprocessed Uranium Current Status and Future Prospects", IAEA publication, (2007).
- [6] International Atomic Energy Agency (IAEA), "Radiological Conditions in Areas of Kuwait with Residues of Depleted Uranium", IAEA publication, (2003).
- [7] Cothorn C.R. and Lappenbusch W.L., *Occurrence of uranium in drinking water in the US*, Health Phys. **45**, 89-99, (1983).
- [8] Lide D.R., "Handbook of Chemistry and Physics", 90th edition, CRC Press, Boca Raton, Florida, (2009).
- [9] Ebbs S.D., Brady D.J. and Kochian L.V., *Role of uranium speciation in the uptake and translocation of uranium by plants*, J. Exp. Bot. **49**, 1183-1190, (1998).
- [10] Morss L.R., Edelstein N.M. and Fuger J., "The Chemistry of the Actinide and Transactinide Element", 4th edition, Springer, Dordrecht, (2006).
- [11] Roessler C.E., Smith Z.A., Bolch W.E. and Prince R.J., *Uranium and radium-226 in Florida phosphate materials*, Health Phys. **37**, 267-269, (1979).
- [12] Merkel B., Planer-Friedrich B. and Wolkersdorfer C., *Uranium in the Aquatic Environment*. Springer-Verlag, Berlin, (2002).

- [13] Dreesen D.R., Williams J.M., Marple M.L. Gladney E.S. and Perrin D.R., *Mobility and bioavailability of uranium mill tailings constituents*, Environ. Sci. Technol. **16**, 702-709, (1982).
- [14] Tadmor J., *Atmospheric release of volatilized species of radioelements from coal-fired plants*, Health Phys. **50**, 270-273, (1986).
- [15] German Federal Environment Agency, “Uranium and Human Bio-monitoring”, (2005).
- [16] United Nations, “Sources and Effects of Ionizing Radiation”, (Report to the General Assembly), Scientific Committee on the Effects of Atomic Radiation (UNSCEAR), UN, New York, (2000).
- [17] Fisenne I.M., Perry P.M., Decker K.M. and Keller H.K., *The daily intake of $^{234,235,238}\text{U}$, $^{228,230,232}\text{Th}$, and $^{226,228}\text{Ra}$ by New York City residents*, Health Phys. **53**, 357-363, (1987).
- [18] Priest N.D., *Toxicity of depleted uranium*, Lancet **357**, 244-246, (2001).
- [19] Agency for Toxic Substances and Disease Registry (ATSDR), “Toxicological Profile for Uranium”, U.S. Department of Health and Human Services, Public Health Service, Atlanta, GA. (1999).
- [20] Fisenne I.M., Perry P.M. and Harley N.H., *Uranium in humans*, Radiat. Prot. Dosim. **24**, 127-131, (1988).
- [21] German National Research Center for Environment and Health, Institute of Radiation Protection, “A Study of Uranium Excreted in Urine An Assessment of Protective Measures Taken by the German Army KFOR Contingent”, Germany, (2001).
- [22] Wrenn M.E., Durbin P.W., Howard B., Lipsztein J., Rundo J., Still E.T. and Willis D.L., *Metabolism of ingested uranium and radium*, Health Phys. **48**, 601-633, (1985).
- [23] International Commission on Radiological Protection (ICRP), “Age Dependent Doses to Members of the Public from Intake of Radionuclides: Part 5: Compilation of Ingestion and Inhalation Dose Coefficients”, ICRP Publication 72, Annals of the ICRP, Vol. 25(2), (1996).

- [24] Leggett R.W. and Harrison J.D., *Fractional absorption of ingested uranium in humans*, Health Phys. **68**, 484-498, (1995).
- [25] International Commission on Radiological Protection (ICRP), “Age Dependent Doses to Members of the Public from Intake of Radionuclides: Part 4 Inhalation Dose Coefficients”, ICRP Publication 71, Annals of the ICRP, (1995).
- [26] World Health Organization (WHO), “Depleted Uranium Sources, Exposure and Health Effects”, Technical Report, (2001).
- [27] International Commission on Radiological Protection (ICRP), “Age Dependent Doses to Members of the Public from Intake of Radionuclides: Part 3 Ingestion Dose Coefficients”, ICRP Publication 69, Annals of the ICRP, Vol. 25(1), (1995).
- [28] Leggett R.W., *Basis for ICRP's age-specific model for uranium*, Health Phys. **67**, 589-610, (1994).
- [29] Sontag W., *Multicompartment kinetic models for the metabolism of americium, plutonium and uranium in rats*, Hum. Toxicol. **5**, 163-173, (1986).
- [30] Berlin M. and Rudell B., “Uranium. In: Handbook on the Toxicology of Metals”, 2nd edition, (Friberg L., Nordberg G.F. and Vouk V.B. Eds.), pp. 623-637, Elsevier Science Publishers, Amsterdam, (1986).
- [31] Tracy B.L., Quinn J.M., Lahey J., Gilman A.P., Mancuso K., Yagminas A.P. and Villeneuve D.C., *Absorption and retention of uranium from drinking water by rats and rabbits*, Health Phys. **62**, 65-73, (1992).
- [32] Cooper J.R., Stradling G.N., Smith H. and Ham G.E., *The behavior of uranium-233 oxide and uranyl-233 nitrate in rats*, Int. J. Radiat. Biol. Re. **41**, 421-433, (1982).
- [33] Stevens W., Bruenger, F. W., Atherton D.R., Smith J.M. and Taylor G.N., *The distribution and retention of hexavalent ²³³U in the beagle*, Radiat. Res. **83**, 109-126, (1980).
- [34] Bowman F.J. and Foulkes, E.C., *Effects of uranium on rabbit renal tubules*, Toxicol. Appl. Pharm. **16**, 391-399, (1970).

- [35] Health Canada, “Uranium in Drinking Water - Supporting Documentation In: Guidelines for Canadian Drinking Water Quality”, Health Canada, Ottawa, Ontario, (1999).
- [36] World Health Organization (WHO), “Guidelines for Drinking Water Quality”, 2nd edition, Addendum to Vol. 2, Health Criteria and Other Supporting Information, WHO_EOS_98.1, Geneva, 283, (1998).
- [37] Gilman A.P., Villeneuve D.C., Secours V.E., Yagminas A.P., Tracy B.L., Quinn J.M., Valli V.E., Willes R.J. and Moss M.A., *Uranyl nitrate: 28-day and 91-day toxicity studies in the Sprague-Dawley rat*, Toxicol. Sci. **41**, 117-128, (1998).
- [38] Zarkadas Ch., Karydas A.G. and Paradellis T., Determination of uranium in human urine by total reflection X-ray fluorescence, Spectrochim. Acta Part B 56, 2505-2511, (2001).
- [39] Singh N.P., Burleigh D.P., Ruth H.M. and Wrenn M.E., Daily U intake in Utah residents from food and drinking water, Health Phys., 59, 333-337, (1990).
- [40] International Commission on Radiological Protection (ICRP), “The Biological Basis for Dose Limitation in the Skin”, ICRP Publication 59, (1992).
- [41] International Commission on Radiological Protection (ICRP), “Recommendations of the International Commission on Radiological Protection”, ICRP Publication 21 (1-3), (1990).
- [42] Bleise A., Danesi P.R. and Burkart W., *Properties, use and health effects of depleted uranium (DU): a general overview*, J. Environ. Radioactiv. **64**, 93-112, (2003).
- [43] United Nations Scientific Committee on the Effects of Atomic Radiation (UNSCEAR), “Sources and Effects of Ionizing Radiation: Report to the General Assembly, with Scientific Annexes”, United Nations, New York, (1993).
- [44] Food and Agriculture Organization of the United Nations, International Atomic Energy Agency, International Labour Organization, OECD Nuclear Energy Agency, Pan American Health Organization, World Health Organization, “International Basic Safety

- Standards for Protection against Ionizing Radiation and for the Safety of Radiation Sources”, Safety Series No. 115, IAEA, Vienna, (1996).
- [45] Putnam D. F., *Composition and concentrative properties of human urine*, National Aeronautics and Space Administration (NASA), Washington, D.C., USA, (1971).
- [46] Taylor D.M. and Taylor S.K., *Environmental uranium and human health*, Rev. Environ. Health **12**, 147-157, (1997).
- [47] International Commission on Radiological Protection (ICRP), “Report of the Task Group on Reference Man”, ICRP Publication 23, Pergamon, Oxford, (1975).
- [48] Dang H.S., Pullat V.R. and Pillai K.C., *Determining the normal concentration of uranium in urine and application of the data to its biokinetic*, Health Phys. **62**, 562-566, (1992).
- [49] Medley D.W., Kathren R.L. and Miller A.G., *Diurnal urinary volume and uranium output in uranium workers and unexposed controls*, Health Phys. **67**, 120-122, (1994).
- [50] Bogard J. S., *Review of uranium bioassay techniques*, Oak Ridge National Laboratory, ORNL-6857, (1996).
- [51] Harley J.H., Radiochemical determination of isotopic uranium, method, E-U-04, HASL-300, Environmental Measurements Laboratory, New York, (1979).
- [52] Dupzyk I.A. and Dupzyk R.J., Separation of uranium from urine for measurement by fluorometry or isotope-dilution mass spectrometry, Health Phys., 36,526-529, (1979).
- [53] Gladney E.S., Moss W.D., Gautier M.A. and Bell M.G., *Determination of U in Urine: Comparison of ICP-Mass Spectrometry and Delayed Neutron Assay*, Health Phys. **57**, 171-175, (1989).
- [54] Moreno E., Reyes P. and de la Rosa J.M., in “Labview - Modeling, Programming and Simulations”, (De Asmundis R., Ed.), pp. 177-200, Intach Open, Croatia, (2011).
- [55] Skoog D. A., Holler F. J., Crouch S. R., “Principles of Instrumental Analysis”, 6th edition, Thomson higher education, USA, (2007).
- [56] Becker R.S., “Theory and Interpretation of Fluorescence and Phosphorescence”, Wiley, USA, (1969).

- [57] Valeur B, "Molecular Fluorescence: Principles and Applications", Wiley-Verlag, Weinheim, Germany, (2001).
- [58] Wehry, E.L., "Modern Fluorescence Spectroscopy", Vol. 1, Plenum press, New York, (1976).
- [59] Hover T., "An Introduction Fluorescence Spectroscopy", ParkinElmer Ltd. Inc, pp. 3-38, (2000).
- [60] Lakowicz J.R., "Principles of Fluorescence Spectroscopy", 3rd edition, Maryland, USA, (2006).
- [61] Hercules D.M., "Fluorescence and Phosphorescence Analysts", Wiley-Interscience, New York, (1965).
- [62] McGlynn S.P., Azumi T. and Kinoshita M., "Molecular Spectroscopy of Triplet State", Prentice-Hall, USA, (1969).
- [63] Barltrop J.A. and Coyle J.D., "Principles of Photochemistry", Wiley, New York, (1978).
- [64] Turro N.J., "Molecular Photochemistry", Benjamin, New York, (1967).
- [65] Chen R.F. and Edelhoch H., "Biochemical Fluorescence: Concepts", Vol. II, Marcel Dekker Inc., New York, (1976).
- [66] Kuijt J., Ariese F., Brinkman U.A. Th. and Gooijer C., *Room temperature phosphorescence in the liquid state as a tool in analytical chemistry*, Analytica Chimica Acta **488**, 135-171, (2003).
- [67] Hollas J.M., "Modern Spectroscopy" 4th edition, John Wiley & Sons, Chichester, England (2004).
- [68] Duarte F. J., in "Tunable Lasers Handbook", (Duarte F.J., Ed.), pp. 167-215, Academic Press, USA, (1995).
- [69] Duarte F.J., in "High Power Dye Lasers", (Duarte F.J., Ed.), pp. 7-43, Springer-Verlag, Berlin, (1991).
- [70] Bass I.L., Bonanno R.E., Hackel R.P. and Hammond P.R., *High-average-power dye laser at Lawrence Livermore National Laboratory*, Appl. Opt. **33**, 6993-7006, (1992).
- [71] Hollberg L., in "Dye Laser Principles" (Duarte F. J. and Hillman L. W. Eds.), pp. 185-238, Academic Press, New York, (1990).

- [72] Finch A., Chen G., Sleat W. and Sibbett W., *Pulse asymmetry in the colliding-pulse mode-locked dye laser*, J. Mod. Optic. **35**, 345-354, (1988).
- [73] Fork R.L., Brito Cruz C.H., Becker P.C. and Shank C.V., *Compression of optical pulses to six femtoseconds by using cubic phase compensation*, Opt. Lett. **12**, 483-485, (1987).
- [74] Demtröder W., “*Laser Spectroscopy Vol. 1: Basic Principles*”, 4th edition, Springer-Verlag, Berlin, (2008).
- [75] Hecht J., “*Dye Lasers: the User Guidebook*”, 2nd edition, McGraw-Hill, New York, (1992).
- [76] Titterton D.H, in “*Handbook of Laser Technology and Applications Vol. 2: Laser Design and Laser systems*”, (Webb E.C. and Jones J.D.C. Eds.), pp. 1115-1142, Institute of Physics, Philadelphia, (2004).
- [77] Koechner W., “*Solid-State Laser Engineering*”, Springer, Berlin, (1992).
- [78] Costela A., García-Moreno I. and Sastre R., in “*Tunable Laser Applications*”, 2nd edition, (Duarte F.J. Ed.), pp. 97-120, CRC Press, New York, (2009).
- [79] Duarte F.J., “*Tunable Laser Optics*”, Academic Press, New York, (2003).
- [80] Regard W.W., *Saturation effects in high gain lasers*, J. Appl. Phys. **36**, 2487-2490, (1965).
- [81] Schäfer F.P., *Organic dye solution laser*, Appl. Phys. Lett. **9**, 306-309, (1966).
- [82] Corney A., “*Atomic and Laser Spectroscopy*”, Oxford University Press, New York, (1977).
- [83] Hänsch T.W., *Repetitively pulsed tunable dye laser for high resolution spectroscopy*, Appl. Optics **11**, 895-898, (1972).
- [84] Vo-Dinh T., “*Room Temperature Phosphorimetry for Chemical Analysis*”, John Wiley and sons, New York, (1984).
- [85] Fisher R.P. and Winefordner J.D., *Pulsed source-time resolved phosphorimetry*, Anal. Chem., **44**, 948-952, (1972).

- [86] Veselsky J.C., Kwiecinska B., Wehrstien E. and Suschny O., *Determination of uranium in minerals by laser fluorometry*, Analyst **113**, 451-455, (1988).
- [87] Hemmila I., *Time-resolved fluorometric determination of terbium in aqueous solution*, Anal Chem. **57**, 1676-1681, (1985).
- [88] Brina R. and Miller A.G., *Direct detection of trace levels of uranium by laser-induced kinetic phosphorimetry*, Anal. Chem. **64**, 1413-1418, (1992).
- [89] Chemchek instruments, "Kinetic Phosphorescence Analyzer, KPA-11 Operation Manual and Documents", (2006).
- [90] Brina R. and Miller A.G., *Determination of uranium and lanthanides in real-world samples by kinetic phosphorescence analysis*, Spectroscopy **8**, 25-31, (1993).
- [91] Croatto P.V., Frank I.W., Johnson K.D., Mason P.B. and Smith M.M., *Evaluation of kinetic phosphorescence analysis for the determination of uranium*, Research and Development Report , New Brunswick Laboratory, Argonne, Illinois, USA, (1997).
- [92] Gaft M., Reisfeld R. and Panczer G., "Luminescence Spectroscopy of Minerals and Materials", Springer-Verlag, Berlin, Heidelberg, (2005).
- [93] Marfunin A.S., "Spectroscopy, Luminescence, and Radiation Centers in Minerals", Springer-Verlag, Berlin, (1979).
- [94] Meinrath G., *Aquatic chemistry of uranium a review focusing on aspects of environmental chemistry*, FOG, Freiberg University, Passau, Germany, Vol.1, (1998).
- [95] Dieke G.H., Duncan A.B.F., "Spectroscopic Properties of Uranium Compounds; National Nuclear Energy Series", Div. III, Vol.2, McGraw-Hill, New York, (1949).
- [96] Jones L.H., *Systematics in the vibrational spectra of uranyl complexes*, Spectrochim. Acta A **10**, 395-403, (1958).
- [97] Rabinowitch E. and Belford R. L., "Spectroscopy and Photochemistry of Uranyl Compounds", Pergamon press, New York, (1964).
- [98] Kaminski R., Purcell F.J. and Russavage E., *Uranyl phosphorescence at the parts-per-trillion level*, Anal. Chem. **53**, 1093-1096, (1981).

- [99] Schulman S.G., "Molecular Luminescence Spectroscopy, Methods and Applications: Part 1", Wiley, New York, (1984).
- [100] Sill C.W. and Peterson H.E., *Fluorescence test for uranium in aqueous solution*, Anal. Chem. **19**, 646-651, (1947).
- [101] Centanni F.A., Ross A.M. and De Sesa M.A., *Fluorometric determination of uranium*, Anal. Chem., **28**, 1651-1675, (1956).
- [102] Thatcher L.L., Barker F.B., *Determination of uranium in natural waters*, Anal. Chem., **29**, 1575-1578, (1967).
- [103] Yokoyama Y., Moriyasu M. and Ikeda S., *Electron transfer mechanism in quenching of uranyl luminescence by halide ions*, J. Inorg. Nucl. Chem. **38**, 1329-1333, (1976).
- [104] Moriyasu M., Yokoyama Y. and Ikeda S., *Quenching mechanisms of uranyl luminescence by metal ions*, J. Inorg. Nucl. Chem. **39**, 2205-2209, (1977).
- [105] Velićković D., Mirić I., Mirić P. and Bojović P., *Determination of natural uranium traces using solid state track detectors*, Proceeding of the 11th Inter. Conf. on SSNTDs, Bristol, pp583, (1981).
- [106] Gohn C.E. and Gold R., *Computer-controlled microscope for automatic scanning of solid-state nuclear track recorders*, Rev. Sci. Inst. **43**, 12-17, (1972).
- [107] Fleisher R.L., Price P.B. and Walker R.M., "Nuclear Tracks in Solids: Principles and Applications", University of California Press, Berkeley, (1975).
- [108] Espinosa G., Meyer K. and Gammage R. B., *Soil measurements by nuclear track detectors*, Radiat. Meas. **25**, 401-404, (1995).
- [109] Nikezic D. and Yub K.N., *Formation and growth of tracks in nuclear track materials*, Mat. Sci. Eng. R. **46**, 51-123, (2004).
- [110] Fleischer R.L., Price P.B. and Walker R.M., *Ion explosion spike mechanism for formation of charged-particle tracks in solids*, J. Appl. Phys. **36**, 3645-3652, (1965).
- [111] Durrani S.A. and Bull R.K., "Solid-State Nuclear Detection; Principles, Methods, and Applications", Pergamon press, UK, (1987).
- [112] Hepburn C. and Windle A.H., *Solid state nuclear track detectors*, J. Mater. Sci. **15**, 279-301, (1980).

- [113] Yammamoto M., Yasuda N., Kiazuka Y., Yamagishi M., Kanai N., Ishigure N., Furukawa A., Kurano M., Miyahara N., Nakazawa M., Doke T. and Ogura K., *CR-39 sensitivity analysis on heavy ion beam with atomic force microscope*, Radiat. Meas. **28**, 227-2330, (1997).
- [114] Price P.B., Lai D., Tamtance A.S. and Perelygin V.P., *Characteristics of tracks of ions of $14 \leq Z \leq 36$ in common rock silicates*, Earth Planet. Sc. Lett. **19**, 377-395, (1973).
- [115] Tsoufanidis N., “Measurement and Detection of Radiation”, 2nd edition, Taylor & Francis, University of Missouri-Rolla, UK, (1987).
- [116] Benton E.V., *On latent track formation in organic nuclear charged particle track detectors*, Radia. Effec. **2**, 273-280, (1970).
- [117] Fleischer R.L., Price P.B. and Walker R.M., *Solid-state track detectors: applications to nuclear science and geophysics*, Ann. Rev. Nucl. Sci. **15**, 1-28, (1965).
- [118] Fleisher R.L. and Price P.B., *Charged particle tracks in glass*, J. Appl. Phys., **34**, 2903-2904, (1963).
- [119] Zaki M.F., *Gamma-Induced modification on optical band gap of CR-39 SSNTD*, Braz. J. Phys. **38**, 558-562, (2008).
- [120] Cassou R.M. and Benton E.V., *Properties and applications of CR-39 polymeric nuclear track detector*, Nucl. Track Detection **2**, 173-179, (1978).
- [121] International Atomic Energy Agency (IAEA), “Analytical Techniques in Uranium Exploration and Ore Processing”, Technical reports series No. 341, IAEA, Vienna, (1992).
- [122] Hashimoto T., *Determination of the uranium content in sea water by a fission track method with condensed aqueous solution*, Anal. Chim. Acta **56**, 347-354, (1971).
- [123] Reimer G.M., *Uranium determination in natural water by the fission-track technique*, J. Geochem. Explor. **4**, 425-431, (1975).
- [124] McCorkell R.H., *A fission track method for determination of uranium in natural waters for geochemical exploration*, CIM Bull. **76**, 89-92, (1983).

- [125] Singh H., Singh J., Singh S. and Bajwa B.S., *Uranium concentration in drinking water samples using the SSNTDs*, Indian J. Phys. **83**, 1039-1044, (2009).
- [126] Chakarvarti S.K., Lal N. and Nagpaul K.K., *Content of uranium trace in urine determined from fission*, Int. J. Appl. Radiat. Iso. **31**, 793-795, (1980).
- [127] Igarashi Y., Yamakawa A., Seki R. and Ikeda N., *Determination of uranium in Japanese human tissues by the fission track method*, Health Phys. **49**, 707-712, (1985).
- [128] Cheng Y.L., Lin J.Y. and Hao X.H., *Trace uranium determination in beverages and mineral water using fission track techniques*, Nucl. Tracks Rad. Meas. **22**, 853-855, (1993).
- [129] Ciubotariu M., Danis A., Staicul L., Iancu E., Dumitrescu G. and Cucu M., *Studies of the uranium biodistribution in animals contaminated by ingestion using fission track method*, Radiat. Meas. **28**, 353-356, (1997).
- [130] Al-Timimi W.A.K., *Determination of depleted uranium concentration in biological sample*, M.Sc. Thesis, Al-Mustansiriyah University, (2000).
- [131] Singh J., Singh L. and Kher S., *A comparison of fission track and laser fluorometry techniques for uranium analysis in water samples*, Radiat. Meas. **36**, 517-519, (2003).
- [132] Al-uboode S.T.A., *Determination of alpha emitters concentration in human urine via PM-355 SSNT Detector*, M.Sc. Thesis, Al-Nahrain University, (2006).
- [133] Sawant P.D., Prabhu S., Kalsi P.C. and Pendharkar K.A., *Estimation of trace levels of plutonium in urine samples by fission track technique*, J. Radioanal. Nucl. Chem. **279**, 179-183, (2009).
- [134] Moore, L.L., Williams, R.L., *A rapid method for determining nanogram quantities of uranium in urine using the kinetic phosphorescence analyzer*, J. Radioanal. Nucl. Chem. **156**, 223-233, (1992).
- [135] Hedaya M.A., Birkenfeld H.P. and Kathren R.L., *A sensitive method for the determination of uranium in biological samples utilizing*

- kinetic phosphorescence analysis (KPA)*, J. Pharmaceut. Biomed. **15**, 1157-1165, (1997).
- [136] Sowder A.G., Clark S.B. and Fjeld R.A., *The effect of sample matrix quenching on the measurement of trace uranium concentrations in aqueous solutions using kinetic phosphorimetry*, J. Radioanal. Nucl. Chem. **234**, 257-260, (1998).
- [137] Pellmar T.C., Fuciarelli A.F., Ejnik J.W., Hamilton M., Hogan J., Strocko S., Emond C., Mottaz H. M. and Landauer M. R., *Distribution of uranium in rats implanted with depleted uranium pellets*, Toxicol. Sci. **49**, 29-39, (1999).
- [138] Miller A.C., Fuciarelli A.F., Jackson W.E., Ejnik E.J., Emond C., Strocko S., Hogan J., Page N. and Pellmar T., *Urinary and serum mutagenicity studies with rats implanted with depleted uranium or tantalum pellets*, Mutagenesis **13**, 643-648, (1998).
- [139] Thomas P.A. and Gates T. E., *Radionuclides in the lichen-caribou-human food chain near uranium mining operations in northern Saskatchewan, Canada*, Environ. Health Persp. **107**, 527-537, (1999).
- [140] Ejnik J.W., Hamilton M.M., Adams P.R. and Carmichael A.J., *Optimal sample preparation conditions for the determination of uranium in biological samples by kinetic phosphorescence analysis (KPA)*, J. Pharm. Biomed. Anal. **24**, 227-235, (2000).
- [141] McDiarmid M.A., Keogh J.P., Hooper F.J., McPhaul K., Squibb K., Kane R., DiPino R., Kabat M., Kaup, B., Anderson L., Hoover D., Brown L., Hamilton M., Jacobson-Kram D., Burrows B. and Walsh M., *Health effects of depleted uranium on exposed Gulf War veterans*, Environ. Res. **82**, 168-180, 2000.
- [142] Finneran K.T., Housewright M.E. and Lovley D.R., *Multiple influences of nitrate on uranium solubility during bioremediation of uranium contaminated subsurface sediments*, Environ. Microbiol. **4**, 510-516, (2002).
- [143] McDiarmid M.A., Engelhardt S., Oliver M., Gucer P., Wilson P.D., Kane R., Kabat M., Kaup B., Anderson L., Hoover D., Brown L., Handwerger B., Albertini R.J., Jacobson-Kram D. and Thorne C.D., Squibb K.S., *Health effects of depleted uranium on exposed Gulf War*

- veterans: a 10-year follow-up, *J. Toxicol. Env. Heal. A* **67**, 277-296, (2004).
- [144] Lestaevel P., Bussy C., Paquet F., Dhieux B., Clarencon D., Houpert P. and Gourmelon P., *Changes in sleep-wake cycle after chronic exposure to uranium in rats*, *Neurotoxicol. Teratol.* **27**, 835-840, (2005).
- [145] Monleau M., Blanchardon E., Claraz M., Paquet F. and Chazel V., *Biokinetic models for rats exposed to repeated inhalation of uranium: implications for the monitoring of nuclear workers*, *Radioprotection* **41**, 85-96, (2006).
- [146] Humaid A.I., Al-Marboui R. and El-Mongy S. A., *Destructive Assay of Uranium Concentration by Reliable Laser Induced Kinetic Phosphorimetry Analysis (KPA)*, *J. of Nucl. Radiat. Phys.* **2**, 69-77, (2007).
- [147] Tawfiq O.A and Shirqi I.S, *Akashat phosphate mine*, Ministry of Industry and Minerals, State Company for Phosphate, 2010.
- [148] International Atomic Energy Agency (IAEA), "The Recovery of Uranium from Phosphoric Acid", IAEA publication, (1989).
- [149] Ghayb D.H., *Measurement of alpha emitters concentration in Tigris river water in Baghdad city using CR-39 plastic track detector*, M.Sc. Thesis, Al- Nahrain University, (2002).
- [150] Alter H.W. and Fleischer R.L., *Passive integrating radon monitor for environmental monitoring*, *Health Phys.* **40**, 693-702, (1981).
- [151] Schramel P., Wendler I., Roth P. and Werner E., *Method for the determination of Thorium and Uranium in urine samples by ICP-MS*, *Mikrochim. Acta* **126**, 263-266, (1997).
- [152] Al-Timimi L.T.A., *Uranium concentration in human blood samples using CR-39*, M.Sc. Thesis, Al-Nahrain University, (2007).
- [153] Al-Jundi J., Werner E., Roth P., Höllriegel V., Wendler I. and Schramel P., *Thorium and uranium contents in human urine: influence of age and residential area*, *J. Environ. Radioact.* **71**, 61-70, (2004).
- [154] Karpas Z., Paz-Tal O., Lorber A., Salonen L., Komulainen H. and Auvinen A., *Urine, hair, and nails as indicators for ingestion of uranium in drinking water*, *Health Phys.* **88**, 229-242, (2005).

- [155] Othman I., *The relationship between uranium in blood and the number of working years in Syrian phosphate mines*, J. Environ. Radioact. **18**, 151-161, (1993).
- [156] Ting B.G., Paschal D.C., Jarrett J.M., Pirkle J.L., Jackson R.J., Sampson E.J., Miller D.T. and Caudill S.P., *Uranium and thorium in urine of United States residents: reference range concentrations*, Environ. Res. **81**, 45-51, (1999).
- [157] Mohagheghi A.H., Shanks S.T., Zigmond J.A., Simmons G.L. and Ward S.L.A., *A survey of uranium and thorium background levels in water, urine, and hair and determination of uranium enrichment by ICP-MS*, J. Radioanal. Nucl. Chem. **263**,189-195, (2005).
- [158] Orloff K.G., Mistry K., Chapp P., Metcalf S., Marino R., Shelly T., Melaro E., Donohoe A.M. and Jones R.L., *Human exposure to uranium in groundwater*, Environ. Res. **94**, 319-326, (2004).

الخلاصة

يعتبر تحديد تراكيز اليورانيوم في الادرار البشري هو الاسلوب الافضل في مجال رصد قيم التعرض الداخلي العرضية او المزمنة للعاملين وعموم الناس والناجمة عن التعرض لليورانيوم . في هذه الدراسة ، تم استخدام طريقتين نموذجيتين لتحديد تراكيز التعرض المهني اليورانيوم في الادرار البشري للعاملين في مناجم الفوسفات وصناعة الاسمدة الفوسفاتية لسكان عدد من المواقع المنتخبة في العراق . تضمن الجزء الاول استخدام تقنية تحليل الفسفرة المستحثة بالليزر والتي تستند على اثاره اليورانيوم في المحاليل المائية باستخدام ليزر الصبغة النبضي ، ثم قياس الوميض الفسفوري المنبعث والمعبّر عن تركيز اليورانيوم في العينة .

تمت معايرة المنظومة قبل اجراء عمليات التحليل باستخدام محاليل قياسية ودراسة خطية استجابة الجهاز مع تغير تركيز اليورانيوم وتبين الحصول على معامل ارتباط خطي واضح لتراكيز تتراوح بين 0.05 و 100 ميكروغرام / لتر . كما تم اختبار دقة وكفاءة المنظومة باستخدام طريقة القياس المتكرر للعينات حيث وجد ان الفارق في النتائج لم يزد عن 3.5 بالمائة وان حدود الكشف بلغت مستويات منخفضة تصل الى 10 نانوغرام / لتر .

بينت نتائج التحليل ان تراكيز اليورانيوم في الادرار البشري للمتطوعين تراوحت بين 0.41 و 5.26 ميكروغرام / لتر مع معدل 1.315 ± 0.730 ميكروغرام / لتر . كما سجلت النتائج اعلى تركيز لليورانيوم في نماذج الادرار الخاصة بالعاملين في مصانع الاسمدة والذين عملوا في السابق ضمن وحدة تنقية اليورانيوم من الصخور الفوسفاتية ، اظهرت النتائج ايضاً ان معدل تركيز اليورانيوم في الادرار يتناسب طردياً مع مختلف الفئات العمرية ولغاية 60 سنة .

بينت النتائج ان تراكيز اليورانيوم في الادرار للسكانين بالقرب من المناجم الفوسفاتية في عكاشات او مواقع طمر النفايات الاشعاعية في عداية والجزيرة اعلى من تراكيز هذا النظير في الادرار للسكانين في المناطق الاخرى . ومن ناحية اخرى وجد ان تركيز اليورانيوم عند الذكور اعلى من الاناث ولمختلف الفئات العمرية .

تم اجراء تحليل النماذج ومقارنة النتائج باستخدام تقنية عد اثار شظايا الانشطار النووي . واطهرت نتائج المقارنة مكانية التقنيتين في اجراء التحليل مع فارق الدقة . حيث اشارت النتائج الى توافق قوي بين تراكيز اليورانيوم المقاسة باستخدام تقنية الليزر التفسري المستحث والقيم العيارية مما يعكس الدقة في النتائج والوثوق في الجهاز المستخدم في اجراء هذا النوع من القياسات .

Brief Curriculum Vitae for Ahmed F. Saleh Al-Jobouri

Personal Data

Full name: Ahmed F. Saleh Murbat Al-Jobouri

Date of birth: 6-7-1974

Place of birth: Baghdad, Iraq

Nationality: Iraqi

Marital Status: Married and I have one Child

Religion: Muslim

Permanent Address: Iraq, Baghdad, Al-za'afarana, Sector (966), St. No. (21),
Building (16).

Phone No.: Mobile (Zain): +964-790-1440-274
(Asiacell): +964-770-4209-489
Office: +964-1-7781899

E-mail Address: phy.asaleh@yahoo.com
afsalih@gmail.com

Title of job: physicist

Name of employer: Ministry of Environment, Radiation Protection Center

Education:

1. B.Sc. on General physics from Baghdad University, Education College, with Nuclear physics courses as a special field of study, from 1992 to 1996.
2. M.Sc. on nuclear physics from Al-Nahrain University, College of Science, from Nov. 2009 to April 2012.

Thesis title “Determination of Uranium Concentration in Human Urine for Selected Regions in Iraq Using Laser-Induced Kinetic Phosphorimetry and CR-39 Nuclear Track Detector”

Employment:

1. After the completion of undergraduate study and joining military service with the Iraqi army for eighteen month from Sep. 1996 to Mar. 1998, I worked in the private sector for six years from 1998 to 2004.
2. Ministry of Environment/Radiation Protection Center from Oct. 2004, till now as a physicist in the Radiological Monitoring Department. In the implementation of the following tasks:
 - 2.1. Issuing authorizations and licenses for all activities dealing with radioactive materials and sources for ex. the possession and use of radiation sources, radioactive sources safe transportation, decommissioning activities.
 - 2.2. Site inspection and radiation survey for medical and research institutes dealing with radioactive sources and X-ray generator equipments.

- 2.3. Plans review and site inspection for the decommissioning activities of Iraqi former nuclear facilities such as; LAMA facility, Geo Survey Pilot Plant and Italian Radioisotope Production Laboratories (IRIL).
- 2.4. Final survey and site release from regulatory control (ex. Geo-Pilot Plant facility).
- 2.5. Monitoring external radiation exposure for workers by supplying them with personal monitoring instruments ex; personal monitoring film.
3. One of regulatory body licensing and inspection team in decommissioning of destroyed nuclear facilities in Iraq.
4. Contributing with United Nations Environment Programme (UNEP) in publishing an international report for “*the radiological conditions in selected areas of southern Iraq with residues of depleted uranium*”.
5. Computer experience with Microsoft software (Windows and Office), installation and operation.

Training and experience

1. Participating in International Atomic Energy Agency (IAEA) technical meeting on Characterization for the Iraq Nuclear Facilities Decommissioning Project, 23 – 27 July 2007, IAEA, Vienna, Austria.
2. Participating in IAEA meeting on Consultancy to Develop Nuclear Regulations for Iraq, 18 – 22 Feb. 2008, IAEA, Vienna, Austria.
3. Participating in the Train and Engage Program: Project Management, Planning and Characterization for Facility Dismantlement, 7 – 23 June 2008, International Radioecology Laboratory, Slavutych and Pripyat, Ukraine.
4. Participating in the United States Department of State Training Workshop on Data Management, Analysis, and Reporting, 19 – 23 Feb. 2012, US Embassy, Baghdad, Iraq.
5. Participating in IAEA Consultants meeting for review of Draft Decommissioning Plan (DP) for Tammuz 2 reactor, 27 Feb. – 2 Mar. 2012, IAEA, Vienna, Austria.
6. Participating in the Frist Lasers and Advanced Materials Engineering Conference, 19 – 20 Mar. 2012, University of Technology and Institute of Laser for Postgraduate Studies, Baghdad, Iraq.

Publications:

1. Ahmed F. Saleh, Mazin M. Elias and Nada F. Tawfik, “*Determination of uranium concentration in urine of Akashat phosphate mine and fertilizer plants workers using laser-induced kinetic phosphorimetry*”, Frist Lasers and Advanced Materials Engineering Conference, Baghdad, Iraq.

بِسْمِ اللَّهِ الرَّحْمَنِ الرَّحِيمِ

﴿ وَقُلِ اعْمَلُوا فَسَيَرَى اللَّهُ عَمَلَكُمْ

وَرَسُولُهُ وَالْمُؤْمِنُونَ

وَسَتُرَدُّونَ إِلَىٰ عَالَمِ الْغَيْبِ وَالشَّهَادَةِ

﴿ فَيُنَبِّئُكُمْ بِمَا كُنْتُمْ تَعْمَلُونَ

صَدَقَ اللَّهُ الْعَظِيمُ

﴿ سورة التوبة : الآية (١٠٥) ﴾